UNIVERSITY OF PAVIA
Department of Electrical Engineering

Cost-effective Evolutionary Strategies for Pareto Optimal Front Approximation in Multiobjective Shape Design Optimization of Electromagnetic Devices

Doctorate dissertation by:

Marco Farina

Supervisors: Professor A. Savini
Assoc. Professor P. Di Barba

Academic Year 2000-2001

To Elena.

Abstract

Il ruolo dell' ottimizzazione multiobiettivo nella progettazione industriale di dispositivi elettromagnetici é sempre piú rilevante. La diponibilitá di codici FEM potenti e flessibili per l'analisi di campo e la crescente potenza di calcolo dei calcolatori forniscono al progettista la possibilitá di costruire modelli parametrici complessi che possono essere utilizzati per realizzare procedure di ottimizzazione automatiche. Come accade in gran parte dei problemi di progettazione, gli obiettivi di cui tener conto quando si progetta un dispositivo elettromagnetico sono molti e spesso in contrasto fra loro. L'approccio classico, tuttora ampiamente utilizzato, per affrontare problemi di ottimizzazione multiobiettivo consiste nel trasformare il problema multiobiettivo in uno mono-obiettivo utilizzando informazioni ulteriori sul problema che formalizzino un grado di preferenza tra gli obiettivi; il problema mono-obiettivo, cosi ottenuto viene successivamente risolto tramite una delle tecniche classiche di ottimizzazione, deterministiche o stocastiche.
In questa ottica il problema multi-obiettivo viene visto come un caso particolare del problema mono-obiettivo.
Questo approccio ha principalmente tre svantaggi

- La varietá di soluzioni di un problema multiobiettivo viene cosi ridotta a una sola soluzione con una consequente significativa perdita di informazione.

- La scelta di una soluzione tra le infinite possibili (meglio tra le n numericamente disponibili) attraverso informazioni aggiuntive viene fatta a priori, cioé senza una completa informazione su tutte e possibili soluzioni.

- In alcuni (frequenti) problemi multiobiettivo (problemi non convessi) l'approccio in oggetto fornisce soluzioni che sarebbe impossibile da un punto di vista matematico ottenere attraverso un approccio classico.

L'approccio derivato dalla teoria di Pareto non richiede una scelta a priori del grado di preferenza e inverte il punto di vista considerando il problema mono-obiettivo come un caso particolare del problema multi-obiettivo. Il risultato dell'ottimizzazione non é piú uno soltanto ma una varietá, un campionamento delle infinite soluzioni Pareto-ottime.
La teoria dei problemi multiobiettivo é d'altra parte matura e fornisce utili teoremi di esistenza e unicitá delle soluzioni, sia quando si considerano le classiche formulazioni scalarizzate, sia quando il problema é affrontato attraverso la teoria degli ottimi di Pareto. Una notevole varietá di metodi evolutivi e non evolutivi specificamente sviluppati per l' ottimizzazione multiobiettivo secondo Pareto sono presenti in letteratura e sono tuttora oggetto di studio nella comunitá scientifica. Allo scopo di confrontare questa varietá enorme di metodi diversi in maniera univoca, specifici criteri di convergenza e misure dell'errore di approssimiazione sono in corso di studio, perché l'estensione all'approssimazione del fronte di Pareto dei suddetti concetti non é per nulla immediata.
D'altra parte l'applicazione dei suddetti algoritmi a problemi di progettazione reali é spesso difficile e poco pratica da un punto di vista del costo computazionale, a causa dell'elevato numero di chiamate alla funzione obiettivo (fissato il numero di soluzioni volute). Questo é perticolarmente vero nel caso dell'ottimzzazione di forma dei dispositivi elettromagnetici industriali, dove la valutazione delle funzioni obiettivo spesso richiede la soluzione di un problema FEM (talvolta 3D, non lineare o accoppiato).

Lo sforzo di questa tesi consiste nel legare la teoria dell'ottimizzazione multiobiettivo secondo Pareto al progetto ottimo automtico di dispositivi elettromagetici, allo scopo di realizzare metodologie efficaci che possano essere utilizzati anche in ambiemte industriale.
I seguenti punti chiave del lavoro sono particolarmente importanti:

- Realizzare strategie a basso costo che richiedano un piccolo numero di chiamate alla funzione obiettivo ad un certo grado di accuratezza nell'approssimzione del fronte di Pareto.
- A questo scopo, considerare la varietá dei metodi evolutivi per l'ottimizzazione multiobiettivo e cercare di modificare le strategie computazionali al fine di renderli pratici per la progettazione industriale.
- Considerare anche strategie classiche, non evolutive (basate sulla funzione preferenza) in maniera critica e legarle alle precedenti tramite algoritmi ibridi.
- Cercare di estendere all'approssimazione del fronte di Pareto i metodi per l'ottimizzazione mono-obiettivo basati sulle superfici di risposta a reti neurali.
- Legare i codici di ottimizzazione sviluppati a codici commerciali per l'analisi FEM.
- Applicare le strategie sviluppate a problemi di progettazione multiobiettivo industriale in collaborazione con progettisti industriali.

Inoltre, le seguenti affermazioni possono essere dimostrate dalla presente tesi.

- L'analisi dell'ottimizzazione multiobiettivo secondo Pareto mostra che l'uso delle funzioni preferenza scalarizzate deve essere considerato con attenzione e in maniera molto critica.
- La scelta a posteriori della soluzione di compromesso da scegliere a partire dalle molte Pareto-ottime disponibili é preferibile rispetto alla scelta a priori di un grado di preferenza.
- Inoltre la disponibilitá di diverse soluzioni Pareto-ottime é utile di per se stessa al progettista.
- La soluzione di problemi di progettazione ottima multiobiettivo industriale tramite la teoria di Pareto é praticabile se si considerano metodi specifici appositamente studiati per fornire soluzioni convergenti e diverse tra loro anche quando il numero di soluzioni che possono essere calcolate é molto piú basso del tipico numero din individui richiesto per la convergenza in un algoritmo evolutivo multiobiettivo classico.

I contributi piu originali del progetto sembrano essere i seguenti:

- Applicazione al progetto della forma dei dispositivi eletromagnetici dell'ottimizzazione multiobiettivo secondo Pareto.
- Sviluppo di algoritmi e strategie speciali con buon comportamento sia in caso di problemi test analitici sia in caso di problemi di progettazione industriale.

Introduction and project statement

The role of multiobjective optimization in industrial design of electromagnetic devices is remarkable and is more and more increasing. The availability of powerful and flexible FEM codes for field analysis and the increasing power of computers gives the designer the chance of building complex parametric models to be considered for an automatic optimization procedures. As in almost all design problems, objectives in an electromagnetic devices design are numerous and often in contrast each other. The classical, and still widely used, approach to such a situation is to transform the multiobjective problem into a single-objective one using some extra knowledge, and to solve it with classical techniques for single-objective optimization.
Under such a perspective the multi-objective problem is considered as a special case of the single-objective one.
This approach has three main drawbacks:

- the variety of solution of a multiobjective problem is reduced to one with a significant reduction of information,
- the choice of one solution using some extra knowledge is done a-priori with no complete information about all possible solutions,
- in some (frequent) multiobjective problems (non-convex problems) the true multiobjective approach gives solutions that would be mathematically impossible to obtain via the classical approach.

On the other hand, when Pareto optima theory is considered, no *a-priori* choice of preferences is required and the perspective is inverted, that is the single-objective problem becomes a special case of the multi-objective one. The aim of the optimization process is the approximation of the infinite Pareto-optimal solution throughout a convergent and equally spaced sampling of the Pareto optimal front.

The mathematical theory of multiobjective optimization is mature and gives useful theorems for existence and uniqueness of solutions both when classical scalar formulations are considered and when the problem is tackled via Pareto optima theory (two reference book are [37], [34] or [10]). A wide variety of evolutionary and non evolutionary methods being specially devoted to Pareto multiobjective optimization (Multiobjective Evolutionary Algorithms MOEAs) have been developing and are being developed in the scientific community. In order to do this huge amount of different strategies univocally a debate is in progress about test functions, specific convergence criteria and approximation errors because the extension to Pareto Optimal Front (POF) approximation of such concepts is non at all straightforward. This is why, for instance, a special section of the first congress on Evolutionary Multiobjective Optimization (EMO2001, Zurich, [13]) was devoted to performance measurements.

On the other hand real-life application of MOEAs is often hard and unpractical due to the complexity of methods [23, 39, 2, 1, 21],[ws1] and the computational cost deriving from the required huge number of objective functions calls [7, 46, 2],[ws2]. This is particularly true when shape design in electromagnetic industrial devices is concerned, where the evaluation of objective functions often requires FEM computations (sometimes 3D or non-linear or coupled). A special section of EMO2001 was devoted to real-life applications.

The effort of this thesis is to link true multiobjective optimization mathe-

matical theory and algorithms with automated optimal design of electromagnetic devices in order to build effective methodologies to be practical in industrial environment. The following key-point will be tackled:

- Build cost effective strategies requiring a small number of objectives function calls at a given accuracy of Pareto Optimal Front approximation.
- In order to do this consider the world of Evolutionary multiobjective Optimization methods and try to modify strategies in order them to be practical in electromagnetic shape design.
- Consider classical non-evolutionary strategies (based of preference function) as well, in a critical way and link them to hybrid stochastic-deterministic search tools.
- Try to extend neural network based single objective response surface methods to POF approximation.
- Link developed strategies to commercial FEM field analysis tools.
- Apply developed strategies to industrial design problem in cooperation with industrial designers.

Contents

List of Figures

List of Tables

Part I

Methodology and Algorithms

Chapter 1

Methodology

1.1 Introduction

1.2 Multi-objective optimization problems

Many realistic optimization procedures in electromagnetic industrial design can be formulated as nonlinear constrained multiobjective optimization problems. The following problem will be thus considered throughout the whole present work:

$$\begin{cases} \min\limits_{\mathbf{x}\in\mathbb{R}^N} & \mathbf{f} = \{f_1(\mathbf{x}), ..., f_M(\mathbf{x})\} \\ subject\ to & \mathbf{g}(\mathbf{x}) \leq 0 \\ & \mathbf{h}(\mathbf{x}) = 0 \end{cases} \tag{1.1}$$

where $\mathbf{x} = (x_1, x_2, ..., x_N)$ is the design variables vector in $\mathbb{R}^N$ and where M objective functions $f_1(\mathbf{x}), f_2(\mathbf{x}), ..., f_M(\mathbf{x})$ are considered assuming, without loss of generality, that all objectives are to be minimized. Moreover $\mathbf{g}(\mathbf{x}) \leq 0$ and $\mathbf{h}(\mathbf{x}) = 0$ are inequality and equality constraints representing the majority of practical and physical constraints arising in industrial design. From a general point of view, design variables may also not belong to $\mathbb{R}^N$ (e.g. discrete variables design optimization); in this work we only consider real variables.

Problem 1.1 give rise to the following subspaces known as design domain search space Ω and objective domain search space Ω_O respectively:

$$\begin{cases} \Omega\ :\ \{\mathbf{x} \in \mathbb{R}^N\ s.t.\ \mathbf{g}(\mathbf{x}) \leq 0\ and\ \mathbf{h}(\mathbf{x}) = 0\} \\ \Omega_O\ :\ \{\mathbf{f}(\mathbf{x}) \in \mathbb{R}^M\ s.t.\ \mathbf{x} \in \Omega\} \end{cases} \tag{1.2}$$

Ω_o being the image of Ω through function $\mathbf{f}$.
Very often the M objectives have different physical dimensions and are non commensurable because they refer to different characteristics or performances of the device (e.g. cost of materials, volume, efficiency, power leakage). The designer is thus forced to look for compromises among all desired objectives. In order problem 1.1 to be non-trivial (that is truly multiobjective) the pair (f_i, f_j) has to represent conflicting objectives $\forall\, i, j = 1, ..., M\ with\ i \neq j$. As a consequence single-objective optimization is to be considered as a special case of multiobjective optimization.
The notion of Pareto-optimality is one of the major issues in multiobjective decision making and it is useful for the designer because it gives a precise mathematical definition of the general concepts such as compromise solution, better or worse solution and so on that are non trivial concepts in multiobjective optimization. When multiple solutions of a given problem are available, it is necessary to rank them according to a certain rule. This can be done in a straightforward way using Pareto

Situation	Consequence
x_1 dominates x_2	x_1 is a better solution than x_2
x_2 dominates x_1	x_2 is a better solution than x_1
None of the two	x_1 and x_2 are equivalent solutions

Table 1.1: Pareto optima theory terminology.

optima theory, although Pareto optima definition is not the unique definition of optima in multiobjective problems, (see Nash optimum definition and its applications). When single-objective optimization is concerned an order criterion among solution is trivial because the objective domain search space is mono-dimensional; on the other hand when multiple objectives are considered the task of an order or partial order criterion in the objective domain search space is non-trivial and is one of the core task of MO optimization. Following Pareto theory, the following order criterion can be stated where minimization of all objective is considered without any loss of generality.

Def 1.1 *For any two points (solutions)* $\boldsymbol{x}_1$ *and* $\boldsymbol{x}_2 \in \Omega$ *if the following conditions hold:*

$$\begin{cases} f_i(\boldsymbol{x}_1) \leq f_i(\boldsymbol{x}_2) & for\, all\, i \in [1,2,...M] \\ f_j(\boldsymbol{x}_1) < f_j(\boldsymbol{x}_2) & for\, at\, least\, one\, j \in [1,2,...M] \end{cases}$$

then x_1 *is said to dominate* $\boldsymbol{x}_2$*.*

Although a detailed treatment of Pareto multiobjective optimization is out of the scope of this work, some basic definitions and concepts will be introduced and explained with reference to simple examples. This should be sufficient when Pareto optima theory is to be applied to multiobjective optimization of electromagnetic devices; a detailed treatment of the full theory can be found in [34],[10],[7],[47, 15, 16, 14].
As a consequence of definition 1.1 in Pareto optima theory when two solution are available, three kinds of different situations can happen and are shown in table 1.1

We can now give a geometric interpretation of definition 1.1. Let us assume to have a set of solutions for a two-objective optimisation problem; in this case we can plot in the design space all points corresponding to the solutions. Looking at figure 1.1 let us now focus on a single point $F^* \in \Omega_O$ being the image through function $\mathbf{f}$ of a point $x^* \in \Omega$ and draw two semiaxes parallel to the main axes, originated from the given point and oriented towards infinity or minus infinity if the related objective has to be minimised or maximised, respectively. The following definitions can be stated:

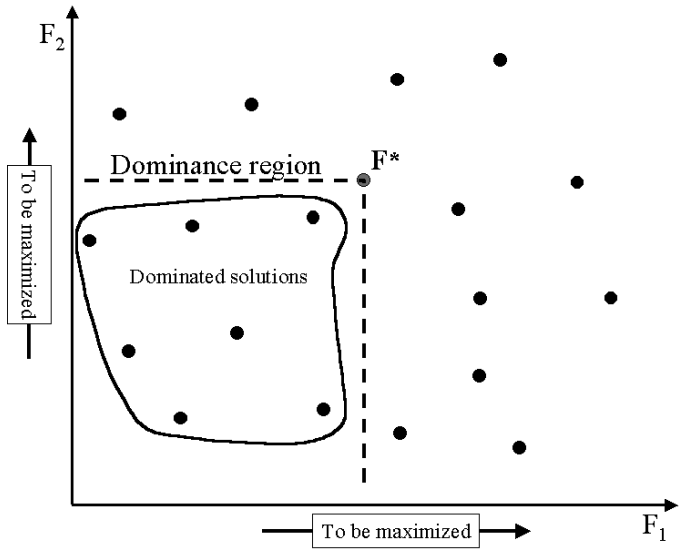

Figure 1.1: Schematic view of dominance region.

Def 1.2 *The region bounded by the semiaxes having origin in the solution* $\boldsymbol{F}^* = \boldsymbol{f}(x^*$ *is said dominance region of* $\boldsymbol{x}^*$*.*

Def 1.3 *All solutions located in the dominance region of* $\boldsymbol{x}^*$ *are said dominated solutions.*

Def 1.4 *If $\boldsymbol{x}^*$ does not belong to any dominance region of other points $\in \Omega$, then $\boldsymbol{x}^*$ is said non-dominated solution or Pareto-optimal (PO) solution; more formally.*
$\boldsymbol{x}^* \in \Omega\, is\ PO\ if \quad \nexists\, \boldsymbol{x} \in \Omega\, s.t.\, f_i(\boldsymbol{x}) \leq f_i(\boldsymbol{x}^*) \forall\, i = 1, ..., M\, and\, f_j(\boldsymbol{x}) < f_j(\boldsymbol{x}^*)$
$for\, at\, least\, one\, j \in [1, ..., M]$

As a consequence of definitions 1.1 and 1.4 the number of solution for problem 1.1 is infinite and two subsets for PO solutions can be thus defined:

Def 1.5 *The set of PO solutions in Ω is called Pareto Optimal Set (POS).*

$$POS = \{\boldsymbol{x}^* \in \Omega\, s.t.\, \widetilde{\boldsymbol{x}}\, is\, PO\} \tag{1.3}$$

Def 1.6 *Given a $POS \in \Omega$ its image in objective domain through function $\boldsymbol{f}$ is called Pareto Optimal Front (POF).*

$$POF = \{\boldsymbol{f}(\boldsymbol{x}^*) \in \Omega_O\, s.t.\, \boldsymbol{x}^* \in POS\} \tag{1.4}$$

Two points in the objective domain, giving some very preliminary information about Ω_O and known as Utopia and Distopia point respectively, can be defined:

Def 1.7 *We call utopia-point U the array containing all single objective minima in the search space.*

$$\boldsymbol{U} = \left[\min_{\boldsymbol{x}\in\Omega} f_i\right] \quad i = 1 : M \tag{1.5}$$

As a consequence of the truly multiobjective nature of problem 1.1 the inverse image of $\mathbf{U}$ does not belong to Ω and $\mathbf{U}$ does no belong to Ω_O. From a more formal viewpoint the following condition ensures non-triviality of the MO problem:

$$\nexists\, \mathbf{x}_U \in \Omega\, s.t.\, f_i(\mathbf{x}_U) = \min_{\mathbf{x}\in\Omega} f_i(\mathbf{x}) \quad \forall i = 1, ..., M \tag{1.6}$$

that is no points in Ω minimize at the same time all objectives (no cooperative objectives). With duality the following definition can be given:

Def 1.8 *We call distopia-point D the array containing all single objective maxima in the search space.*

$$\boldsymbol{D} = \left[\max_{\boldsymbol{x}\in\Omega} f_i\right] \quad i = 1, ..., M \tag{1.7}$$

Some primary information on the POF may be obtained from the evaluation of the following matrix

$$[\widetilde{\mathbf{M}}] = \begin{cases} U_i & \text{i=j,} \\ f_j(\widetilde{\mathbf{x}})\ when\ f_i(\widetilde{\mathbf{x}}) = U_i & \text{otherwise.} \end{cases} \tag{1.8}$$

When matrix $[\widetilde{\mathbf{M}}]$ is computed the Nadir point R can be computed as follows:

Def 1.9 *We call nadir-point R the array containing all extremal point in the POF.*

The evaluation of the nadir point is simple in a 2D problems but it becomes not at all trivial in case of more than two objectives. The following formula can be for approximating the nadir point.

$$R_i = \max_{j=1:M} [\widetilde{M}_{i,j}] \tag{1.9}$$

From a practical point of view we remark that the computation of the $M \times M$ matrix $[\widetilde{\mathbf{M}}]$ and thus $\mathbf{R}$ and $\mathbf{U}$, only requires M single-objective optimization.
A schematic view of POS and POF in a typical situation is represented in figure 1.2 As can be seen visualization of POF is straightforward when the number of objective is two; it becomes difficult for three objectives problems and impossible for more than three objectives. The same holds for visualizing POS when the number of design variables is more than two or three. When dealing with approximation of POS and POF, visualization is much more useful than the corresponding single-objective solution visualization and this is why the problem of visualizing results

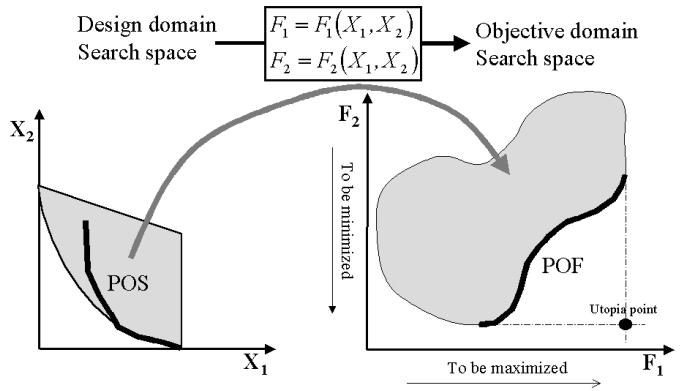

Figure 1.2: Example of search spaces in both domains and utopia point.

is not at all a trivial task and could be an interesting topic for future research. Utopia U, distopia D and nadir R are shown on a schematic example in figure 1.3; the computation of all this points is essential for a preliminary bounding of the POF.
The shape of POF is fundamental in determining the difficulties encountered by the optimizer in converging towards it and thus the strategies to overcome these difficulties. We will schematically show the most typical kinds of POF that are encountered when dealing with realistic optimization in electromagnetics: deceptive, discontinuous, convex, non-convex and multimodal. Such terms are here defined. The POF can be written as a function of one objective versus all the others in the following way:

$$f_M^{POF} = POF(f_1, ..., f_{M-1}) \tag{1.10}$$

only for some very simple cases the function 1.10 can be written in a closed form.

Def 1.10 *A multiobjective problem is said* ***convex*** *if and only if all objective function are convex and* ***non-convex*** *if and only if one or more objective function are non convex.*

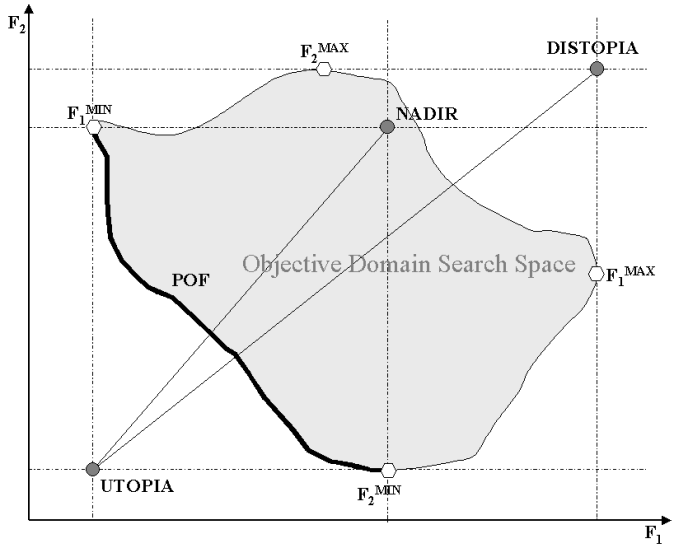

Figure 1.3: Example of objective domain search spaces key-points.

For a convex problem function 1.10 is convex and *vice-versa*.

Def 1.11 *A multiobjective problem is said* ***discontinuous*** *if and only if function 1.10 is discontinuous.*

If $\mathbf{S}_\Omega$ is random exhaustive sampling of Ω we consider $\mathbf{S}_{\Omega_O} = \mathbf{f}(\mathbf{S}_\Omega)$ as a sampling of Ω_O.

Def 1.12 *A multiobjective problem is said* ***deceptive*** *if and only if* $\boldsymbol{S}_{\Omega_O}$ *is non uniform when* $\boldsymbol{S}_\Omega$ *is uniform.*

If the POF is in a non-uniform density region of $\mathbf{S}_{\Omega_O}$ the POF too can be said deceptive.

Def 1.13 *A multiobjective problem is said* ***multimodal*** *if and only if more than one local POF exists.*

The main difficulties when tackling approximation of discontinuous *POF* is the approximation of all the branches of the front. Usually solutions tend to converge towards an extremal point of the front; a schematic example of a discontinuous front is shown in 1.4

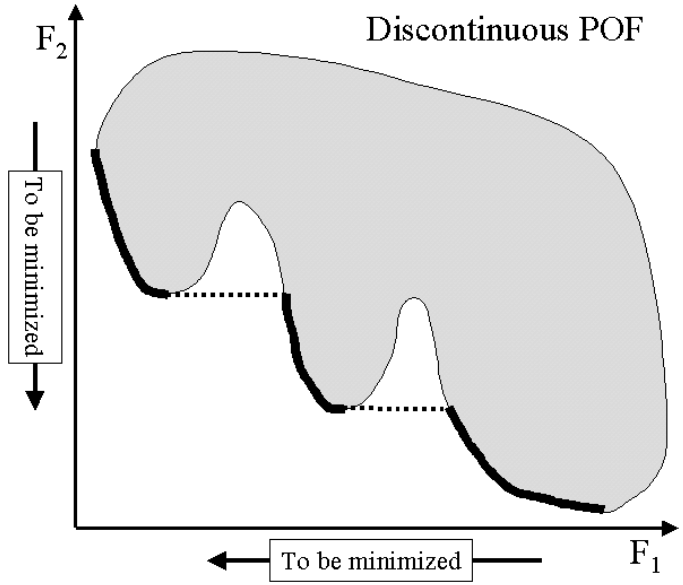

Figure 1.4: Schematic view of a problem with a discontinuous front.

Another remarkable difficulty for the *POF* approximation arises when the density of search space in objective domain is non uniform. This can be viewed considering an uniform random distribution of sampling points in the design domain search space; when the image throughout function **f** of each point is plotted in the objective space a non-uniform distribution of point arises. This happens in the whole objective-domain search space.

In figure 1.5 we schematically represent with non-uniform grey the non-uniformity of the search space and with non-uniformly distributed dots the consequent non-uniformity of the *POF*. When approximating deceptive *POF* solutions tend to converge towards the regions with higher density (the lower part in figure 1.5).

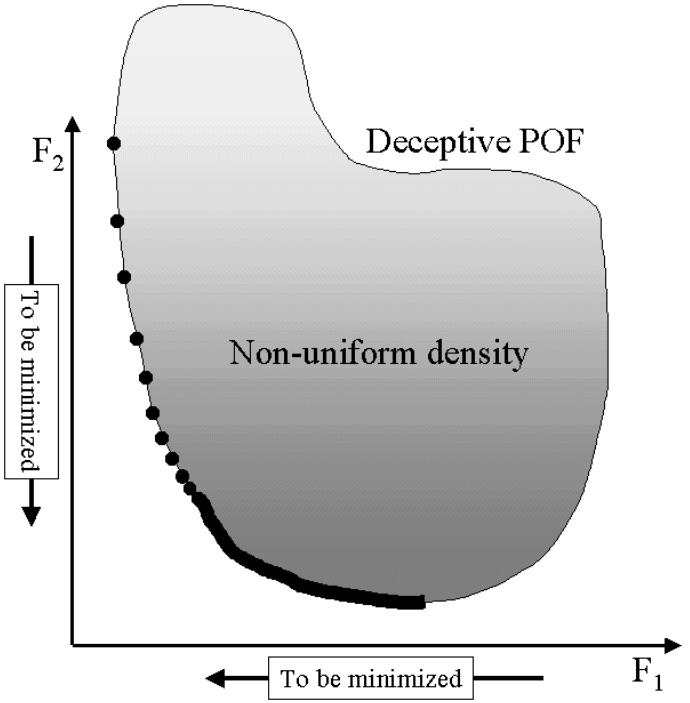

Figure 1.5: Schematic view of a deceptive problem.

Convexity of *POF* is a key feature for approximation; this property will be deeply discussed in the following section; here a schematic view of both a convex and a non-convex front is shown in figure 1.6 Another interesting and typical situation happens when the objective domain search space is characterized by several local *POF*. Such a situation can be viewed

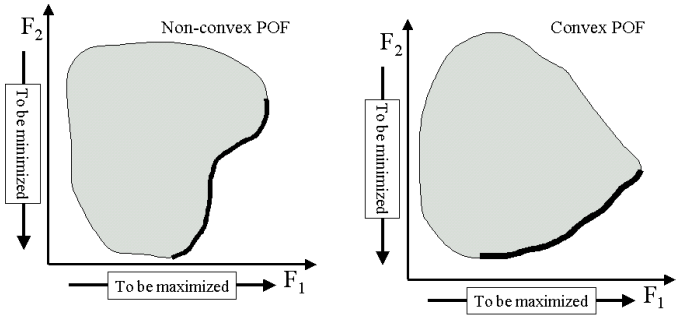

Figure 1.6: Schematic view of convex and non-convex multiobjective problem.

when an uniform sampling points random distribution in design domain search space is considered and the corresponding points are plotted in the objective domain; the distribution of points is schematically represented in figure 1.7. We point out that presence of local front does not depend on a coarse search space sampling. We will see some optimization tests on such a problem later on but we can say here that the multimodal problem is essentially the extension to multiobjective optimization of the concept of multiple minima in single-objective optimization.

We introduce here the concept of Pareto ranking or Pareto sorting that will be remarkable when dealing with *POF* approximation algorithms. Let us consider a set of points in the objective space as it is shown in figure 1.8; a first *POF* can be defined and it is labelled as I in figure 1.8. If we remove points belonging to this first front from the full set of points we can define the *POF* for this reduced set of points (labelled II in figure 1.8). This procedure can go on until all points in the initial set are considered. We will use the term Pareto Sorting Algorithm PSA or Non Pareto Sorting Algorithm NPSA when we refer to an algorithm that uses Pareto sorting or not for fitness assignment; we will go into deeper details about algorithms in section 2.2.

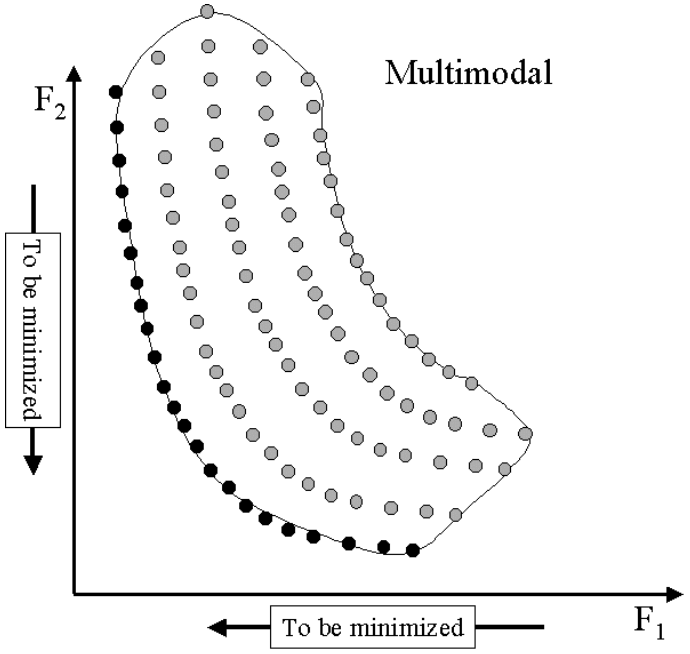

Figure 1.7: Schematic view of a multimodal multiobjective problem.

1.3 Preference-function Formulations *versus* Pareto Formulation

The traditional approach to multiobjective optimization in electromagnetic design has generally consisted of building up a scalar objective function expressing a compromise among the various objectives and depending on either weight coefficients or threshold values; afterward the optimization is performed via standard single-objective optimization methods. Although being simple and widely used, scalar formulations presents several drawbacks; first of all the result of an optimization is only one solution which is supposed to be optimal. The first criticism is that it is not al-

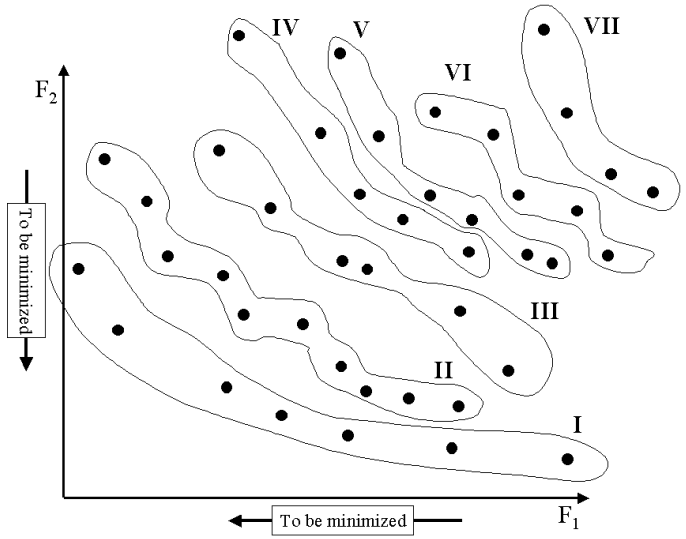

Figure 1.8: Example of Pareto ranking.

ways clear where this solution is located with respect to the POF, being sometimes even a dominated solution. Second and more important aspect is that the mathematical solution of a multiobjective optimization problem is a variety of solution, which are spread on the POF; knowing this variety is often very useful for the designer, who has a wide range of possibilities for an a-posteriori more conscious choice.

In order to obtain many different solutions located on the POF one could run several single-objective optimizations of different scalar functions without introducing at all the idea of solution ranking in the Pareto sense; this strategy may work for some formulation on some particular cases but in many other cases it is conceptually wrong giving rice to dominated solutions, or it leads to difficulties in obtaining a uniform sampling of the POF. For a more detailed treatment of the topic we now consider the three most popular scalar formulations which are commonly used in electromagnetic design and show limits of each of them when applied to the sampling of a POF; three task will be addressed for each formulation:

- When performing a single-objective optimization on the preference function to be considered is the solution a non-dominated one and in which sense can it be said to be optimal ?
- When performing several runs with different weights or threshold values can the POF be identified in an exhaustive way ?
- If the answer to the previous question is yes, does a uniform distribution of solutions on the POF correspond to a uniform a-priori choice of weights or threshold values ?

1.3.1 Normalised weighted sum

The formulation is the following:

$$\begin{cases} \min\limits_{\mathbf{x}\in\Omega} \widetilde{f}(\mathbf{x}) = \sum\limits_{i=1}^{M} \dfrac{w_i f_i(\mathbf{x})}{R_i - U_i} \\ \sum\limits_{i=1}^{M} w_i = 1 \end{cases} \tag{1.11}$$

Where R_i and U_i are nadir and utopia points components respectively. The use of such a normalization value is essential for weights w_i to express desired compromises. As regards the first two questions the following theorem holds:

Theorem 1.1 *Let the POF be convex. If* $\boldsymbol{f}^* = \boldsymbol{f}(\boldsymbol{x}^*) \in POF$ *then there exist a weighting vector* w $(w_i >= 0, i = 1, ..., M, \sum w_i = 1)$ *such that* $\boldsymbol{x}^*$ *is a solution of the problem:* $\min\limits_{\boldsymbol{x}\in\Omega} w^T F$

For the proof see [34]; a simple geometric interpretation of theorem 1.1 in two dimensions is shown in figure 1.9 where the general equipotential line of function $\widetilde{f}$ is plotted with dashed line in the objective domain; a POF and the search space of a general multiobjective optimization problem are also shown. Once the weights w_1 and w_2 are fixed the minimization process can be viewed as searching for the point of the dashed lines which

is externally tangent to the POF and it is external to the search domain. As is evident from figure 1.9, only in the case of convex POF all point of the front can be sampled with this scalar function. Moreover it is not at all easy to know a priori the distribution of weights that give rise to a uniform distribution of solution on the POF. For instance one may consider a linear distribution of weights and obtain solution concentrated in one region of the POF. An example of this is shown in figure 1.10 where the following two monodimensional objective function are considered

$$\begin{cases} \min\limits_{(x)\in[0:2]} F_1(x) = x(x-1.5)(x-3)(x-4) \\ \min\limits_{(x)\in[0:2]} F_2(x) = (4-\sqrt{x}) \end{cases} \tag{1.12}$$

The search space in design domain is a curve; the distribution of solutions corresponding to a uniform distribution of weights is concentrated around the point corresponding to the minimum of f_1 and the approximation of the other POF regions is poor. A non-uniform distribution of weights should be considered but it is difficult to know a-priori the distribution of weights that corresponds to an equispaced distribution of solutions.

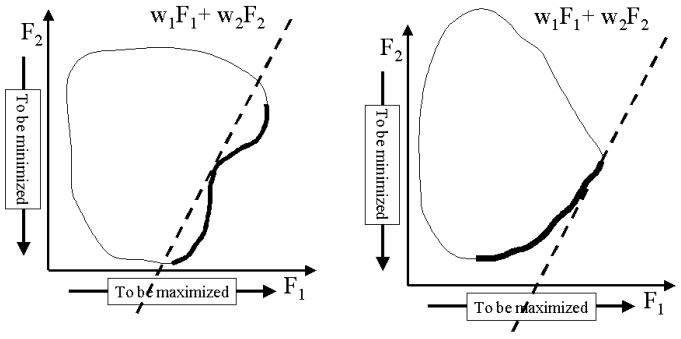

Figure 1.9: Visualization of Theorem 1.1 for both convex and non convex problems.

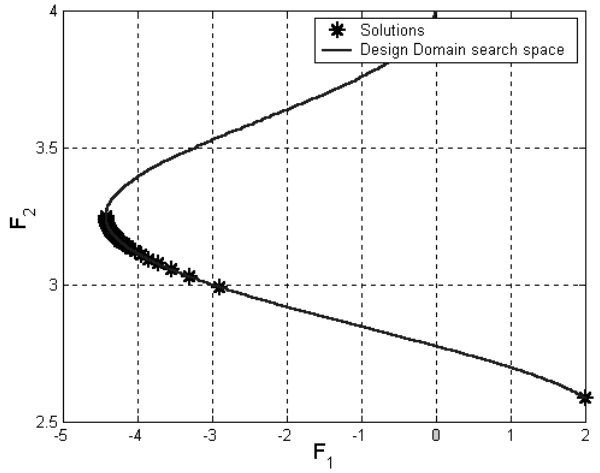

Figure 1.10: Example of non equispaced solutions corresponding to a linear distribution of weights.

1.3.2 Normalized weighted sum with membership function

The formulation is the following:

$$\begin{cases} \min\limits_{\mathbf{x}\in\Omega} \widetilde{f}(\mathbf{x}) = & \sum\limits_{i=1}^{M} \dfrac{w_i \mu_i(f_i(\mathbf{x}))}{R_i - U_i} \\ \sum\limits_{i=1}^{nobj} w_i = & 1 \end{cases} \tag{1.13}$$

where $\mu_i(f_i(\mathbf{x}))$ are membership function of a fuzzy classification of $f_i(\mathbf{x})$ possible values; various shapes can be used such as linear or arctan-like. For a simple example that easily answers the aforementioned three questions we consider a two objective problem and we build up linear two values membership for each objective. So doing one has $3 \times M$ degrees of

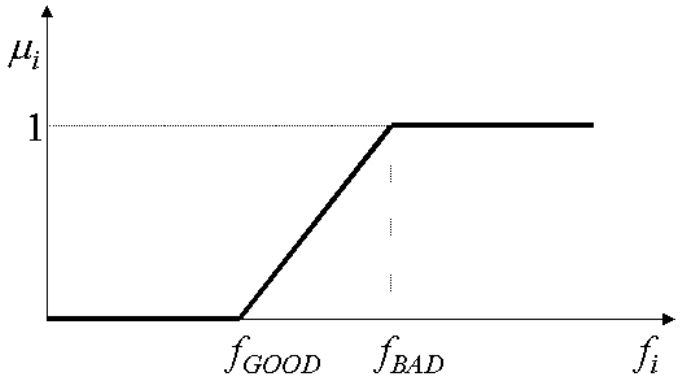

Figure 1.11: Membership function for the *i-th* objective function in the min-max formulation of 1.13.

	w_1	w_2	$f_{G,1}$	$f_{B,1}$	$f_{G,2}$	$f_{B,2}$
A	0.25	0.75	0.1	0.3	0.2	0.4
B	0.4	0.6	0.3	0.6	0.4	0.7
C	0.5	0.5	0.4	0.5	0.5	0.6
D	0.75	0.25	0.5	0.7	0.6	0.8

Table 1.2: Weights and threshold values for figures 1.14 and 1.15.

freedom (M weights w_i and $2 \times M$ membership functions threshold values). The general membership μ_i is shown in figure 1.11 where threshold values f_G (good value for f))and f_B (bad value for f) are also defined. Weights and threshold values are shown in table 1.2, we consider four different weights and four different threshold values for each objective function.

Figure 1.14 shows the $\widetilde{f}$ function as a function of f_1 and f_2 for two different situations: variable weights and fixed threshold values or fixed weights and variable threshold values. This is the scalarised function that is given to the optimizer. In analogy to what have been done in the case of normalised weighted sum we plot the contour lines of $\widetilde{f}$ together with a general POF for all different situations (figure 1.15). We can now try to answer to the aforementioned three questions. First of all for some combination of weights and thresholds values the solution may be dominated (see case A-3 or A-4 in figure 1.15) because a remarkable part of the front lies in a completely flat region and there is no reason why the optimizer, once reaching that region should converge towards a point on the POF; moreover in order to have multiple solution on the POF with different scalar function one should choose a-priori weights and threshold values similar to th obes in case A-1 where the formulation behaves as a normalised weighted sum in the region of the POF and move both weights and threshold values in order the oblique line region to overlap the front. This procedure is almost impossible to be done a-priori, that is when the POF is unknown. This is why we can conclude that the use of linear membership seems to be highly unsuitable for POF approximation. For what regards atan-like membership function the risk of dominated solutions is avoided because no flat region for function $\widetilde{f}$ are present in Ω_O; this can be easily seen in figure 1.12 and 1.13. Nevertheless the difficulty in controlling diversity of solutions throughout weights and threshold values changing still holds.

1.3.3 Normalised weighted Min-Max formulation

The following equation gives the scalarised function for this formultion:

$$\begin{cases} \min\limits_{\mathbf{x}\in\Omega} \widetilde{f}_\infty(\mathbf{x}) &= \max\limits_{i=1:M} \dfrac{w_i|f_i(\mathbf{x}) - f_i^*|}{R_i - U_i} \\ \sum\limits_{i=1}^{M} w_i &= 1 \end{cases} \tag{1.14}$$

where f_i^* are the a priori fixed goals for each objective. The ∞ symbol as a subscript of formulation 1.14 defines the L^p-norm in Ω_O that is used in 1.14.

As for previous cases the contours of the $\widetilde{f}$ function are plotted in figure 1.16 as function of f_1 and f_2 against a generic POF in objective domain.

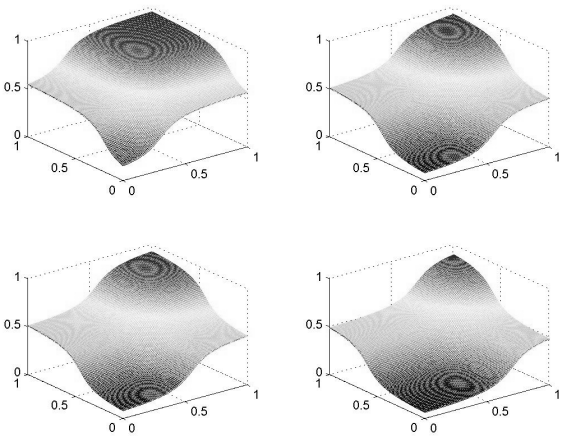

Figure 1.12: Surface of function $\widetilde{f}$ versus f_1 and f_2 with atan-like membership functions μ_i

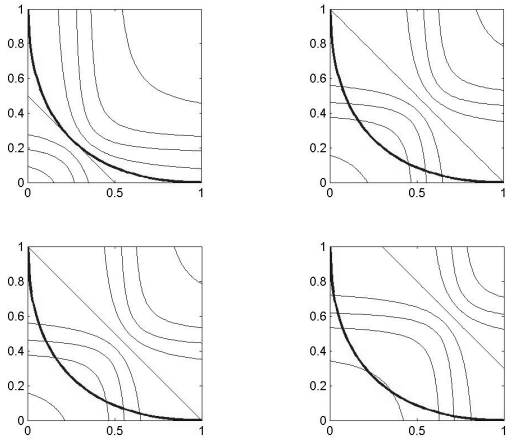

Figure 1.13: Equi-value lines of function $\widetilde{f}$ versus f_1 and f_2 with atan-like membership functions μ_i.

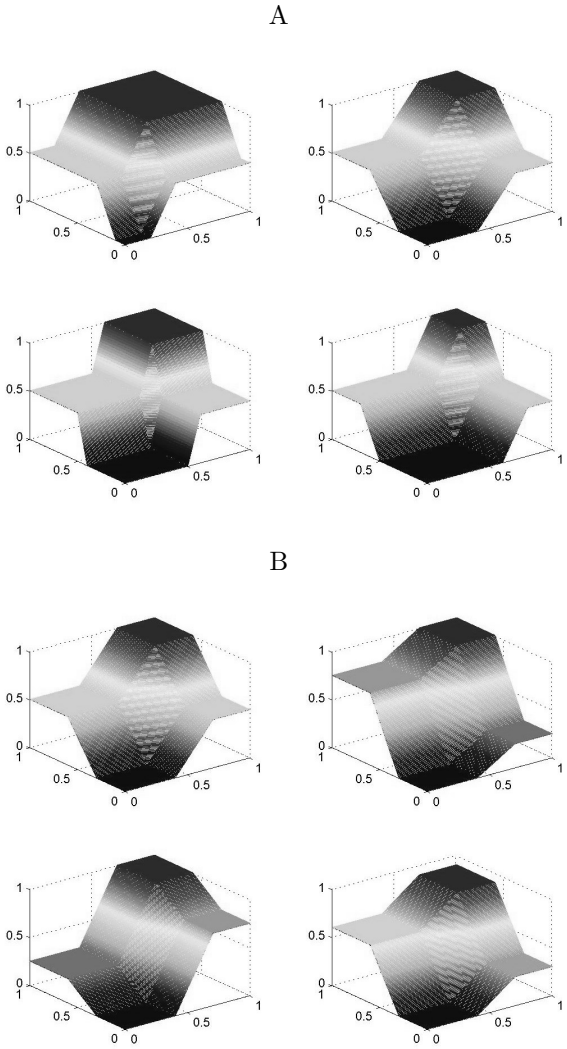

Figure 1.14: Scalarised Objective function $\widetilde{f}$; A: variable weights and fixed threshold values. B: Fixed weights and variable threshold values.

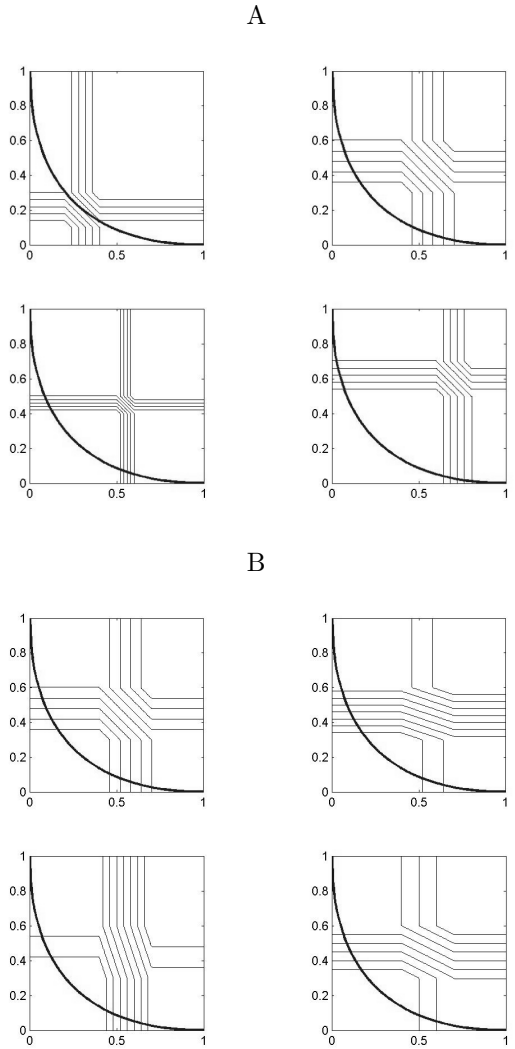

Figure 1.15: Various example of weights and threshold values for membership functions: surface of function $\widetilde{f}$ and contour lines with a convex *POF* (2D Shaffer's problem).

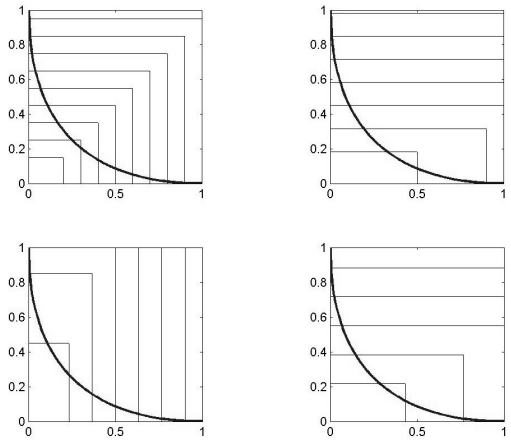

Figure 1.16: Various example of weights for min-max formulation: contour lines of fcap function with a general POF.

It should be noted that this approach is able to produce non-dominated solutions lying on non convex regions of the POF because the corner of a contour line of $\widetilde{f}$ may be tangent to the POF even in non-convex case; convergence of such a formulation toward the POF is assured by theorems (see [34]) even in case of non-convex problems. However the difficulty in the a-priori choice of a weights distribution giving a regular distribution of solutions on the POF still holds.

1.3.4 Obtaining variety of solutions with variables goals

The degrees of freedom in formulation 1.14 affecting the location of optimal solution on the POF are weights w_i and goals f_i^*. From the point of view of diversity, a possible strategy consist of choosing a suitable distribution of points f_i^* in order to have a good equi-spacing of solution on the POF; the values of weights w_i are fixed. In order this preference function to be effective in converging towards the POF for all possible choices of f_i^* (internal point of the objective domain search space Ω_o or external), the sign in the L^∞-distance is to be considered, that is the modulus in equation 1.14 is to be removed. This can be easily understood looking at figure 1.18 (schematic case) where two different f_i^* locations are considered. Contour lines of preference function $\widetilde{f}_\infty$ are plotted in the two upper cases while in the lower two cases preference function $\widetilde{f}_\infty$ without modulus is plotted; as can be seen the L^∞ norm preference function works only when the center f_i^* is outside Ω_O; if f_i^* is internal to Ω_O the search algorithm would converge towards f_i^* and not towards the POF.

We thus at the end deal with the following preference function:

$$\widetilde{f} = \max_{i=1:M} \left[\frac{\frac{1}{M}(f_i - f_i^*)}{R_i - U_i} \right] \tag{1.15}$$

where diversity of solution is obtained by means of targets f_i^* variation with fixed weights (defining parallel search directions in objective domain). An example of a problem where both internal and external f_i^* are used is shown in figure 1.21. As can be seen approximation quality does not depend on the position of centers and also a convex POF can be approximated with equally spaced solutions.

The validity of the strategy is shown in figures 1.21, 1.19, 1.17 and 1.20 where several different problems are considered both with two or three objectives. As can be seen the quality of solution is satisfactorily both in terms of convergence and diversity. The choice of goals f_i^* may be driven by different criteria; all examples here shown consider a linear distribution of goals on the line (or triangular surface in 3D problems) linking extreme points on the POF. More details on this strategy can be found in [cjp1].

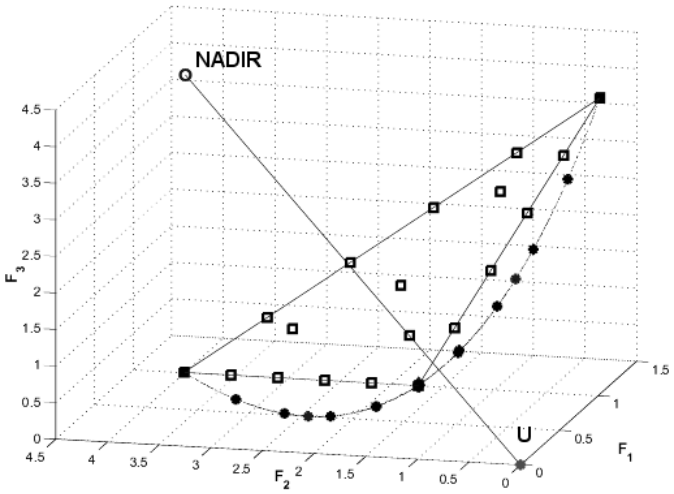

Figure 1.17: F3Db+ test case: results in the objective space of a run with 19 centers (□), 13 diverse solution (•) over the analytical POF curve (gray dots) with linear f_i^* 's choice.

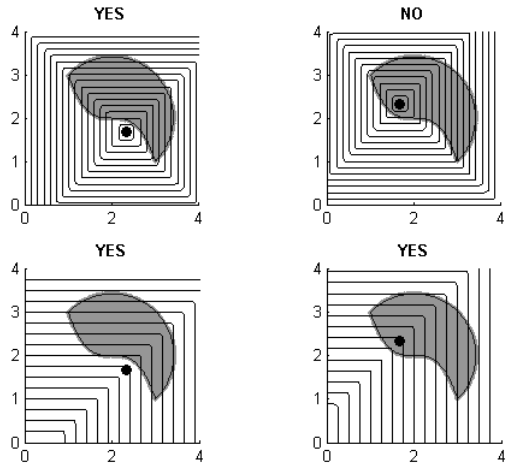

Figure 1.18: Contour lines on objective space of $\widetilde{f}_\infty$ (first two plots) and $\widetilde{f}$ (second two plots) preference function for two different f_i^* locations (•) on a schematic objective domain search space Ω_O .

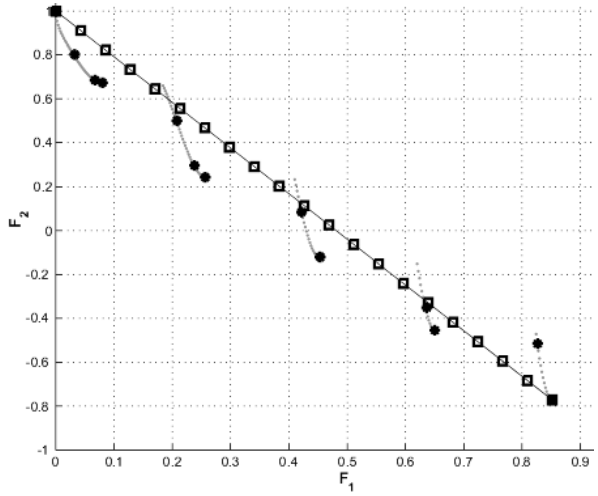

Figure 1.19: DTZ3 test case: results in the objective space of a run with 21 centers (□), 13 diverse solution (•) over the analytical POF (gray dots) with linear f_i^* 's choice.

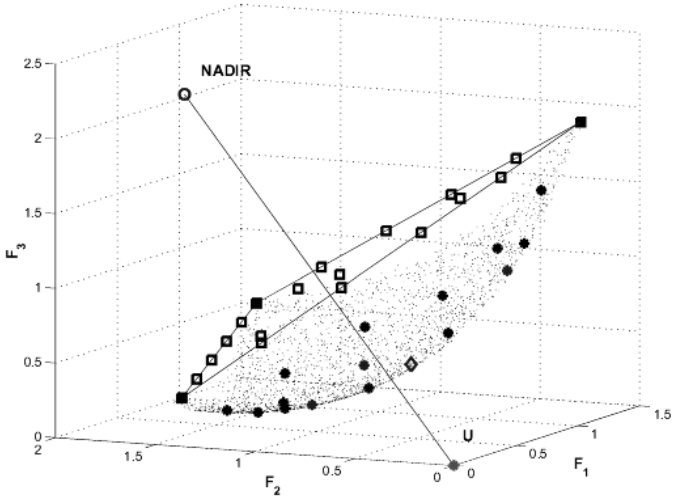

Figure 1.20: F3Db- test case: results in the objective space of a run with 19 centers (□), 19 diverse solution (•) over the analytical POF surface (gray dots) with linear f_i^*'s choice.

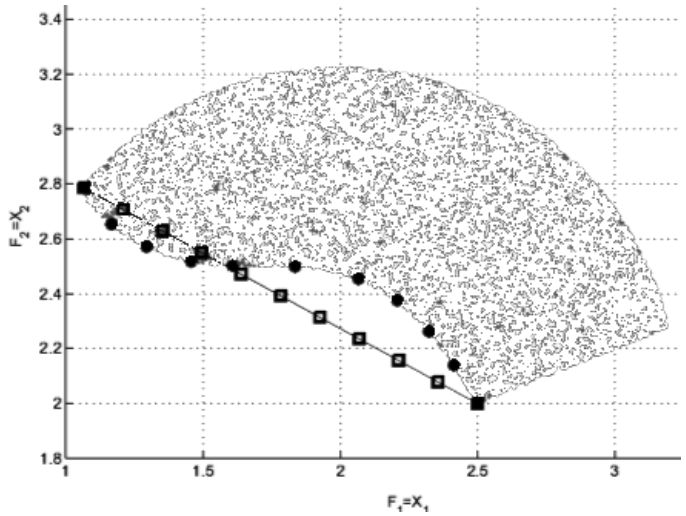

Figure 1.21: F2D test case: results in the objective space of a run with 11 centers (□), 11 diverse solution (•) over exhaustive sampling (gray dots), with linear f_i^* s choice.

1.3.5 Best Compromise Optimal Solution

The Best Compromise Optimal Solution (BCOS) $\widehat{\mathbf{x}}$ may be defined as follows:

$$\begin{cases} \widehat{\mathbf{x}} \in POS \\ \widehat{\mathbf{f}} = \mathbf{f}(\widehat{\mathbf{x}}) \in POF \\ \min\limits_{\mathbf{f} \in POF} \sum\limits_{1<i,j<M,\, i \neq j} \left(\frac{f_i - U_i}{R_i - U_i} - \frac{f_j - U_j}{R_j - U_j} \right) \end{cases} \tag{1.16}$$

and it may be obtained as solution of formulation 1.14 with $w_i = \frac{1}{M}$ and and $f_i^* = U_i$;

1.3.6 Search directions in objective domain

Sometimes one may be interested in computing a particular solution located on the POF in the intersection point with a line linking utopia point **U** and another point **B**. This is a solution corresponding to a particular search direction. In order the solution to be effective even in case of non-convex problem formulation 1.14 is to be used. Nevertheless an equivalent weighted sum preference function can be considered for computing weights to be used in formulation 1.14 corresponding to desired search directions.

$$\breve{f} = \left(\sum_{i=1}^{M-1} \frac{w_i f_i}{N_i} \right) + \frac{\left(1 - \sum\limits_{i=1}^{M-1} w_i \right) f_M}{N_M} \tag{1.17}$$

where **N** is the normalization array. This formulation is equivalent to 1.14 only in case of a convex problem but it can be used for computing weights that correspond to desired search directions.

The equation of the hyper-planes normal to desired search direction can

be computed as follows

$$f_M = \frac{N_M \breve{f}}{1 - \sum_{i=1}^{M-1} w_i} - \frac{N_M \sum_{i=1}^{M-1} \frac{w_i f_i}{N_i}}{1 - \sum_{i=1}^{M-1} w_i} \tag{1.18}$$

weights corresponding to the U-B direction can be computed in the following way:

$$\frac{B_M - U_M}{B_i - U_i} = \frac{N_M w_i}{N_i \left(1 - \sum_{i=1}^{M-1} w_i\right)} \quad i = 1 : M-1 \tag{1.19}$$

and the following linear system is to be solved

$$\mathbf{l} = [\mathbf{S}]\mathbf{c} \tag{1.20}$$

where

$$S_{i,i} = (B_M - U_M)N_i + (B_i - U_i)N_M \quad , \quad S_{i,j} = (B_M - U_M)N_i \tag{1.21}$$

and where $l_i = (B_M - U_M)N_i$.
A closed form solution may be easily computed in 2D and 3D cases.
2D case

$$c = \frac{1}{1 + \frac{N_2}{N_1}\frac{B_1 - U_1}{B_2 - U_2}} \tag{1.22}$$

3D case

$$c_1 = \frac{k_2(B_2 - U_2)N_1}{k_3 N_2 (B_1 - U_1)} \quad , \quad c_2 = \frac{k_2}{k_3} \tag{1.23}$$

where

$$k_1 = \frac{(B_2 - U_2)N_1 N_3}{N_2} \quad , \quad k_2 = (B_3 - U_3)N_1 \quad , \quad k_3 = k_1 + k_2 + \frac{k_1 k_2}{N_3(B_1 - U_1)} \tag{1.24}$$

1.3.7 Conclusive remarks

As conclusive remarks we point out that scalar formulations with variable weights and threshold values can be used with success as POF sampling techniques only in some cases;the main risk of this approach to multiobjective optimization is that in some cases solutions may be dominated. This is why Pareto formulation of multiobjective problems where no scalar function is considered and all conflicting objectives are kept separate seems to be much more reliable for both a theoretical and a practical point of view and it will be considered here onwards in this work. So doing the additional knowledge which is necessary in order to choose one solution among the infinite solutions of a multiobjective problem, is used a posteriori (that is after the optimization process) and not a priori (before the optimization process). A schematic view of such a logic procedure is shown in figure 1.22.
One of the key-points of Pareto optimality methods [40, 30, 29] is the *a-priori* or *a-posteriori* use of higher-level information when the decision maker has to choose among compromises. Very often in industrial electromagnetic design the a-posteriori choice implies more consciousness in such a decision because it is performed after considering all available POF sampling solutions. More details on Pareto Multiobjective Optimization Theory can be found in [17, 19, 6, 4, 5]

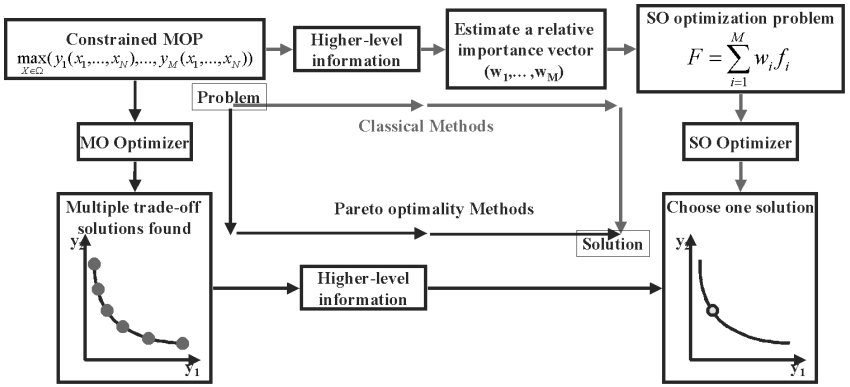

Figure 1.22: Classical and Pareto-based methods from the point of view of A-posteriori and a-priory choice.

Chapter 2

Multiobjective Optimization Strategies

2.1 Introduction

From a general point of view a wide variety of strategies for *POF* approximation can be considered [22, 28, 20, 43, 26, 44]. We focus our attention on cost effective algorithms that is algorithms where the number of objective function calls is reduced at a give degree of POF approximation accuracy (we recall that when MO optimization is concerned, accuracy=diversity+convergence). When building cost effective algorithms for multiobjective optimisation the simplest idea would be to consider deterministic search algorithms on different scalarised formulations and thus consider Non Pareto-sorting Algorithms (NPSA) where individuals do not interact among each other during optimization. This is why stochastic search engine are not strictly necessary for convergence towards the front as is the case for Pareto sorting algorithms (PSA).

2.2 The algorithms

.

A wide variety of stochastic methods are available in literature for Pareto multiobjective optimization [27, 18, 3, 31, 32, 45, 12],[ws2,ws3,ws4] and a comprehensive study of comparison and state of the art is presented in [47]. All this algorithms have been developed for solving optimization problems where the cost of objective functions evaluation is moderate. As a consequence the number of individuals used is usually very high because the majority of such methods derives from standard GA where the typical individuals number in the population size is 30-500. When dealing with design optimization of electromagnetic devices the evaluation of objective usually requires a FEM field computation that may be coupled and nonlinear; typical duration of such a computation even on powerful computers makes the use of this methods unpractical.

Let us consider as an example a real life case where one of the objective requires a FEM torque computation of 5 minutes; if the population size is 50 and 100 iteration are necessary for convergence we have at least 25000 minutes which is an unaffordable time for industrial design timing. This is why, having discarded deterministic methods for the problem of local minima the development of stochastic methods for Pareto Optimization that reduces the number of objective function evaluation is necessary.

Before going into details in the description of the developed algorithms we give in figure 2.1 a schematic classification of different algorithms that have been developed and used in this work in order to make clear since the beginning the used terminology (see table 2.1).

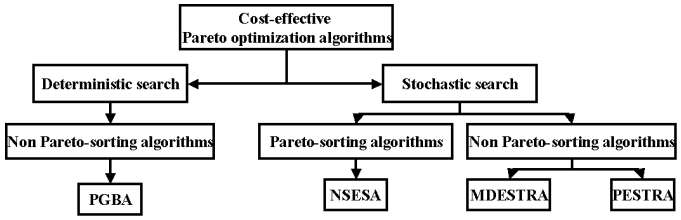

Figure 2.1: Classification of developed algorithms.

PGBA	Pareto Gradient Based Algorithm
NSGA	Non-dominated Sorting Genetic Algorithm
NSESA	Non-dominated Sorting Evolution Strategy Algorithm
PESTRA	Pareto Evolution STRAtegy
MDESTRA	Multi Direction Evolution STRAtegy

Table 2.1: Acronyms for the algorithm's names.

2.2.1 Pareto Gradient Based Algorithms (PGBA)

One possibility is thus to approximate the *POF* via deterministic search; a standard gradient based algorithm can be run for several individuals with one of the scalarised formulation previously presented with different weights or different threshold values. The logical sequence of operations of such an algorithm is shown in table 2.2. Though being the simplest and most immediate strategy the risk of being trapped in local minima is remarkable. PGBA can hardly be used as a global POF approximation strategy but it may be used as a second part of an hybrid stochastic-deterministic and global-local strategy (see section 2.3.5).

2.2.2 Non-dominated Sorting Evolution Strategy Algorithm (NSESA)

The algorithm is derived from Shrinivas and Deb's NSGA [42, 8, 9, 11, 25] from the point of view of the general structure. The differences are mainly

Start
1-Build a random starting population of npop individuals
2-Compute all npop *times* M starting objectives values
3-Build a uniform distribution of npop *times* M weights
4-Build scalarised functions with different weights
5-Run npop deterministic search with different scalarised functions
end

Table 2.2: PGBA sequence of operations.

in the fitness assignment strategy and in the evolutionary operators which are generation, mutation and annealing of a (1+1)ES algo [1]. Often the use of GA-based strategies is computationally unaffordable or highly unpractical from an industrial point of view. Therefore we have decided to adopt a (1+1)ES algorithm as the optimization engine of the multiobjective strategy because, in our experience, it is robust and gives good convergence even when few individuals are considered. It should be noted that generation, mutation and annealing steps are implemented in parallel; this is possible because in our implementation individuals do not interact each other during the whole process, apart from the steps of Pareto ranking and fitness evaluation.
As it can be seen from the flow-chart in the **first step** of the algorithm we generate, in a random way, an initial population of individuals in the design domain search space. In the **second step** we classify individuals into Pareto sets. This means that we first apply the dominance region criterion to the whole population and we thus collect all non-dominated individuals in the first front, then we remove these individuals from the population and we apply the same criterion in order to obtain the second front and so on. The **third step** consists of assigning a fitness value to each individual; two criteria must be followed in this step:

1. forcing convergence to the Pareto optimal set
2. forcing diversity among solutions

In order to do this the fitness value for each individual has to depend on

the Pareto set which the individual belongs to and a sharing procedure is to be implemented in order to favor isolated solution and to thus avoid clustering of solutions. The schematic effect of sharing procedures may be viewed in a schematic way in figure 2.2.
When implementing a fitness sharing procedure, diversity of individuals in either design space or objective space can be considered. Moreover solutions with strong diversity in shape can be characterised by weak diversity in objective value (the opposite as well). Both procedures can lead to results useful for industrial designer who is interested in both shape and performance diversity of optimal solutions. This is why a sharing procedure in only one of the two spaces cannot guarantee a satisfactory approximation of the Pareto optimal front in the other space (see [cjp6]). Once the current population has been divided into Pareto sets, all relative distances among individuals in each front can are evaluated in both spaces. A bigger fitness value is assigned to isolated individuals either in design or in objective space, while a smaller fitness value is assigned to close individuals reducing their survival probability. More into details, we at first consider the first front and we assign a dummy fitness $dfit_1$ to the individuals as follows:

$$dfit_1 = \|U - cw^1\|_2^{-1} \tag{2.1}$$

where cw^1 is the center of weight of the first front. As previously mentioned, in order to build the sharing procedure we then evaluate the normalized average distances $d_{i,j}$ among elements in both design and objectives domain as follows, ($dx_{i,j}$ or $df_{i,j}$ when shape or performance diversity has to be enhanced respectively):

$$dx_{ij}^k = \sqrt{\sum_{p=1}^{N} \frac{(x_{i,p}^k - x_{j,p}^k)^2}{(xmax_p^k - xmin_p^k)^2}} \qquad i,j = 1 : nset^k \tag{2.2}$$

$$df_{ij}^k = \sqrt{\sum_{q=1}^{M} \frac{(f_{i,q}^k - f_{j,q}^k)^2}{(fmax_q^k - fmin_q^k)^2}} \qquad i,j = 1 : nset^k \tag{2.3}$$

where k stands for the *k-th* front nset is the number of individuals in the set, $[x]^k$ the set of individual values (a nset×N matrix), $[f]^k$ the set of

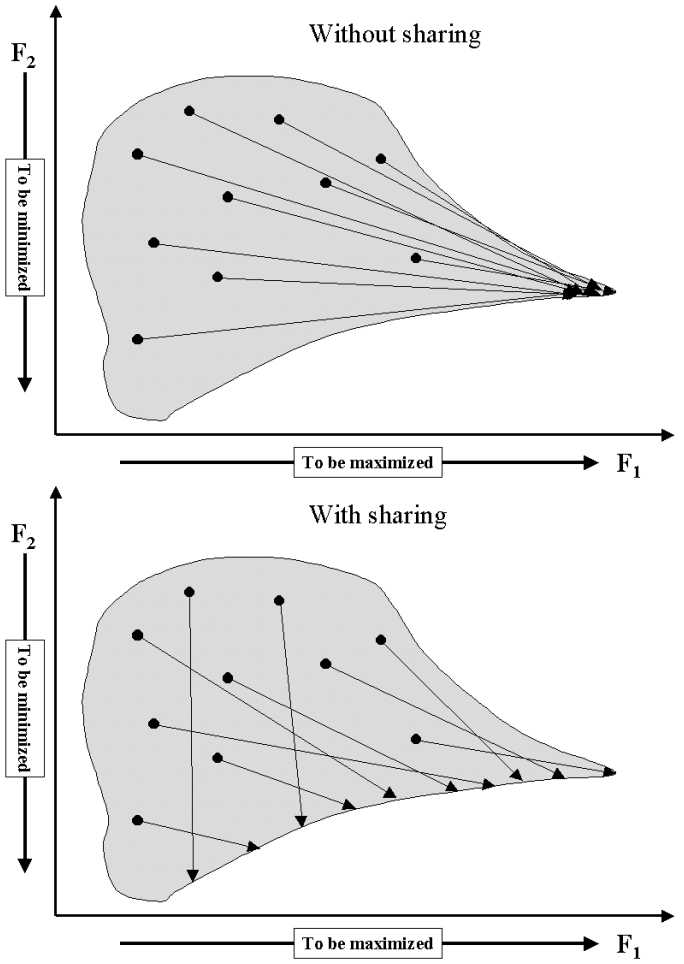

Figure 2.2: Schematic view of the effect of sharing procedures on solutions diversity.

objective values (a nset×M matrix). Moreover $xmax_p^k$ and $xmin_p^k$ are maximum and minimum values of the *p-th* columns of the $[x]^k$ matrix respectively, while $fmax_p^k$ and $fmin_p^k$ are maximum and minimum values of the *p-th* columns of the $[f]^k$ matrix respectively. Afterwards we evaluate for each individual couple in the front the following value:

$$sh_{i,j}^k = \begin{cases} 1 - (\frac{d_{i,j}^k}{\sigma^k})^2 & \text{if } d_{i,j}^k < \sigma^k \\ 0 & \text{else} \end{cases} \quad i,j = 1 : nset \tag{2.4}$$

where $d_{i,j}^k$ can assume one of the previous values ($dx_{i,j}^k$ or $df_{i,j}^k$), and where σ^k can assume one of the following values when shape or performances diversity has to be enhanced respectively.

$$\sigma_x^k = \frac{1}{nset^k - 1}\sqrt{\sum_{p=1}^{N}(xmax_p^k - xmin_p^k)^2} \tag{2.5}$$

$$\sigma_f^k = \frac{1}{nset^k - 1}\sqrt{\sum_{q=1}^{M}(fmax_p^k - fmin_p^k)^2} \tag{2.6}$$

σ^k is the threshold value defining numerically if points are near or far away from each other (in one of the two domains). After this, the following parameter m_i^k measuring how the fitness of the i-th individual has to be reduced with respect to the dummy fitness $dfit^k$, is evaluated

$$m_i^k = \sum_{j=1}^{nset^k} sh_{i,j}^k \tag{2.7}$$

Finally the fitness value for the i-th individual is evaluated:

$$fit_i^k = \frac{dfit_i^k{}^k}{m_i} \qquad i = 1 : nset^k \tag{2.8}$$

Before moving to the k+1-th front a new dummy fitness $dfit_{k+1}$ has to be evaluated:

$$dfit^{k+1} = \min_{i=1:nset_k} fit_i^k - \|cw^{k+1} - cw^k\|_2^{-1} \tag{2.9}$$

where cw^k, cw^{k+1} are the center of weights of current and next front respectively. The procedure is repeated for all successive fronts. We point out that convergence towards the front is always performed in the objective space while sharing procedures can be performed either in the design space or in the objective one.

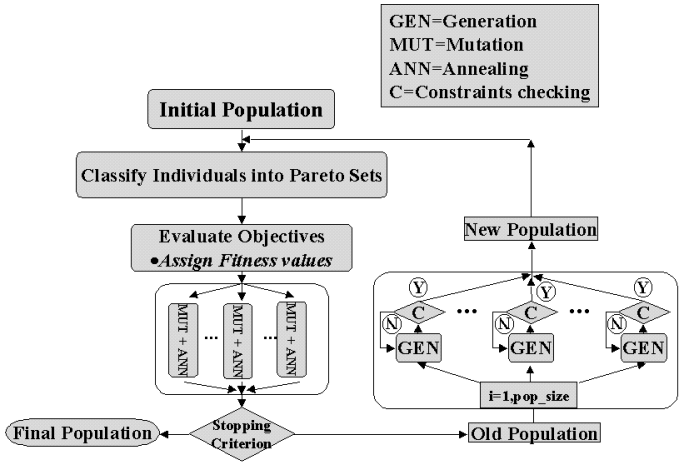

Figure 2.3: General flowchart of an NSESA algorithm: a zoom on fitness assignment is shown in figure 2.4.

2.2.3 Pareto Evolution Strategy Algorithm (PESTRA)

PESTRA is a very simple algorithm where a (1+1) ES is adopted in which a new design vector is accepted if it dominates in the Pareto sense the parent. Starting from an initial population of individuals that span the feasible region in a random way, the aforementioned criterion of optimization is applied to each individual; the results is a final population that gives a first approximation of the Pareto optimal front. The main advantage of the method is the reduced computational cost not in term of

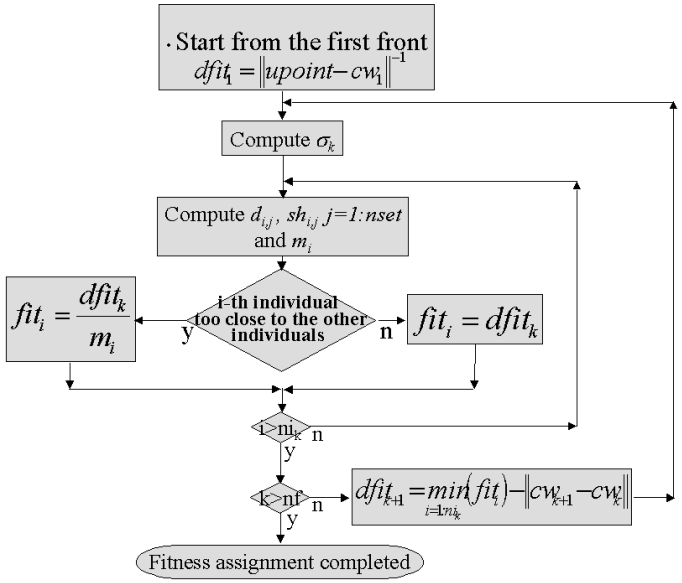

Figure 2.4: Flowchart of an NSESA fitness assignment.

number of objective function evaluation but in terms of algorithm complexity, since there is no need to sort the current population into Pareto sets at each iteration and then to assign a suitable fitness to the individuals of each set . On the other hand, individuals do not interact during evolution and therefore a clustering effect of solution could occur.

In figure 2.5 the simplified flow-chart of the algorithm is reported; it can be noted that each step of the procedure has been implemented in parallel. The major drawback of the algorithm is the lack of an algorithm forcing the spread of non-inferior solutions; as a consequence, they may cluster around a small subregion of the Pareto optimal front. To prevent this occurrence, a large number of individuals in the initial population is in order.

Start
1-Build a starting population of npop individuals
2-Build an uniform weight distribution of the unitary M-cube with npop values
3-Build npop scalar formulations using previously defined weight vectors
4-Run npop independent evolution strategy searches
Stop

Table 2.3: MDESTRA scheme.

2.2.4 Multi Directional Evolution Strategy Algorithm (MDESTRA)

Another very simple strategy is outlined in table 2.3. This algorithm is equal to PGBA in terms of multiple search direction building but deterministic search is substituted by stochastic one. This similarity will be fully exploited in order to compare deterministic search with stochastic one when the same scalarised formulations are considered. Moreover we have considered normalised weighted sum as an example but any scalar formulation with different weights or different threshold values may be considered taking into account what has been shown about limits and drawbacks of scalar formulations.

2.3 Performances measurements on analytical test cases: convergence and errors

Validation and performance measurement for evolutionary multiobjective optimisation algorithms is much more complex than the single-objective counterpart mainly because convergence is not anymore towards a point but towards the *POF* witch is a curve for 2 objective problems, a surface for three objective problems and an M-1 hyper-surface in an m-dimensional space for M objective problems; moreover even if the equation of all single objective is known ad simple it is not always easy to analytically compute the *POF* equation. This is why especially devoted

convergence indexes and error evaluation formulas are necessary . Here some solution to this problem are proposed and applied to validate algorithms. In order to do this several analytical test cases are available in literature presenting one or more of those pathological behaviour that have been presented; some more test cases have been developed, being especially devoted to test algorithms for multiobjective optimisation of electromagnetic devices.

2.3.1 Convergence

When convergence towards POF has to be represented, the following two convergence indexes can be evaluated for each iteration of the optimization process

$$\begin{cases} C_x(iter) = \frac{1}{npop} \sum_{i=1}^{npop} \sqrt{\sum_{j=1}^{N} (x_{ij}^{iter} - x_{ij}^{iter-1})^2} \\ C_f(iter) = \frac{1}{npop} \sum_{i=1}^{npop} \sqrt{\sum_{l=1}^{M} (f_{il}^{iter} - f_{il}^{iter-1})^2} \end{cases} \tag{2.10}$$

where x_{ij}^{iter} is the $j-th$ component of the $i-th$ individual of population at iteration iter while f_{il}^{iter} is the $l-th$ objective value for the $i-th$ individual at iteration $iter$; the first index represent convergence in the design space while the second one in the objective space. The first of the two monitors convergence towards POS while the second one monitors convergence towards POF.
Because of the relationship between POF and POS is complex and problem dependent, the relationship between the two convergence indexes is highly problem dependent and this is why both indexes have to be considered. Moreover from a designer practical point of view both design space and objective space convergence can give useful information on the solution quality. We point out that definitions 2.10 make sense only when individuals do not interact during evolution (with the exception of fitness value assignment); it is thus possible to identify each individual all along its evolution. Moreover the number of individuals must be constant during evolution. This is the case of all the strategies shown on the previous paragraph but not the case of several GA-based strategies where individuals interact each others and the number of individuals varies during evolution (NSGA as an example).

2.3.2 Approximation errors

The exact definition of approximation error in both design and objective spaces is possible only when the POF and POS equation are known and it is thus problem dependent; generally speaking, if the POF and POS equation can be put in the form:

$$\begin{cases} G(f_1, ..., f_M) = 0 \\ H(x_1, ..., x_N) = 0 \end{cases} \tag{2.11}$$

At each iteration iter of the optimiser the following errors both converging to zero when iter increases can be computed:

$$\begin{cases} error_{POF} = \sum_{i-1}^{npop} G(f_{1i}^k, ..., f_{m_i}^k) \\ error_{POS} = \sum_{i-1}^{npop} H(x_{1i}^k, ..., x_{n_i}^k) \end{cases} \tag{2.12}$$

where f_{ji}^k is the value of the j-th objective for i-th individual of population at iteration k and where $x_{i,j}^k$ is the value of the j-th component for the i-th individual. If POS and POF equations in this form are not available, an alternative error measurement have to e computed for each single case.

2.3.3 Cost *versus* random search

When dealing with non-deterministic strategies as all methodologies we are dealing with are, it is extremely important to check performances with respect to random search. In order to do this the following performance measurement has been developed. When the POF analytical equation is known, a strip of variable width ε can be considered around the POF see figure 2.13; ε can be considered a precision tolerance on the POF approximation. The number NOFC of objective function calls (the cost

of the optimization process) can be plotted versus ε when all individuals are inside the ε-width strip that is when the following holds:

$$d_i \leq \varepsilon \quad i = 1 : npop \tag{2.13}$$

where d_i is the minimum Euclidean distance between the point characterising the i-th individual in objective space and POF; npop is the number of individuals. NOFC(ε) can be compared to random search in an easy way because random search can be stopped when 2.13 holds and the total number of random trials can be compared to NOFC; this will be shown on an example. A schematic view of tolerance ε evaluation in POF approximation is shown in figure 2.6

2.3.4 Test cases

Several test cases have been recently collected and proposed in [10]. Some of them have been considered for testing algorithms and some more have been developed. Four test cases are presented here representing different difficulties for the multiobjective evolutionary optimiser.

Test Case 1

As a first example we present the following classical two variables - two objectives problem (Shaffer's 2D function) :

$$\begin{cases} \min\limits_{(x,y)\in\Re^2} F_1(x_1,x_2) = x_1^2 + x_2^2 \\ \min\limits_{(x,y)\in\Re^2} F_2(x_1,x_2) = (x_1 - \frac{\sqrt{2}}{2})^2 + (x_2 - \frac{\sqrt{2}}{2})^2 \end{cases} \tag{2.14}$$

The Pareto optimal front equations for this two-objective analytical problem are:

$$\begin{cases} F_1(x_1,x_2) + 1 - 2\sqrt{F_1(x_1,x_2)} - F_2(x_1,x_2) = 0 \\ x_1 = x_2 \quad (x_1,x_2) \in [0, \frac{\sqrt{2}}{2}] \times [0, \frac{\sqrt{2}}{2}] \end{cases} \tag{2.15}$$

In order to compute the error between current population and Pareto optimal front in both design and objective spaces, the following two distances df and dx has been defined in the objective space and in the design space respectively.

$$df(iter) = \frac{1}{npop} \sum_{1}^{npop} |1 + f_{1i}^{iter} - 2\sqrt{f_{1i}^{iter}} - f_{2i}^{iter}| \tag{2.16}$$

$$dx(iter) = \sum_{i=1}^{npop} |x_{1i}^{iter} - x_{2i}^{iter}| \tag{2.17}$$

where $(x_{1i}, x_{2i})^{iter}$ and $(f_{1i}, f_{2i})^{iter}$ are the current population i-th individual and its objective values at iteration iter respectively.

Test Case 2

A second test case with three objectives and two design variables can be easily built from the previous one and it seems to be particularly suited for an investigation on concepts like scale effect in computational cost when the number of objective increases; it is defined as follows:

$$\begin{cases} \min\limits_{(x,y)\in\Re^2} F_1(x_1,x_2) = x_1^2 + x_2^2 \\ \min\limits_{(x,y)\in\Re^2} F_2(x_1,x_2) = (x_1 - \frac{\sqrt{2}}{2})^2 + (x_2 - \frac{\sqrt{2}}{2})^2 \\ \min\limits_{(x,y)\in\Re^2} F_3(x_1,x_2) = (x_1)^2 + (x_2 - \frac{\sqrt{2}}{2})^2 \end{cases} \tag{2.18}$$

The equations of the POF in search space are the following:

$$0 < x_1 < \frac{\sqrt{2}}{2} \quad , \quad x_1 < x_2 < \frac{\sqrt{2}}{2} \tag{2.19}$$

Test Case 3

A very useful test problem set with different difficulties in introduced in [10, 25, 8] and has been considered for testing the developed strategies; here results for one of them are shown, namely the Deb's DTZ3 problem; the problem,giving rise to a non-connected Pareto front, can be defined as follows:

$$\begin{cases} \min\limits_{(x_1,x_2)\in[0,1]\times[0,1]}(f_1,f_2) \\ f_1(x_1) = x_1 \\ f_2(x_1,x_2) = 1 + 9x_2 - \sqrt{x_1(1+9x_2)} - x_1\sin(10\pi x_1) \end{cases} \tag{2.20}$$

The analytical POF can be determined as the nondominated part of the curve defined by the following equation:

$$f_2 - 1 + \sqrt{f_1} + f_1\sin(10\pi f_1) = 0 \tag{2.21}$$

In order to quantify the POF approximation error all along the evolution, given the i-th individual at niter-th iteration, the following two expressions have been used in design space and in objective space, respectively,:

$$\begin{cases} errorx_i^{iter} = x_{2i}^{iter} \\ errorf_i^{iter} = f_{2i}^{iter} - 1 + \sqrt{f_{1i}^{iter}} + f_{1i}^{iter}\sin(10\pi f_{1i}^{iter}) = 0 \end{cases} \tag{2.22}$$

Test Case 4

This last case is particularly interesting because the POF is non continuous and multimodal but the two single objective function seems to be innocuous as can be seen from 2.7; the problem is the following:

$$\begin{cases} \min\limits_{(x_1,x_2)\in[-6,6]\times[-6,6]}(f_1,f_2) \\ f_1(x_1,x_2) = k_1\sum_{i=1}^{2}(x_i+0.5)^4 - 30x_i^2 - 20x_i \\ f_2(x_1,x_2) = k_2(10 - x_1^3 - x_2^2) \end{cases} \tag{2.23}$$

despite the simplicity of polynomial objective functions the POF and POS analytical equation are not available and no approximation errors can be evaluated.

The assignment of very different magnitude order values to k_1 and k_2 may be used to simulate incommensurability of objectives in real-life cases.

2.3.5 Deterministic search (PGBA) versus stochastic search (MDESTRA) and hybrid strategies

As example let us consider a comparison of results obtained with PGBA and those obtained with a MDESTRA on two different test cases, a non-multimodal (no local fronts) one (test problem 1) and a multimodal (with local fronts) one (test problem 4). When considering results on test problem 1, the quality of approximation is bigger and the speed of convergence is higher than the case of stochastic search (see column 1 in table 2.4). The behaviour of PGBA is similar to single-objective optimization problems where deterministic methods overcome stochastic ones when no local minima are present. But when a multimodal problem is tackled the deterministic method is trapped in local POF and the behaviour is similar to local minima traps in single-objective optimization. Let us now consider a comparison between hybrid search and full stochastic search. In order to compare comparable results the same number of starting points have been considered (20). The number of objective function calls is much higher in the case of stochastic search and one may conclude that the use of deterministic search for POF sampling has a similar behaviour to the use of deterministic search for single objective optimization from the local front traps point of view. In analogy to hybrid methods in single-objective optimization, stochastic search can be used as local search in an hybrid strategy where a deterministic algorithm is used at the end in order to improve quality of solution. An example of such a strategy can be viewed in figure 2.8; the cost in terms of objective function calls is much reduced (see second column in table 2.4) and the quality of solution is much better in terms of both diversity of solutions and convergence towards the POF.

	Test problem 1	Test problem 4
Deterministic	197	237
Stochastic	2840	7680
Hybrid	-	2243

Table 2.4: Comparison of Cost in terms of objective function calls number for three different strategies on two test problems.

2.3.6 Tests on PESTRA

An example of the story of a PESTRA optimisation run on test problem 1 is shown in figure 2.9 in design space and in figure 2.10 for objective space. For comparison the analitycal front in the two domains is also shown. This kind of visualisation gives quite a good and immediate understanding of the optimization process but it is not at all quantitative. As can be seen the optimiser is able to reach the POF and POS regions with few big jumps according to the typical behavior of evolution strategy algorithms. The main drawback of PESTRA is the non uniform distribution of solutions on the POF ; this is because no interaction among individuals happens during optimisation and each evolution is independent from all the others.

Some much more quantitative information on optimization run can be seen in figure 2.11 where convergence index C_x and C_f are plotted against progressive number of iteration. As can be seen both convergence indexes decrease towards zero with typical stochastic strategies behaviour and a quick drop of both C_f and C_x happens in the first iterations, moreover after the 200-th iteration C_f is stable below 10^{-6} while stabilisation of C_x is slower. When considering the approximation errors d_x and d_f (figure 2.12) the typical behaviour of stochastic methods is evident in the stairs-like plot decreasing of both errors, moreover after the 400-th iteration df reduces below 10^{-5} and dx states below 10^{-3}.

As previously mentioned the most important performance test when dealing with stochastic optimization is the comparison to random search. An example of such a comparison is shown in figure 2.13 for PESTRA method where ε has been normalised with respect to the maximum distance between two points in the objective domain search space. As can be seen the optimization strategy overcomes random sampling when ε takes significant values for practical application (10^{-2},10^{-3}) of more than one magnitude order in the number of objective function calls. This is quite an interesting results because it involves the concept of tolerance that is typical of a design environment. Let us now consider a PESTRA twenty individuals solution of test problem 3; individuals are distributed along three of the five branches the POF is composed of. As previously mentioned when introducing discontinuous POF individuals tend to converge towards one of the branch of the front; as for all optimization on test problems the starting population was chosen in a random way in the design space. As previously explained quantitative information on quality of approximation is given in figure 2.15 where both convergence indexes and approximation errors are plotted in logarithmic scale. The decrease of both performance parameters is remarkable.

2.3.7 Tests on NSESA: comparison to PESTRA and scaling effect

In order to compare NSESA with PESTRA the latter is tested at first on test problem 1. A qualitative representation of solution is given in figure 2.16 while quantitative information on both convergence and approximation errors are given in figures 2.18 and 2.19. As can be seen the first important difference is that NSESA is able to control POF sampling points distribution; a second important difference is the behavior of convergence errors. Due to the working principle of NSESA both errors plots are highly oscillatory around a fast decreasing mean value. Another interesting consequences of the increased complexity of NSESA with respect to PESTRA is that objective space convergence indexes behavior is different from design space one; the latter one present a fast decrease in the first iterations while the latter is highly oscillating at the beginning, being apparently increasing. A typical problem in stochastic optimisation is the increasing cost and difficulty in solving an optimisation problem as the number of design variables or design objective increases (scaling effect); test problem 2 is particularly suited to the aim of evaluating the

scaling effect with respect to the number of objective functions. The increased dimensionality of both POF and POS implies a bigger number of individuals in view of a satisfactory sampling. An example of this can be seen in figure 2.20. and where a 50 individual solution of test problem 2 is shown. The POF is a surface whose boundaries are dotted in figure 2.20. In order both test problem 1 and test problem 2 to have the same sampling distance between solutions, it is evident that the number of individuals for test problem 1 should be bigger than the number of individuals for test problem 2. The behavior of convergence index for NSESA algorithm is different from the Pareto ESTRA one shown for the previous test case. Due to the different working principle the current population convergence for NSESA oscillated around a deeply decreasing mean value as can be seen in figure 2.17 where the log of C_f is plotted for a solution of test problem 2. If the optimisation cost is thus highly affected by the scaling effect due to increased objectives number, this is not for convergence index; figure 2.17 shows that the number of iteration required for convergence does not increase significantly. A slower convergence speed would appear in case of a design variable number increase but this would be analogous to the scaling effect for single-objective optimisation and we then refer to literature for this.

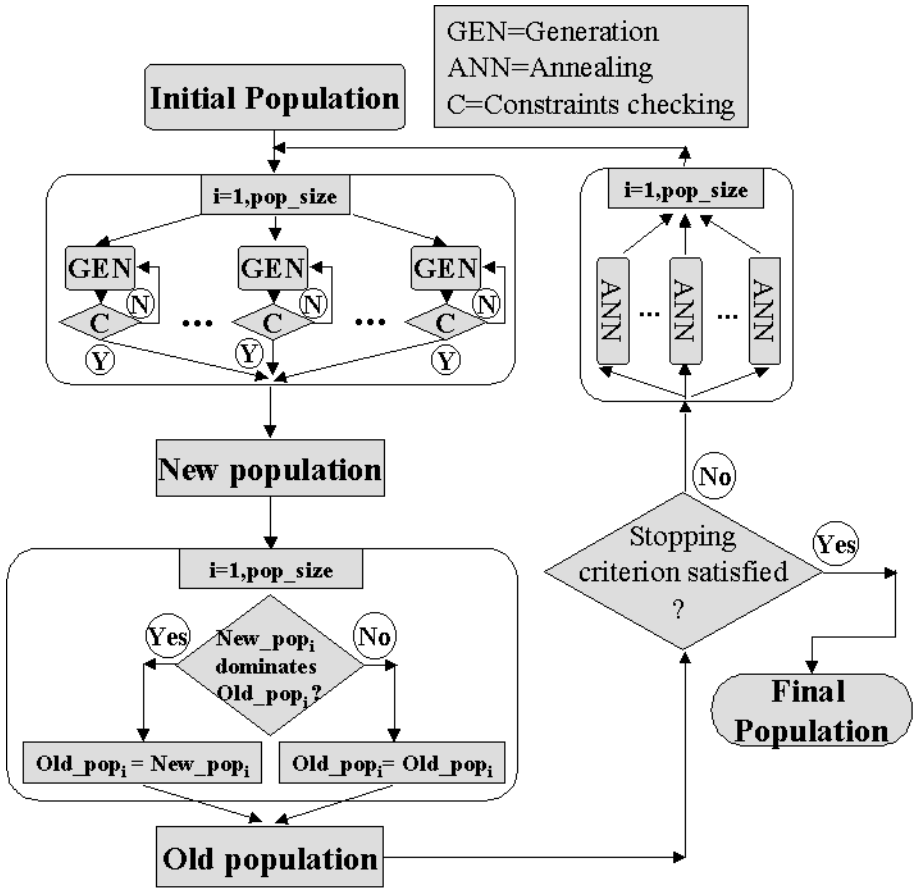

Figure 2.5: General flowchart of PESTRA algorithm.

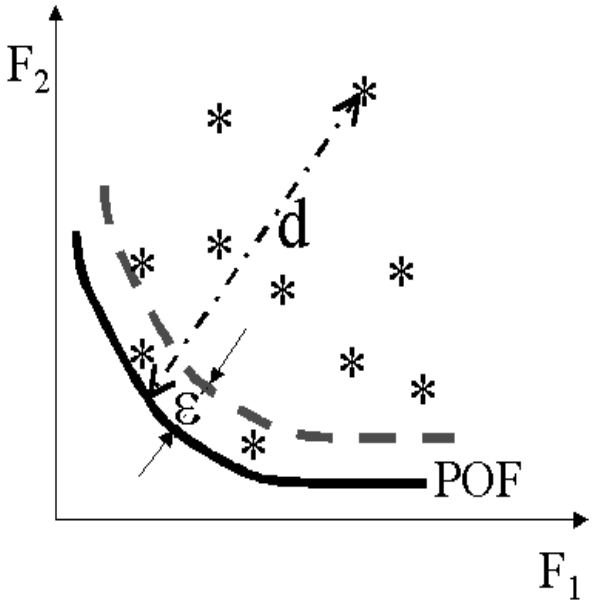

Figure 2.6: Schematic view of ε definition and distance from the POF measurement.

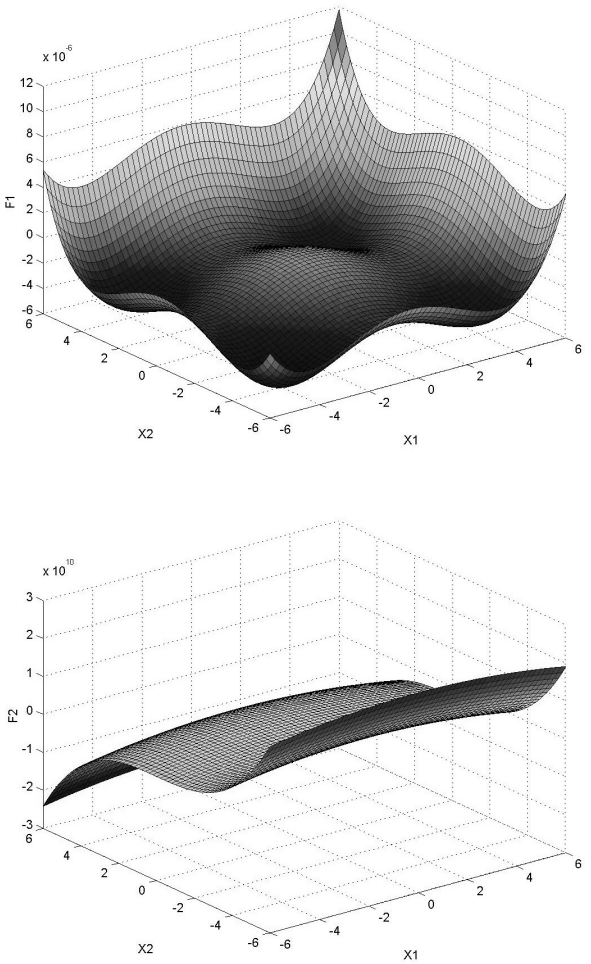

Figure 2.7: Objective functions surfaces for test problem 4.

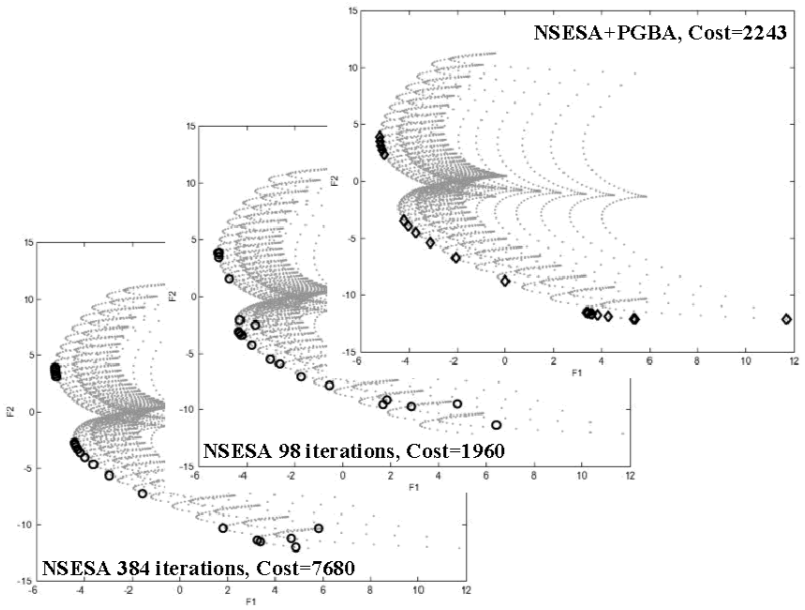

Figure 2.8: 20 individuals solutions comparison: stochastic search up to full convergence, first part of hybrid strategy and full hybrid strategy on two test problems.

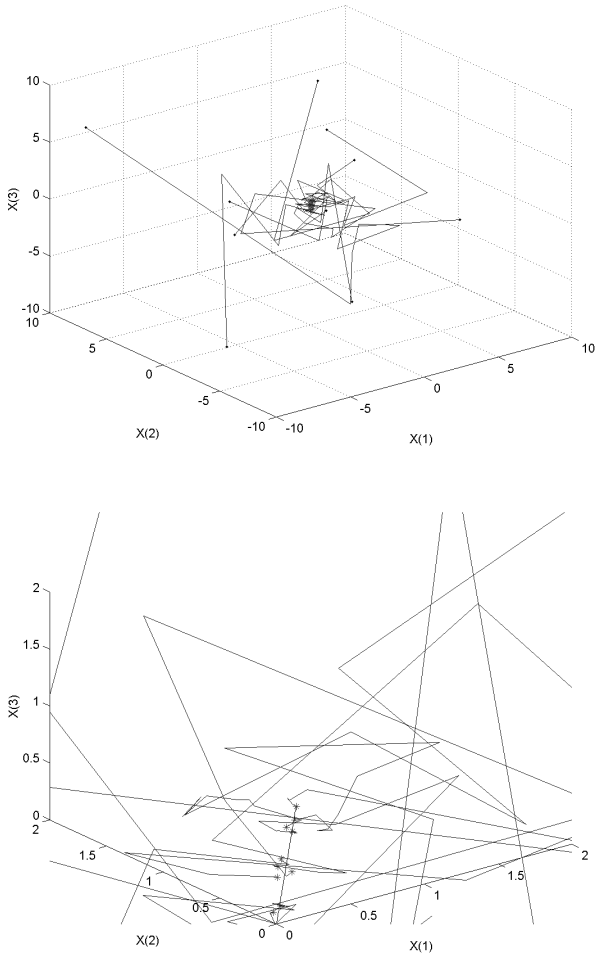

Figure 2.9: Example of a Pareto ESTRA optimization story on test problem 1 in design space (top: global view, bottom: zoom).

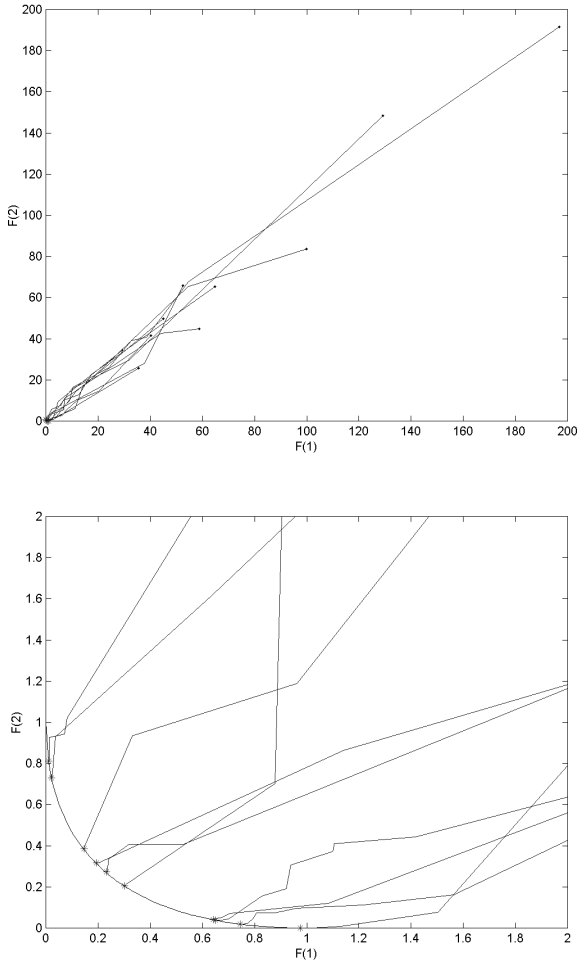

Figure 2.10: Example of a Pareto ESTRA optimization story on test problem 1 in objective space (top: global view, bottom: zoom).

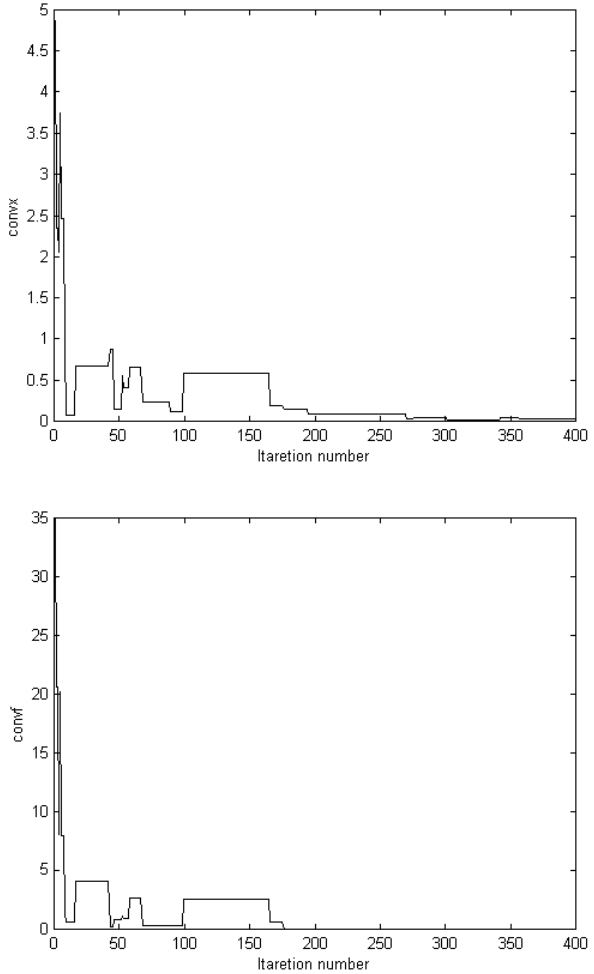

Figure 2.11: Pareto ESTRA convergence indexes for test problem 1 (design and objective domains respectively).

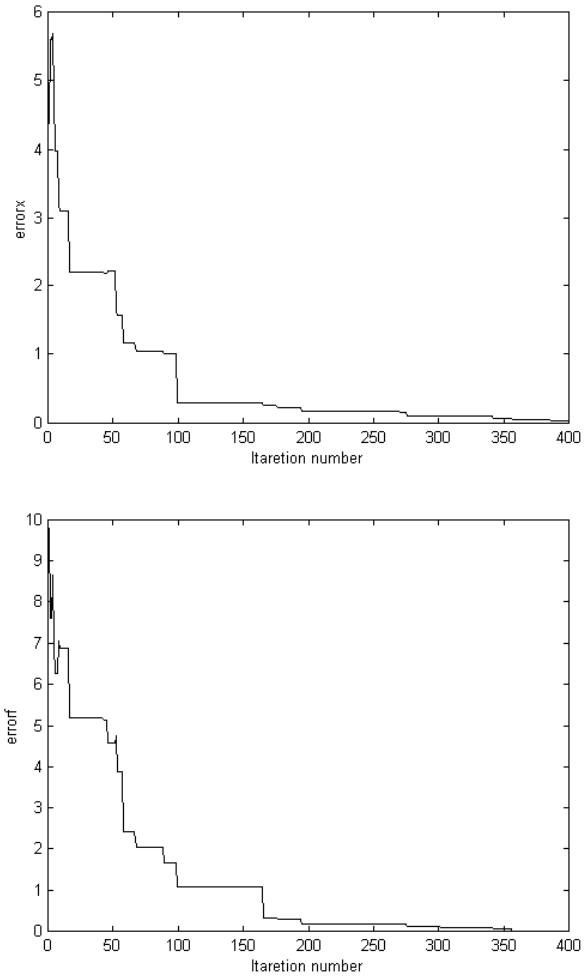

Figure 2.12: Pareto ESTRA approximation errors for test problem 1 (design and objective domains respectively).

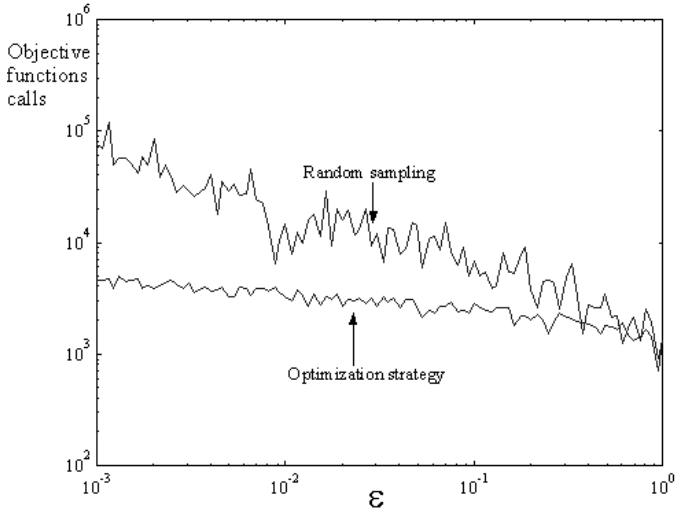

Figure 2.13: Pareto ESTRA *vs* random sampling for test problem 1: NOFC(ε).

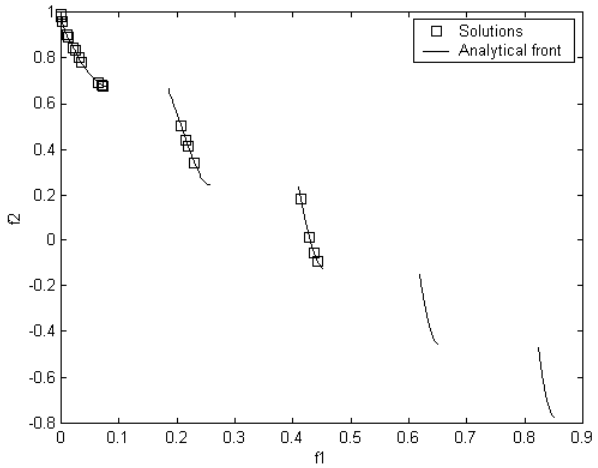

Figure 2.14: Pareto ESTRA solution for test problem 3.

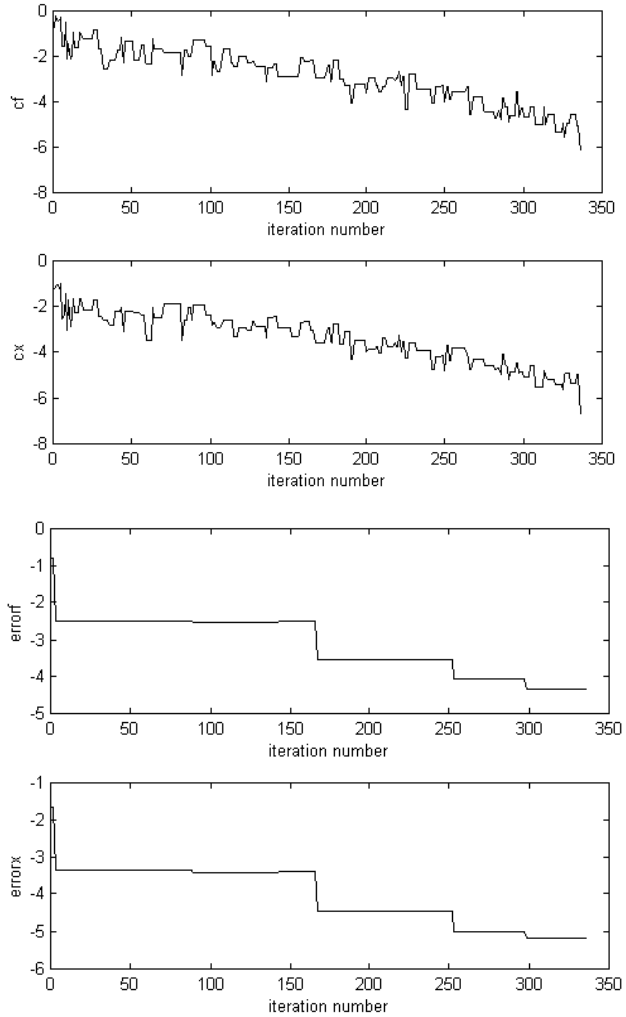

Figure 2.15: Pareto ESTRA solution for test problem 3: convergence indexes and approximation errors in design and objective domain.

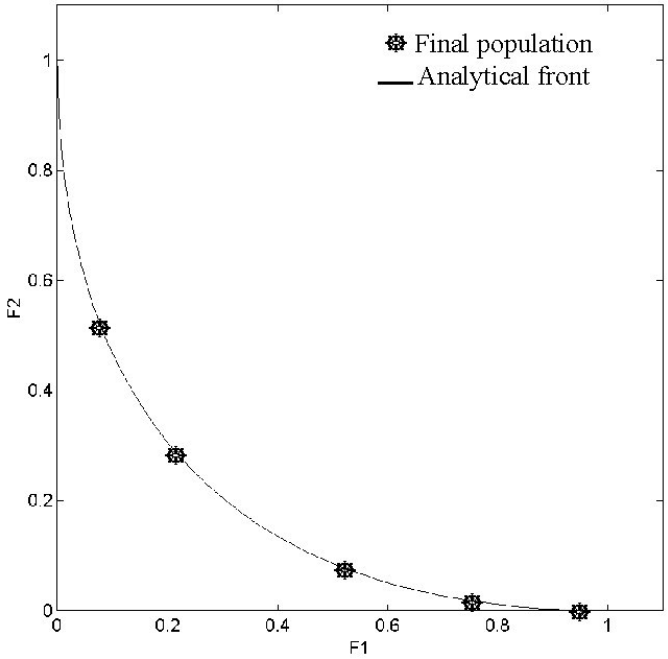

Figure 2.16: 5 individuals solution on Shaffer's problem with NSESA.

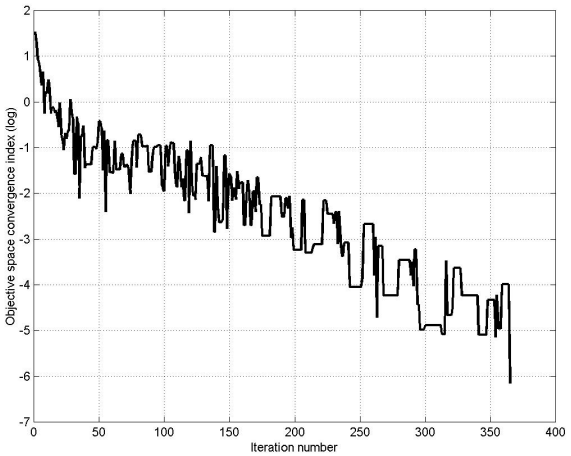

Figure 2.17: Design space convergence index for test in figure 2.20.

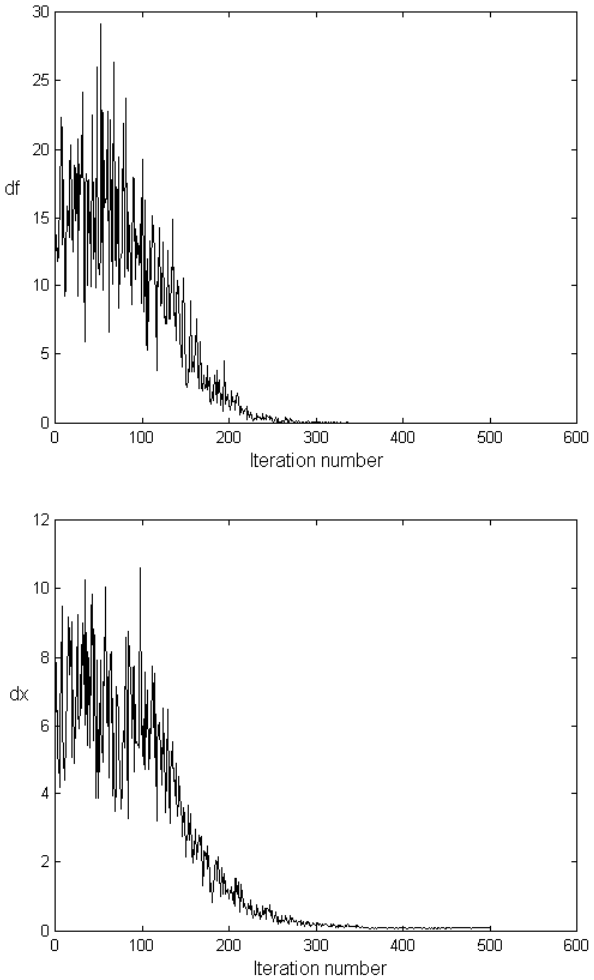

Figure 2.18: Design and objective domain errors for the NSESA 5 individual solution.

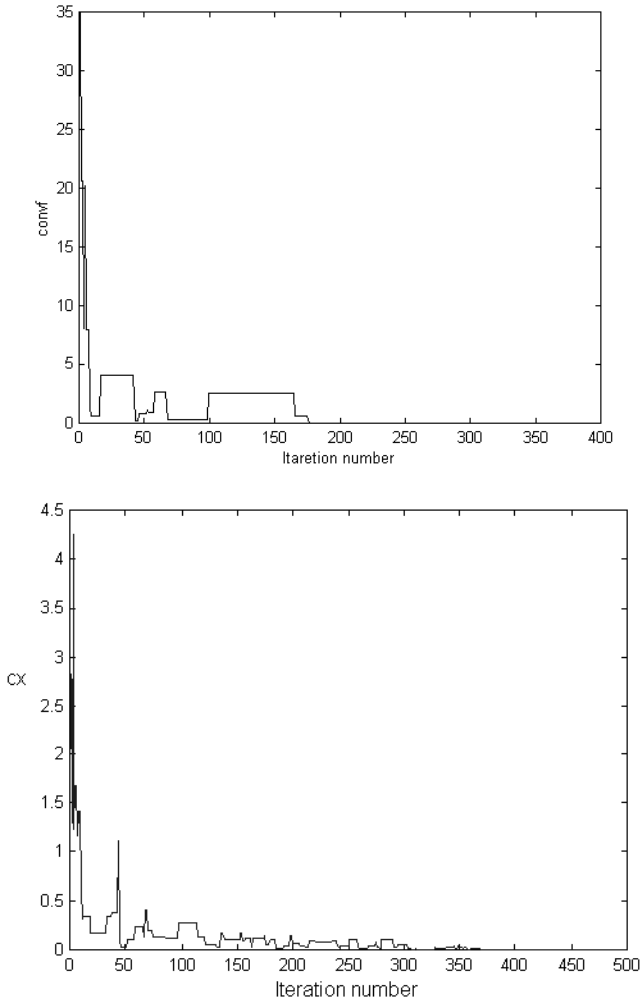

Figure 2.19: Design and objectives domain convergence indexes for the NSESA 5 individual solution

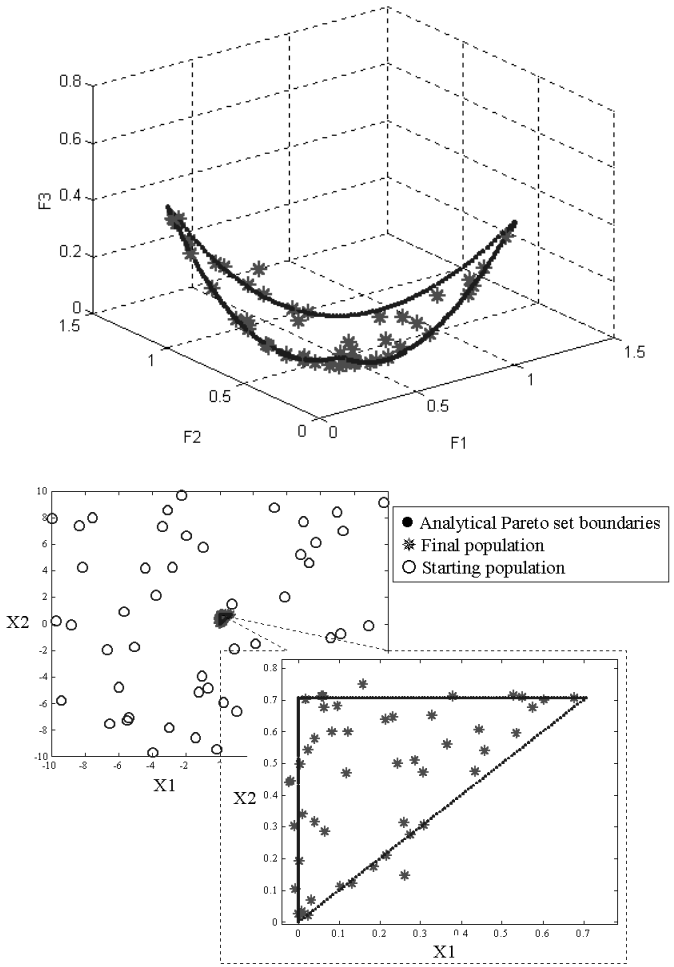

Figure 2.20: A 50 individuals NSESA solution of test problem 2 in design space and objective space.

Part II

Tests and Industrial Applications

Chapter 3

Semi-analytical electromagnetic test cases

3.1 Introduction

As a link between analytical test cases that have been presented and discussed in the previous chapter and real-life numerical test cases that will be shown in next chapter, this chapter is devoted to the discussion of two semi-numerical cases, that is simple electromagnetic problems with a closed form expression available for objective functions [cjp2].

Tackling such problems with the strategies shown in the previous chapter is a very useful exercise because the objective computation time is very low and several test can be computed for the tuning and comparison of strategies. Although very simple the two multiobjective shape optimization problems presented in this chapter share with real-life problems some common features and difficulties such as incommensurability of objectives and non-trivial POF shapes.

At first a multiobjective problem is considered on Brook's solenoid, which is maybe the simplest electromagnetic device but which gives rice to non-trivial POF shape. After that an electrostatic micromotor is considered where a multiobjective design problem gives a fully non-convex POF [cjp10],[cjp12].

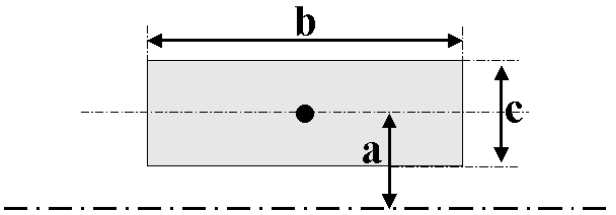

Figure 3.1: Cross section of the solenoid and design variables.

3.2 Shape design of an air-cored solenoid

Brook's solenoid is a classical benchmark in electromagnetic single-objective optimization, due to its simplicity and due to the availability of closed formulas for computing objective. A multiobjective shape optimization problem of a coreless solenoid of rectangular cross-section b × c and mean radius a is tackled (see figure 3.1)[cjp11].

3.2.1 The model and Optimization Problem

If current is supposed to be uniformly distributed over the cross-section, given the geometry of the solenoid and the number N of turns, the induc-

tance L [mH] can be approximated by the following formula :

$$L = \frac{31.49 \times \dfrac{a^2 N^2}{b}}{9 + 6\dfrac{a}{b} + 10\dfrac{c}{b}} \tag{3.1}$$

The multiobjective design problem can be cast in these terms: maximize inductance L(a,b,c) and minimize volume V(a,b,c) for given length k_1=10 m and cross section $k_2 = 10^{-6} m^2$ of the current carrying wire. Due to constraints, two variables only, e.g. a and b, can be considered; finally functions L and V become

$$\begin{cases} F_1 = \dfrac{31.49\dfrac{k_1^2}{4 * \pi^2 b}}{9 + 6\dfrac{a}{b} + 5\dfrac{k_1 k_2}{\pi a b^2}} \\ \\ F_2 = \dfrac{\pi a^2 b}{4} + \dfrac{k_1^2 k_2^2}{4\pi a^2 b} + \dfrac{k_1 k_2}{2} \end{cases} \tag{3.2}$$

respectively. Now the problem reads: maximise $F_1(a, b)$ and minimise $F_2(a, b)$, subject to:

$$a > \sqrt{\frac{k_1 k_2}{4\pi b}} \tag{3.3}$$

and a set of bilateral bounds ensuring the geometrical congruency of the model. Despite the simplicity of formulas for both objective functions, the multiobjective optimization problem is not trivial and cannot be tackled analitically. The two objective functions are shown in figure 3.2.

3.2.2 Discussion and results

Although the maximum region for F_1 and the minimum region for F_2 seems to be coincident, the addition of constraint makes the problem truly multiobjective. Nevertheless from a physical point of view the problem is weakly multiobjective because the Pareto optimal front lies in a thin region poorly sensitive with respect to volume variations (see figure 3.2). For the same reason the Pareto optimal front exhibits an attraction point for solutions located in the lower right corner of design domain space. This gives rise to numerical difficulties in the Pareto front approximation, which is why the problem has been chosen as case study. This can be seen in a clear and immediate way from the search space sampling in figure 3.3. In particular the Pareto optimal front lies in a thin region in the design domain search space. Two different 5-individual solutions obtained with NSESA are shown with enhanced diversity in design domain and in objective domain (figure 3.4). The starting population is always randomly generated and the number of individuals has been set to five in order to simulate the case of an expensive FEM objective function evaluation where a big population is computationally unaffordable. In both cases the solutions lie on the optimal Pareto front and distribute themselves in the front. The effectiveness of either one or the other sharing strategy is problem dependent. This is why in the considered problem both strategies seem to be equivalent as concern solutions diversity.

The history of both convergence indexes c_x and c_f are plotted in figures 3.5 for the firs of the two runs shown in figure 3.4 . After the 300th iteration both values are stable below 10^{-3}, clearly showing the method's stability. The design domain index decrease is quicker although both values oscillate around a decreasing mean value. The behavior is similar to the analytical test cases.

3.3 Shape design of an electrostatic micromotor

The design of micro-electromechanical devices is a remarkable chapter of electromagnetic devices design because special computational tools are to be developed, being specifically devoted to micro-scale effects. We do not go into deeper detail here and we only consider a simple model of an electrostatic micromotor.

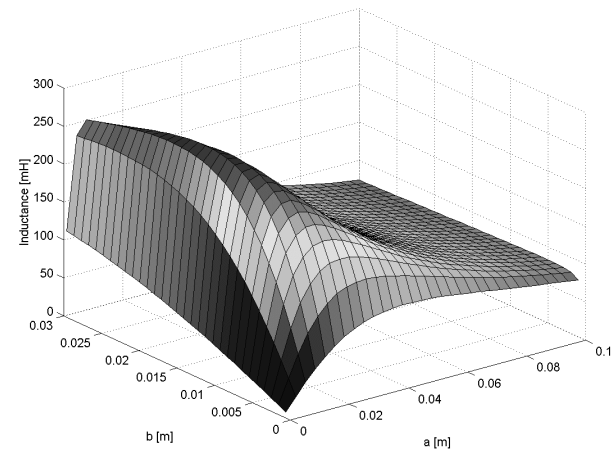

Figure 3.2: Objective function surfaces for the solenoid test case: Inductance L [mH] and volume $[m^3]$.

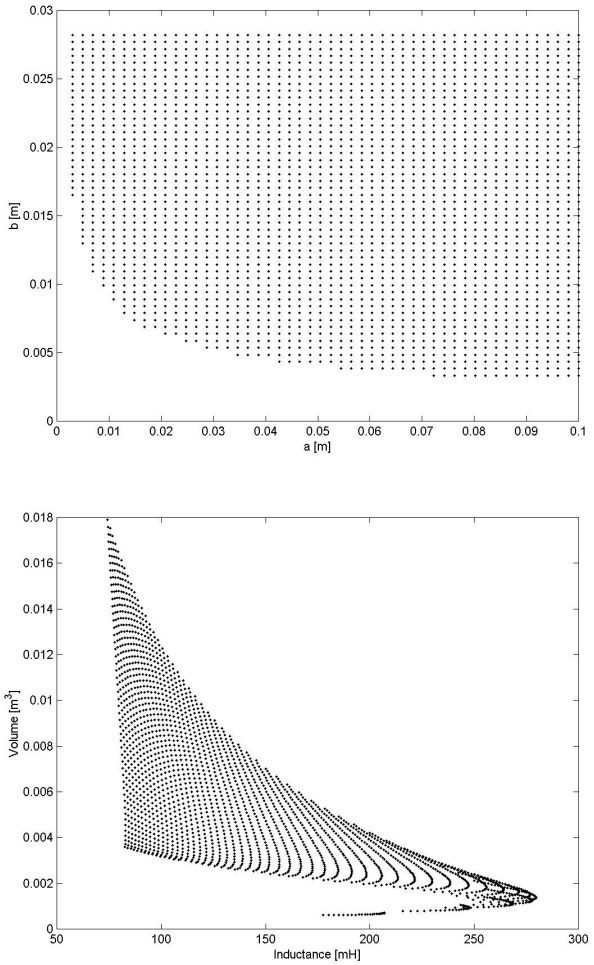

Figure 3.3: Exhaustive sampling of search spaces in design and objective domain for the solenoid problem.

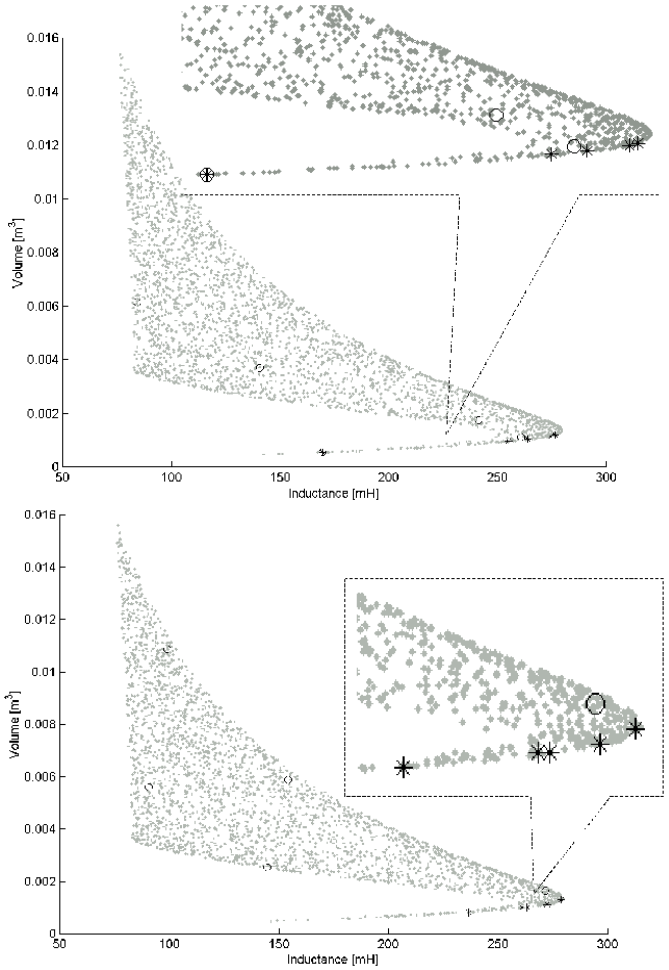

Figure 3.4: 5 individual solutions with enhanced diversity in objective space od resign space. Starting (∘), final (∗) population and exhaustive sampling (·).

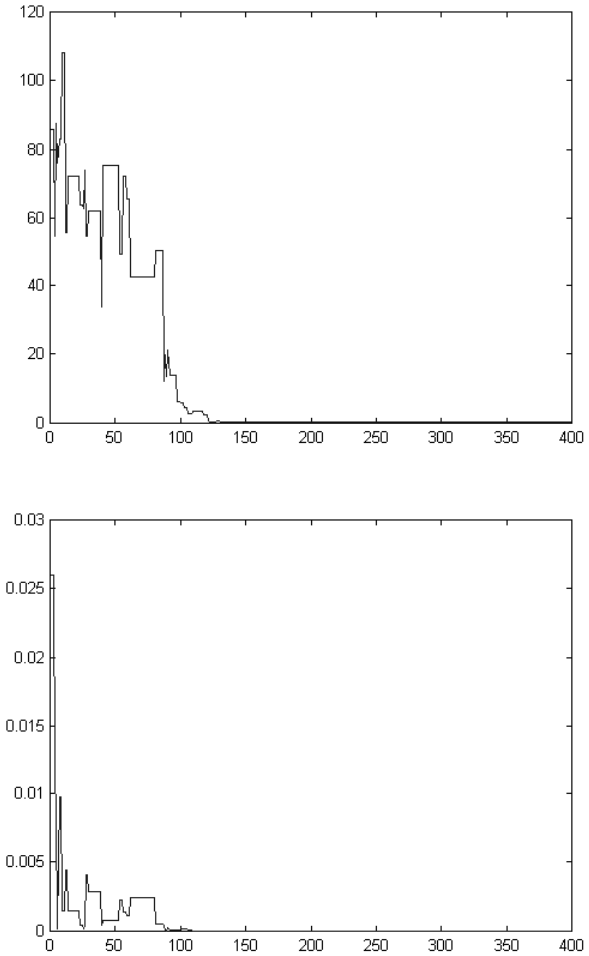

Figure 3.5: Convergence indexes in design domain and objective domain for run in figure 3.4, left.

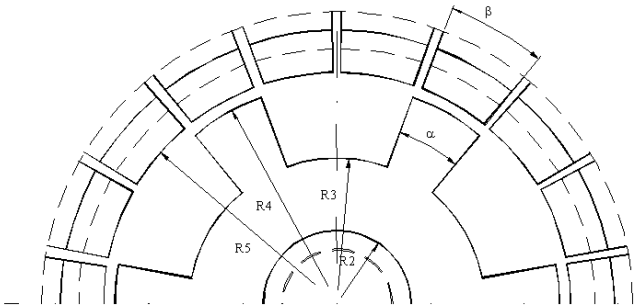

Figure 3.6: Cross section of the micromotor.

When dealing with design of such a device, several models can be taken into account with different degree of accuracy, starting from a simple circuital model to a full electostatic field computation via FEM. We consider here a non-trivial circuital model that gives close form expressions for equivalent capacitances and torque. A detailed analysis of electrostatic micromotors is out of the scopes of this thesis .

3.3.1 The model and Optimization Problem

A variable-capacitance rotating microactuator with radial field is considered. A simplified scheme of the geometry of the device is shown in figure 3.6. The device, etched on a polySilicon structure, is characterized by 24 or 30 stator electrodes (N_S) and 16 or 10 rotor teeth (N_R), respectively (3/2 geometry or 3/1 geometry). For a prototype configuration, the radial dimensions [μm] of the device are: R2=22, R3=40, R4=60, R5=63. Referring to figure 3.6, denoting $x_1 = \alpha$ and $x_2 = \beta$, we switch on one phase of the 3-phase system of square voltages of amplitude equal to V = 100 V and consider the equivalent capacitance $C_{eq}(\varphi, x_1, x_2)$ where φ is the rotor angle. In order to build objective function expressions different capacitances and torque formulas are to be computed in the following way.

The basic formula for computing both no-load commutation torque Γ_0 and static torque Γ_s is

$$\Gamma(\varphi, x_1, x_2) = \frac{1}{2} V^2 \frac{\partial C_{eq}(\varphi, x_1, x_2)}{\partial \varphi} \tag{3.4}$$

When Γ_s has to be computed, equation 3.4 becomes:

$$\Gamma_s(\varphi, x_1, x_2) = \frac{1}{4} V^2 N_R (C_{max}(x_1, x_2) - C_{min}(x_1, x_2)) \sin(N_R \varphi) \tag{3.5}$$

where $C_{max}(x_1, x_2)$ and $C_{min}(x_1, x_2)$ are the maximum and minimum capacity with respect to the rotor angle φ; N_R is the number of rotor teeth. When $C_{max}(x_1, x_2)$ is to be computed two different cases have to be considered (case A1 and case B1 in figure 3.7)

Case A1: $x_1 < x_2$

$$\begin{cases} C_{max} = \varepsilon_0 \varepsilon_r \alpha \dfrac{(2rp + rr)h}{2rr} & \text{where} \\ \alpha = 2 \arcsin(S \cos(\frac{x_1}{2}) - c \sin(\frac{x_1}{2})) \\ S = \frac{r_3}{rr} \sin(\frac{x_2}{2} - \frac{x_1}{2}) \\ C = -\sqrt{1 - S^2} \\ rp = \dfrac{r_2 \sin(\frac{x_1}{2})}{S \cos(\frac{x_1}{2}) - C \sin(\frac{x_1}{2})} \\ rr = \sqrt{r_2^2 + r_3^2 - 2 r_2 r_3 \cos(\frac{x_2}{2} - \frac{x_1}{2})} \end{cases} \tag{3.6}$$

where h is the micromotor's depth and the angle α is shown in figure 3.7

Case B1: $x_1 > x_2$

$$C_{max} = \varepsilon_0 \varepsilon_r h \frac{x_2 \dfrac{r_2 + r_3}{2(r_3 - r_2)} + \det(A_t)}{(r_3 - r_2)^2} \tag{3.7}$$

where

$$A_t = \begin{bmatrix} 1 & r_2\sin(\frac{x_1}{2}) & r_2\cos(\frac{x_1}{2}) \\ 1 & r_2\sin(\frac{x_2}{2}) & r_2\cos(\frac{x_2}{2}) \\ 1 & r_3\sin(\frac{x_2}{2}) & r_3\cos(\frac{x_2}{2}) \end{bmatrix}. \tag{3.8}$$

The first term in the brackets corresponds to the capacitance of the circular sector while the second one is an approximation of the capacitance of the two side "triangles" (see figure 3.7); an alternative approximated formula can be the following one where an equivalent circular sector of angular size $\frac{(x_1+x_2)}{2}$:

$$C_{max} = \varepsilon_0\varepsilon_r h\frac{(x_1+x_2)(r_2+r_3)}{4(r_3-r_2)} \tag{3.9}$$

On the other hand, when C_min is to be computed the following two different cases have to be considered (case A2 and case B2 in figure 3.8)
Case A2: $x_2 < \frac{2\pi}{N_R} - x_1$

$$C_{max} = \varepsilon_0\varepsilon_r h\frac{x_2\frac{r_1+r_3}{2(r_3-r_1)} + \det(A_t)}{(r_3-r_1)^2} \tag{3.10}$$

where

$$A_t = \begin{bmatrix} 1 & r_1\sin(\frac{\pi}{N_R} - \frac{x_1}{2}) & r_1\cos(\frac{\pi}{N_R} - \frac{x_1}{2}) \\ 1 & r_1\sin(\frac{x_2}{2}) & r_1\cos(\frac{x_2}{2}) \\ 1 & r_3\sin(\frac{x_2}{2}) & r_3\cos(\frac{x_2}{2}) \end{bmatrix}. \tag{3.11}$$

or, as an alternative,

$$C_{max} = \varepsilon_0\varepsilon_r h\frac{\frac{\pi}{N_R}(x_1+x_2)(r_1+r_3)}{4(r_3-r_1)} \tag{3.12}$$

Case B2: $x_2 > \frac{2\pi}{N_R} - x_1$

$$\begin{cases} \alpha_A = \frac{2\pi}{N_R} - x_1 \\ \alpha_B = x_2 - \alpha_A \\ C^A_{min} = \varepsilon_0\varepsilon_r h\alpha_A\frac{r_1+r_3}{2(r_3-r_1)} \\ C^B_{min} = \varepsilon_0\varepsilon_r h\alpha_B\frac{r_2+r_3}{2(r_3-r_2)} \\ C_{min} = C^A_{min} + C^B_{min} \end{cases} \tag{3.13}$$

where two parallel connected capacitance are considered corresponding to the A and B circular sector in figure 3.8.
When Γ_0 has to be computed, equation 3.4 becomes:

$$\Gamma_0(x_1,x_2) = \frac{1}{2}V^2N_S\frac{C^A_{eq}(x_1,x_2) - C^B_{eq}(x_1,x_2)}{2\pi} \tag{3.14}$$

where $C^A_{eq}(x_1,x_2)$ is the capacitance of the maximum coenergy configuration in which the axis of the supplied electrode is coincident with the axis of the rotor tooth; $C^B_{eq}(x_1,x_2)$ is the equivalent capacitance when the rotor position is the same, but the supply has been switched to the next phase and N_S is the number of stator electrodes. The following formula holds:

$$C^A_{eq} = C_{max} \tag{3.15}$$

and thus

$$\Gamma_0 = N_SV_2\frac{C_{max} - C^B_{eq}}{4\pi} \tag{3.16}$$

When $C^B_{eq}(x_1,x_2)$ is to be evaluated the following three cases have to be considered (see figures 3.9 and 3.10 :
Case A3 $\frac{2\pi}{N_R} - \frac{2\pi}{N_S} + x_2 < x_1 < \frac{2\pi}{N_R}$

$$C_B = \varepsilon_0\varepsilon_r h(x_2\frac{r_2+r_3}{2(r_3-r_2)} + \frac{\det(A_t)}{(r_3-r_2)^2}) \tag{3.17}$$

where

$$A_t = \begin{bmatrix} 1 & r_2 \sin(\frac{\pi}{N_S} - \frac{\pi}{N_R} + x_1) & r_2 \cos(\frac{\pi}{N_S} - \frac{\pi}{N_R} + x_1) \\ 1 & r_2 \sin(\frac{x_2}{2}) & r_2 \cos(\frac{x_2}{2}) \\ 1 & r_3 \sin(\frac{x_2}{2}) & r_3 \cos(\frac{x_2}{2}) \end{bmatrix}. \quad (3.18)$$

or, as an alternative:

$$C_B = \varepsilon_0 \varepsilon_r h \frac{x_1 - \frac{\pi}{N_R} + \frac{\pi}{N_S} + x_2)(r_2 + r_3)}{4(r_3 - r_2)} \quad (3.19)$$

Case B3 $\frac{2\pi}{N_R} - \frac{2\pi}{N_S} - x_2 < x_1 < \frac{2\pi}{N_R} - \frac{2\pi}{N_S} + x_2$

$$\begin{cases} \alpha_A = \frac{2\pi}{N_R} - x_1 - \frac{2\pi}{N_S} + x_2 \\ \alpha_B = x_2 - \alpha_A \\ C_B^A = \varepsilon_0 \varepsilon_r h \alpha_A \frac{r_1 + r_3}{2(r_3 - r_1)} \\ C_B^B = \varepsilon_0 \varepsilon_r h \alpha_B \frac{r_2 + r_3}{2(r_3 - r_2)} \\ C_B = C_B^A + C_B^B \end{cases} \quad (3.20)$$

Case C3 $0 < x_1 < \frac{2\pi}{N_R} - \frac{2\pi}{N_S} - x_2$

$$A_t = \begin{bmatrix} 1 & r_1 \sin(\frac{\pi}{N_S} + \frac{\pi}{N_R} - \frac{x_1}{2}) & r_1 r_1 \cos(\frac{\pi}{N_S} + \frac{\pi}{N_R} - \frac{x_1}{2}) \\ 1 & r_1 \sin(\frac{x_2}{2}) & r_1 \cos(\frac{x_2}{2}) \\ 1 & r_3 \sin(\frac{x_2}{2}) & r_3 \cos(\frac{x_2}{2}) \end{bmatrix}. \quad (3.21)$$

$$C_B = \varepsilon_0 \varepsilon_r h (x_2 \frac{r_1 + r_3}{2(r_3 - r_1)} + \frac{\det(A_t)}{(r_3 - r_1)^2}) \quad (3.22)$$

or, as an alternative,

$$C_B = \varepsilon_0 \varepsilon_r h \frac{x_1 - \frac{\pi}{N_R} + \frac{\pi}{N_S} + x_2)(r_1 + r_3)}{4(r_3 - r_1)} \quad (3.23)$$

We are now able to set up two objective functions we will deal with, plotted in figure 3.11, i.e maximum static torque F_1 to be maximized and torque ripple F_2 to be minimized .

$$\begin{cases} \max F_1(x_1, x_2) = \frac{1}{4} V^2 N_R (C_{max}(x_1, x_2) - C_{min}(x_1, x_2)) \\ \min F_2(x_1, x_2) = \frac{F_1 - \Gamma_0}{F_1} \end{cases}, \quad (3.24)$$

Several definition of the ripple are possible, the simplest is the previous one and a little bit more precise one is the following:

$$F_2(x_1, x_2) = \frac{F_1 - \frac{\sin(a)}{\sin(2a)} \Gamma_0}{F_1(\cos(N_R a) - \cos(N_R b))} \quad (3.25)$$

where

$$a = \pi(\frac{1}{2N_R} - \frac{1}{N_S}) \quad b = a + \frac{\pi}{N_S} \quad (3.26)$$

When the friction $\Gamma_f(x_1, x_2)$ is considered the following simple equation can be considered:

$$\Gamma_f(x_1, x_2) = \frac{1}{3} V^2 \frac{\varepsilon h \delta_r (x_1 + x_2)}{d^2} \quad (3.27)$$

where C_{max}, C_{min}, C_{eq}^A and C_{eq}^B are suitable expressions of capacitance at various relative positions φ between stator and rotor under different operating conditions, d is the friction radius, f is the static friction coefficient, h is the rotor thickness, r is the outer rotor radius and d is the air gap width.

3.3.2 Discussion and results

First of all we point out that because of the POF is fully non-convex (see exhaustive sampling in figure 3.12), an equivalent scalar weighted sum formulation would give as solution one of the two extreme points on the POF whatever the values of weights is chosen. Apart from the concavity

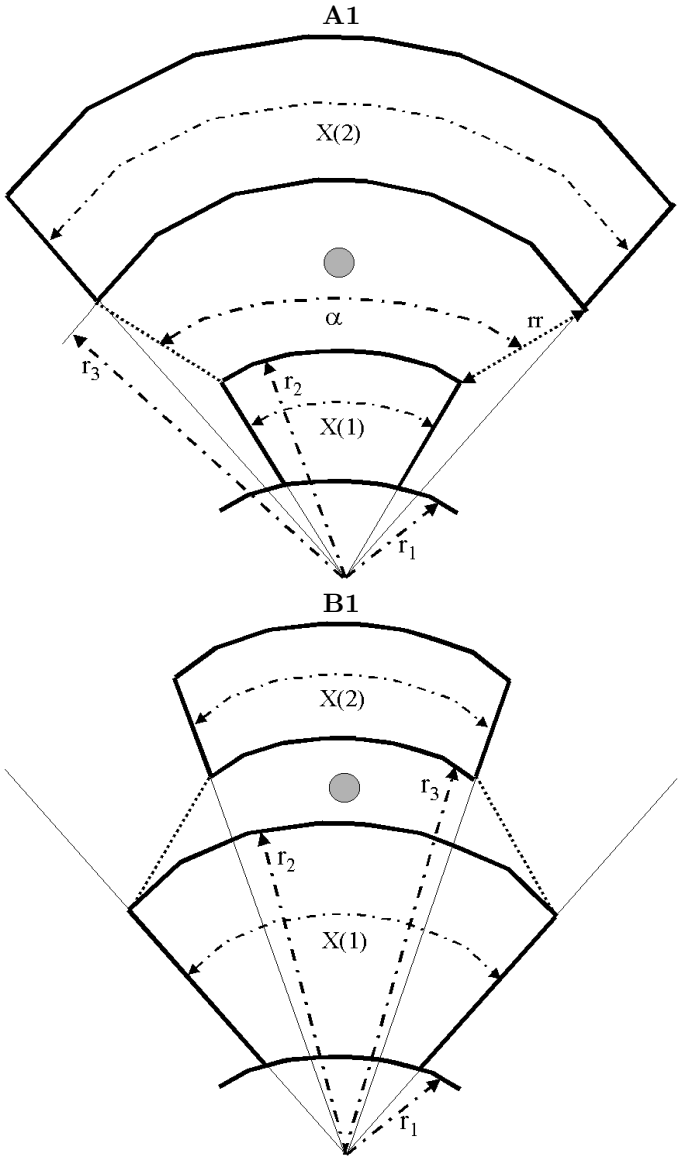

Figure 3.7: Different cases for C_{max} computation

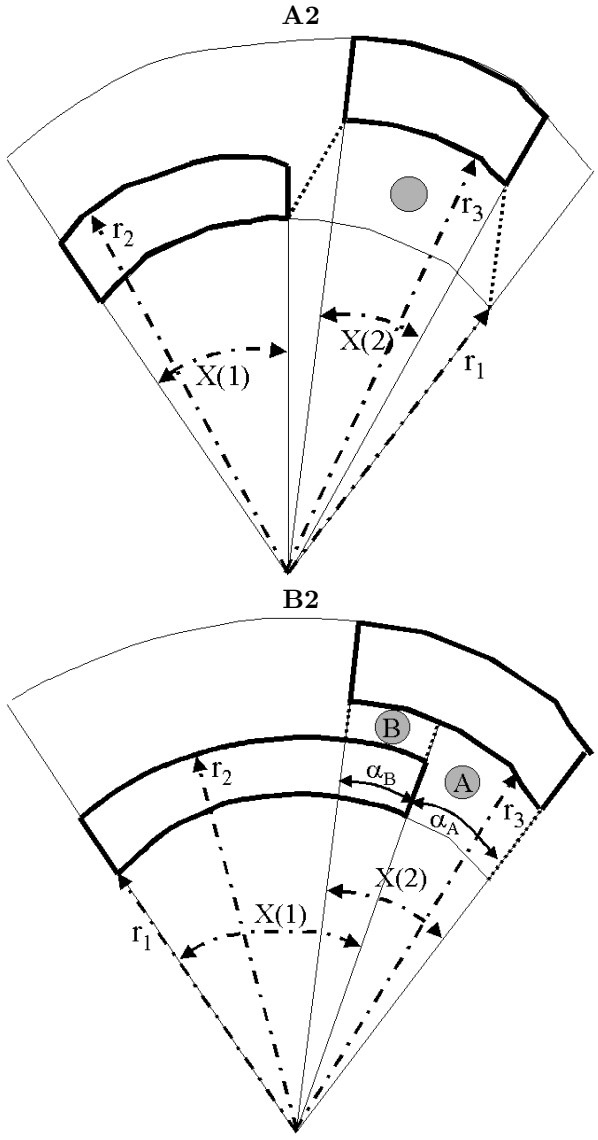

Figure 3.8: Different cases for C_{min} computation.

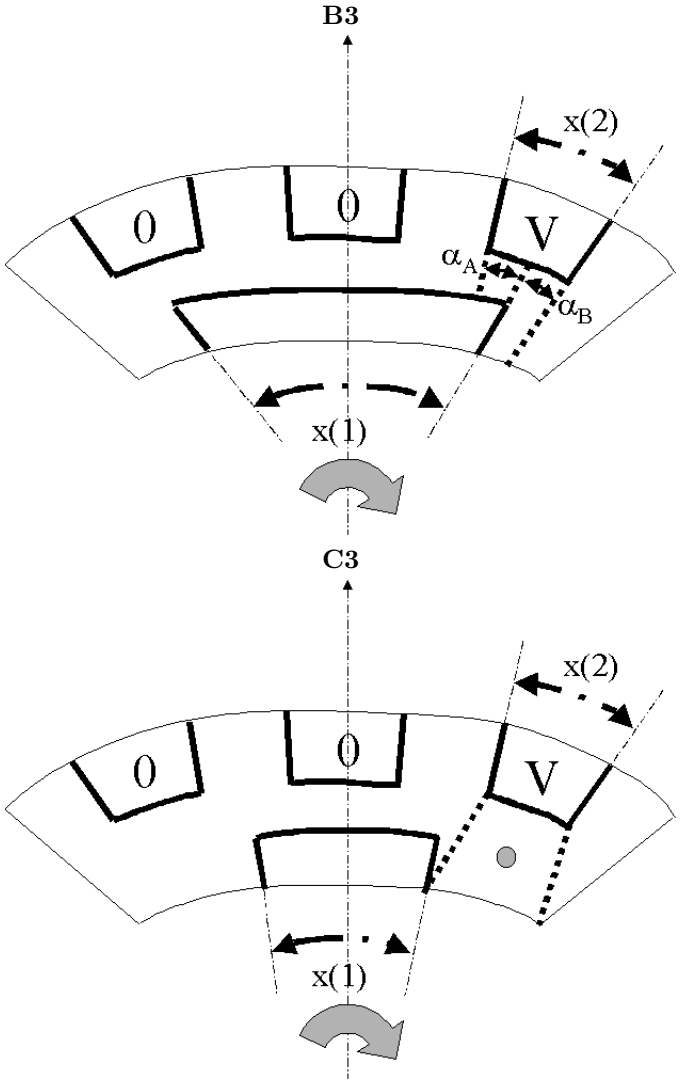

Figure 3.9: Different cases for C_B computation: first two cases

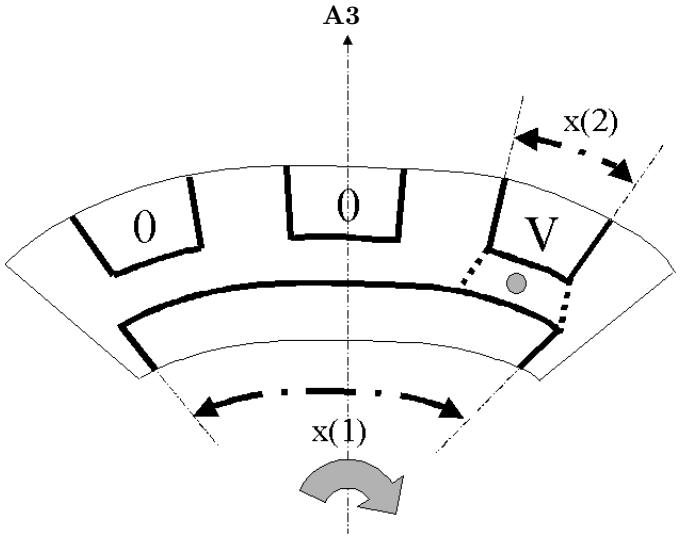

Figure 3.10: Different cases for C_B computation: third case

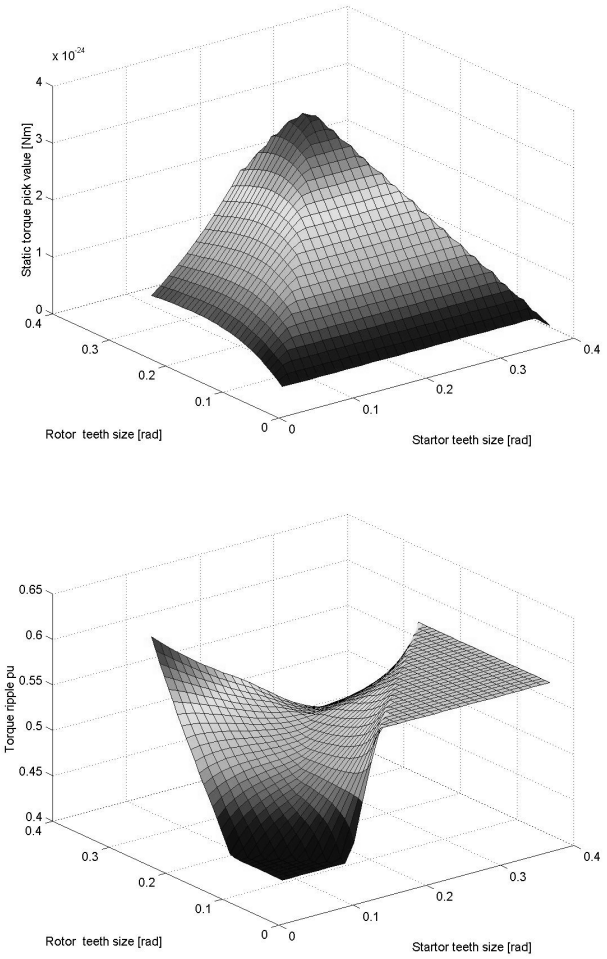

Figure 3.11: Objective function surfaces for the micromotor problem without friction.

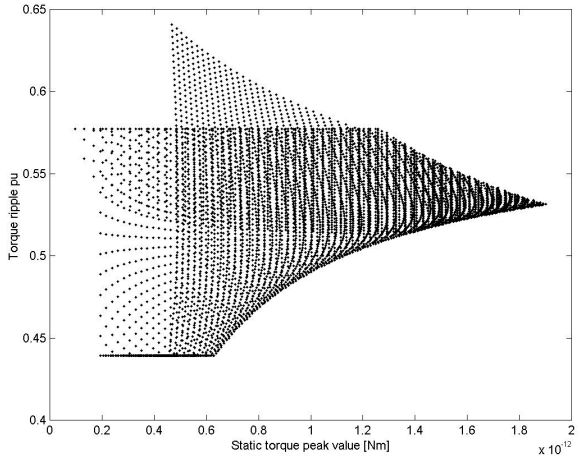

Figure 3.12: Micromotor test case: exhaustive sampling of objective domain search space.

of the POF the problem is not a difficult one and the optimization procedure is straightforward. An example of a 50 individuals solution with obtained NSESA is shown in figure 3.13. As can be seen all individuals are located on the POF and POS respectively.
The evolution of the population during optimization can be seen in figure 3.14 where correspondent iteration numbers are also shown. As can be seen all individuals gradually moves towards the POF under the pressure of fitness assignment and selection. The last result of this chapter is a comparison in both design domain and objective domain of different solutions obtained with or without the addition of the friction and of a third design variable, being the air gap width *d*. As can be seen in figure **??** the POF essentially translates while the POS does not show significant changing.

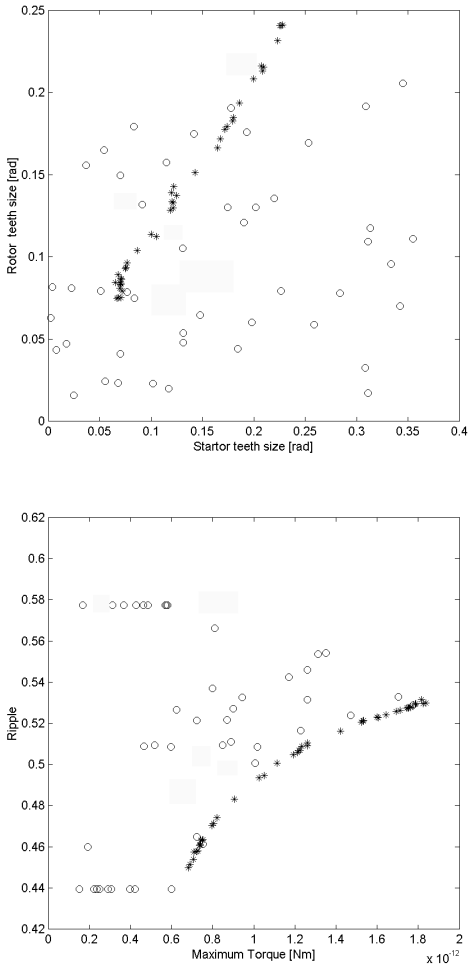

Figure 3.13: Micro-motor test case: 50 individual solution with NSESA in design domain and in objective domain.

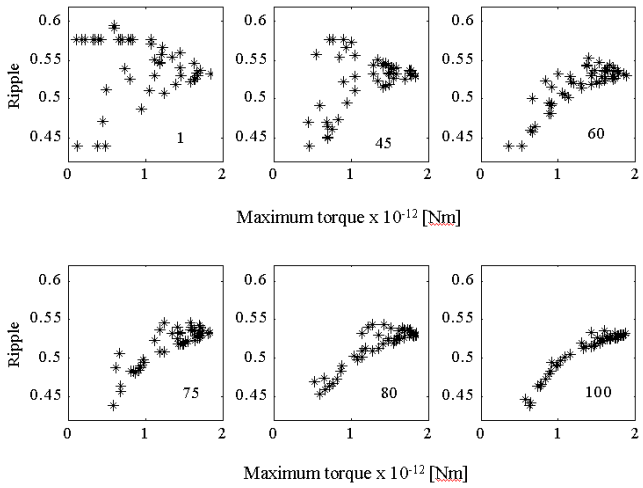

Figure 3.14: Story of population evolution for a run with NSESA on micromotr test case.

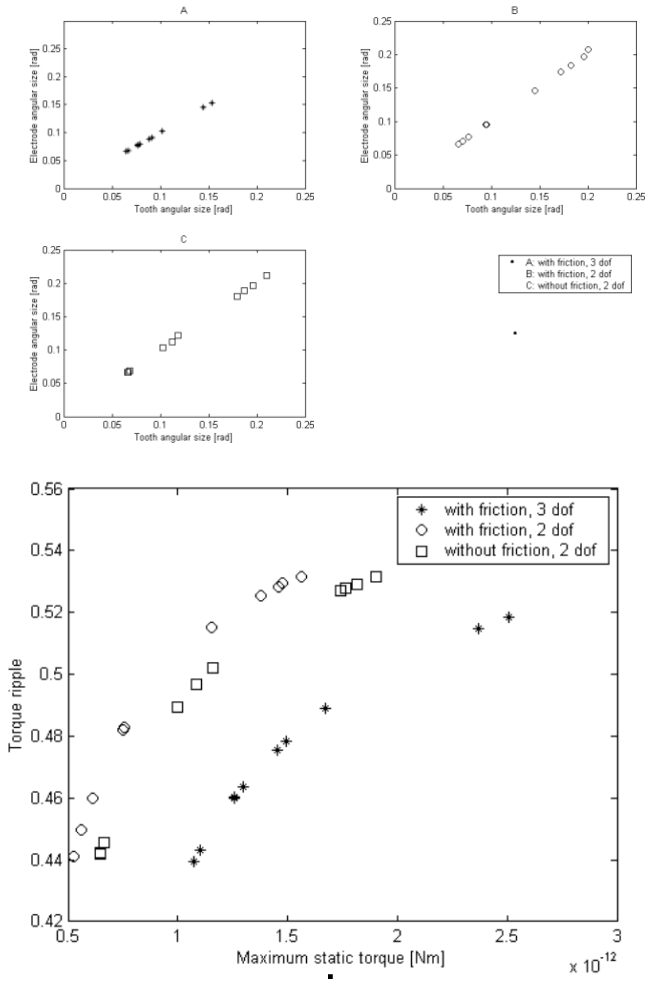

Figure 3.15: Different POF and POS with or without friction and with two or three design variables.

Chapter 4

Real-life electromagnetic test cases

4.1 Introduction

This chapter is devoted to multiobjective optimization of electromagnetic devices for real-life application [35, 38, 36, 33, 39]. The design of an industrial device usually has to fulfill many requirements that can be viewed as objectives. One may divide them into two categories; for the first one a formal mathematical expression is possible (numerical, FEM) such that the objective may be written as a function of design variables (to be computed numerically). For the second category no numerical relations are available linking design variables and objectives. The multiobjective optimization problem can be solved tacking into account all objectives belonging to the first category and the solution is a sampling of the POF. Because of the existence of this second category the approximation of the POF seems to be useful to the designer that will choose a-posteriori one of the available Pareto-Optimal solution tacking into account all objectives belonging to the second category.

When a FEM field computation is to be performed for the evaluation of one or more of the objective the MatLab coded optimizer is to be linked to a commercial Electromagnetic FEM package. Such a procedure may be sometimes non-trivial and a bit of interaction with the FEM package technical assistance is to be taken into account. Two different devices will be considered in this chapter: a single-phase series reactor for power applications and an inductor for transverse-flux-heating of a non-ferrous strip.

The multiobjective optimization of the second device requires a coupled magneto-thermal analysis for the computation of objective values. The MatLab code for such analysis was developed by the Electrothermal heating lab, department of Electrical Engineering, University of Padova, Italy, and it was linked to the optimizers in the frame of a scientific cooperation [cjp8],[ccp1].

4.2 Shape design of a single-phase series reactor for power applications

The reactor is employed to reduce the peak value of the short-circuit current and so mitigate its electrodynamics effects. The design operations, prototyping and final development will be performed by Tamini Transformers S.r.l, Melegnano, Italy.

4.2.1 The model and Optimization Problem

The reactor, the cross-section of which is shown in figure 4.1, is characterized by a coreless winding with cylindrical shape (foil winding); it is

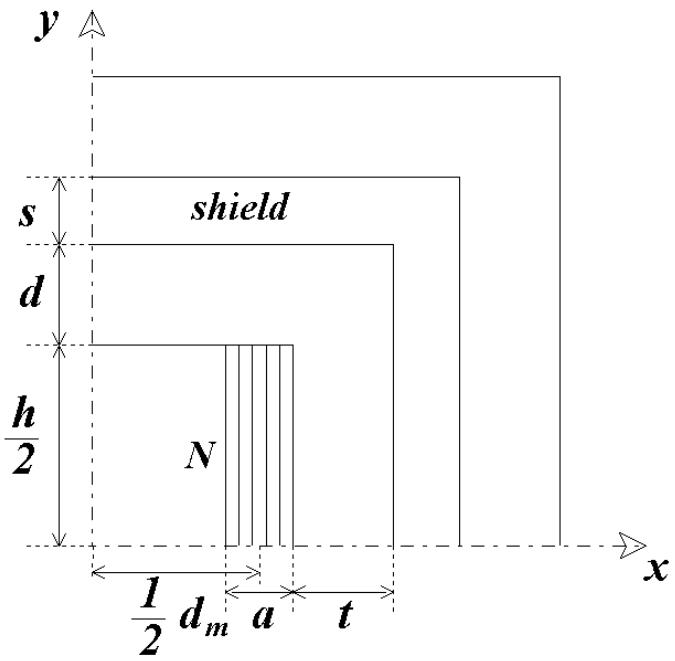

Figure 4.1: Cross-section of the reactor (one quarter) and design variables.

$h[mm]$	$d_m[mm]$	$a[mm]$	$d[mm]$	$t[mm]$	N	k_s
500	590	210	80	40	212	0.504

Table 4.1: Prototype values

boxed in a laminated magnetic screen with parallelepiped shape in order to shield the surrounding environment from the strong stray field. The latter, in turn, gives rise to power losses in the winding that limit the operation of the device; on the other hand the realization of a higher winding and screen, though reducing the effect of leakage, causes an increase of volume and cost of the reactor so that a conflict of design criteria is originated. For a prototype reactor rating a power of 5.9 [MVA] the values shown in Table 4.1 hold:
The distribution of magnetostatic field in the reactor, for which the Cartesian symmetry is assumed to be valid, is governed by the Poisson's equation of vector potential $\mathbf{A} = (0, 0, A)$:

$$\begin{cases} -\nabla \cdot (\frac{1}{\mu}\nabla A) = J & \\ A = 0 & along \quad x = 0 \\ \frac{\partial A}{\partial n} = 0 & elsewhere \end{cases} \tag{4.1}$$

where $J = 3.57[\frac{A}{mm^2}]$ is the current density in the winding while $\mu_r = 1$ and $\mu_r = 104$ are the values of relative permeability of non-magnetic materials and iron, respectively. To solve 4.1 numerically, the two-dimensional field region shown in figure 4.1, including an external layer of air, has been discretized by means of a regular grid of finite elements, namely triangles with quadratic variation of potentials ; the total number of elements is $N_e = 950$ approximately. The evolutionary optimizer calls the a commercial FEM code for performing the field analysis and then updates the finite element grid at each iteration when geometry changes due to design variable changing. In general, up to seven design variables defining the shape of the device can be considered: geometric height h, mean diameter d_m, thickness a of the winding, number of turns N, axial

distance d between winding and magnetic shield, thickness s of the shield, radial distance t between winding and shield.
Two conflicting criteria can be defined:

- **the material cost** f_1 of the reactor, namely the weighted sum of copper and iron weights, **to be minimized**:

$$F_1 = 4k_i w_i[s(\frac{d_m + a}{2} + t)l + s(\frac{h}{2} + d + s)l] + k_c w_c k_s lah \quad (4.2)$$

  with $k_i = 1$, $k_c = 3$ while $w_i = 7860[kgm^{-3}]$ and $w_c = 8930[kgm^{-3}]$ are specific weights of iron and copper, respectively;

- **the fringing field** f_2 inside the winding, i.e. the mean radial component of magnetic induction in the cross-section of the winding, **to be minimized** as well:

$$F_2 = \frac{1}{NW}\sum_{i=1}^{NW} |B_x(i)| \quad (4.3)$$

  where $NW = 64$ is the number of points of a grid sampling the radial induction in the winding.

The following **constraints** have been prescribed:

- the rated value of inductance $L = 23.57[mH]$;
- the induction in the core, not exceeding 0.8 T, when the current per turn is equal to with I_n=893 A;
- the insulation gap between winding and core.

Three independent **design variables** have been selected, i.e.

- height h
- mean diameter d_m
- number of turns N of the winding

Finally, a set of bounds preserves the geometrical congruency of the model, namely:

$$\begin{array}{c} 0.5 \le h \le 1.5 \quad [m] \\ 0.1 + 2a \le d_m \le 1.8[m] \\ 162 \le N \le 262 \end{array} \quad (4.4)$$

The objective functions surfaces of both F_1 and F_2 against (h, d_m) for a given number of turns N=200 are reported in figure 4.2.

4.2.2 Discussion and results

The clash between the two objectives is evident from the comparison of both surfaces. For the sake of comparison, two popular scalar formulations of the multiobjective problem have been considered too, namely the objective weighting and the far-from-worst programming for which the following preference functions have been defined, respectively:

$$\widetilde{f} = c_1 f_1 + c_2 f_2 \quad (4.5)$$

to be minimised, where $c_1 = 10^{-4}$ and $c_2 = 25$ are dimensional coefficients ensuring in and heuristic way (see chapter 1 for discussion about weights choice) equal preference to each objective and

$$\widetilde{f} = (1 - c_1 f_1)(1 - c_2 f_2) \quad (4.6)$$

to be maximized, subject to the prescribed constraints.
Prior to tackle the procedure of optimization, a preliminary identification of the Pareto optimal front has been achieved by sampling, in a random way, the feasible region in both design and objective spaces.
In figure 4.3 the corresponding distribution of samples in the objective space is represented; it can be noted that the design criteria defined transform a quasi-uniform distribution in the design space into a non-uniform one in the objective space. In particular, the Pareto optimal front is approximated by the lower boundary of the latter distribution and is characterized by two branches. The first one corresponds to devices exhibiting a nearly constant cost, while the second branch is characterized

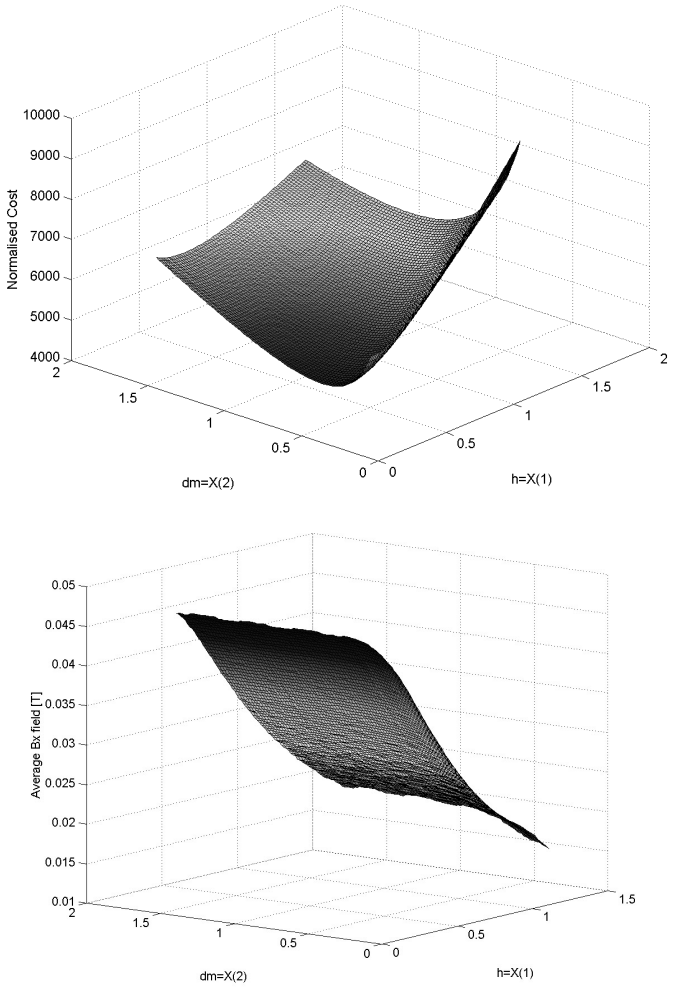

Figure 4.2: Normalized cost of the reactor as a function of mean diameter d_m and height h of the winding. Average B_x field in the winding as a function of mean diameter d_m and height h of the winding itself.

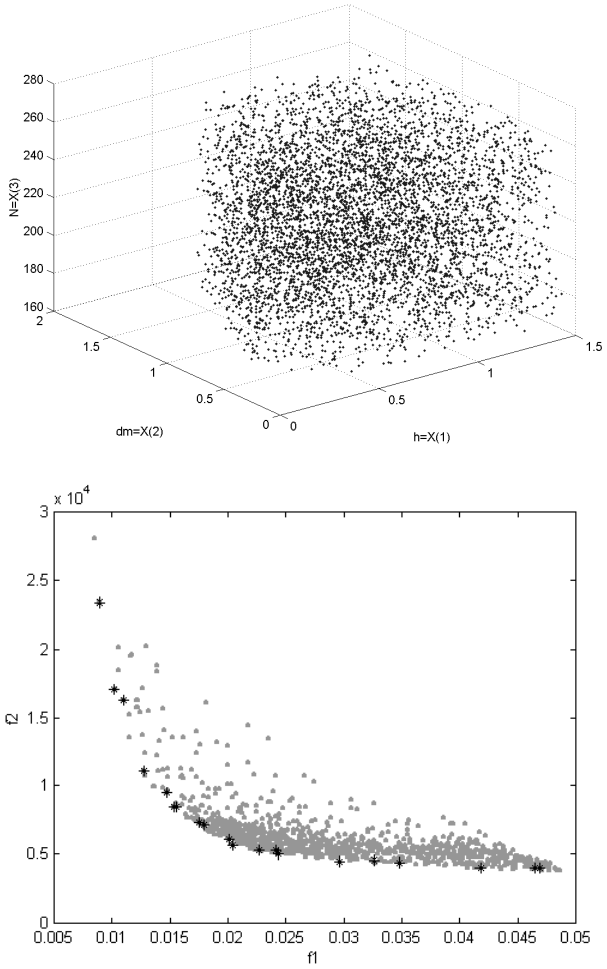

Figure 4.3: Sampling (1000 points) of the feasible region in the design space (geometric dimensions in m) and in the objective space is shown; constraints and bounds are taken into account.

by a remarkable variability and corresponds to devices for which both stray field and cost are actually in mutual conflict. Therefore the Pareto optimal front links two incommensurable objectives and appears to be convex and connected. Moreover it can be noted that, though starting from a quasi-uniform sampling of design space, the approximation of the Pareto optimal front is poorer in the branch of mutual conflict than in the branch of constant cost; this fact confirms the physical expectation that building a low-stray winding is a non-trivial task. As a consequence the approximation of the branch of mutual conflict is a moderately stiff problem from the numerical viewpoint.

PESTRA has been run in two cases, considering 10 and 20 individuals, respectively. After overlapping, in the objective space, the results obtained in the two cases, a few solutions appeared to be weakly dominated and therefore it has been decided to filter them out.

As a result, 24 non-dominated solutions distributed along the Pareto optimal front have been finally obtained; they are shown in figure 4.4. It can be noted that the solutions found represent a subset of Pareto optimal front, characterized by a stray variation of 62.5 % and a corresponding cost variation of 46.7 % approximately. The objective values for the prototype are also shown. As can be seen some solution in the front dominates the prototype and some other solutions are equivalent in the Pareto sense.

In figure 4.5 the shapes of the 24 non-dominated solutions are shown; they are ranked starting from the minimum stray (upper left) device to the to minimum cost (lower right) device; the variability of geometry is evident.

In figure. 4.6 the distribution of magnetic induction in the reactor is shown for the two extremal solutions belonging to the set of 24 non-dominated solutions.

For the sake of comparison, two scalar optimizations have been run considering preference functions p_1 and p_2, respectively; the standard (1+1)-evolution strategy has been applied. The corresponding optima are reported in figure 4.7; it can be noted that the two scalar solutions are practically coincident and represent a non-dominated point located near the center of gravity of Pareto optimal front. The computational cost of

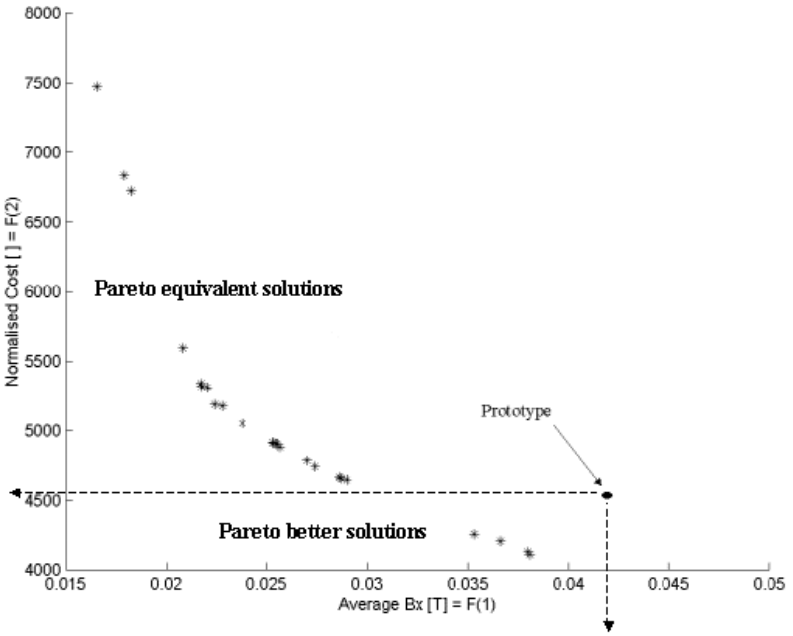

Figure 4.4: Approximation of the Pareto optimal front by means of 24 individuals after filtering 10+20 solutions.

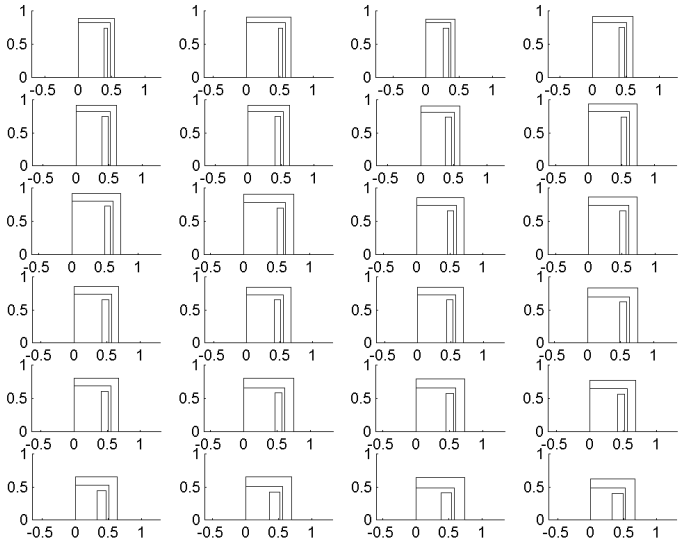

Figure 4.5: Non-dominated solutions: final shapes of the reactor (24 individuals, sizes in m). Shapes are ranked from the minimum stray (upper left) to minimum cost (lower right).

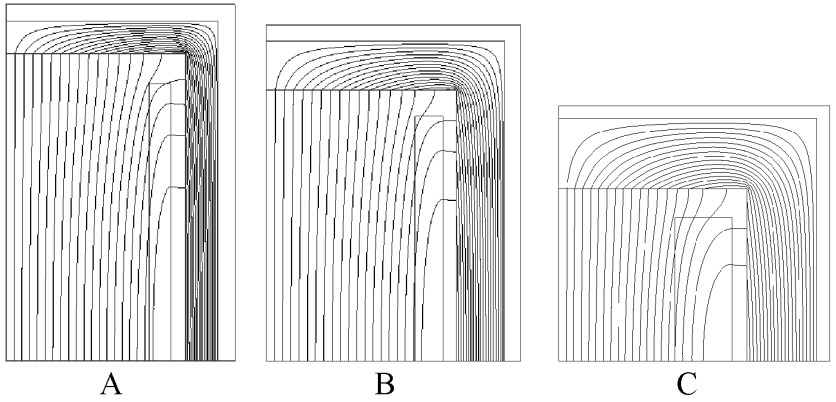

Figure 4.6: Contour plot of magnetic induction for minimum stray field (A) and minimum cost (C) non-dominated solution.

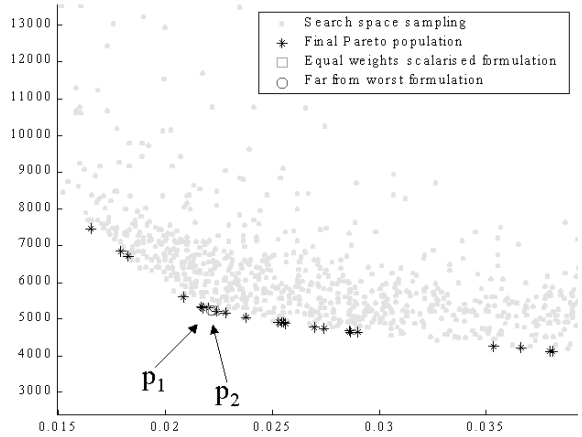

Figure 4.7: Final results: comparison of scalar and vector optimization.

the optimization procedure can be evaluated as follows:

$$c = n_{pop} \times M \times n_{iter} \tag{4.7}$$

where n_{pop} is the number of individuals, M the number of objective functions and n_{iter} the total iteration number. In the case study considered M=2 and n_{pop}=10; when a grid of about 950 triangles of second order is considered, typical figures are c=40 s on a Pentium II 433 MHz processor and n_{iter}=400. The overall procedure has proved to be fast for a twofold reason: on one hand, the algorithm is convergent for any value of n_{pop}, whereas a GA-based strategy would require a high number of individuals, typically some hundreds; on the other hand, there is no need either for classifying individuals into Pareto set during the evolution or for attributing a fitness to each individual, both being time-consuming operations.
A conclusive remark of this first real-life test case can be the following. The optimal shape design of a shielded reactor has been achieved by means of a multiobjective evolutionary optimisation based on the concept of non-dominated solutions. A wide number of configurations belonging to the Pareto optimal front have been identified, so offering the designer an effective choice among devices that rank from the best performing one to the less costly one. The computational cost of the methodology developed is light and compatible with resources of PC based platforms. More generally, the following remarks can be drawn.

- A wide choice among optimal solutions implies a better compatibility of the design with industrial normalization and technological constraints.
- Multi-objective optimisation enhances the diversity of performances of optimal designs and therefore could highlight non-trivial solutions that are a priori unpredictable.
- Having a set of optimal solutions makes it easy to fulfil a posteriori time-varying constraints that are typical of real-life engineering (like the ones imposed by suppliers of materials), whereas in scalar optimization they have to be carefully prescribed in order the only solution be feasible.

4.3 Shape Design of an Inductor for Transverse-flux-heating of a Non-ferrous Strip

Transverse flux induction heating (TFH) has been well known for many years and it is well suited for heating flat metal products. In this case, unlike longitudinal flux heating, TFH allows to obtain a high electrical efficiency by using low frequency values. This advantage becomes more pronounced with the reduction of the strip thickness and increase of the electrical conductivity of the material to be heated. Unlike longitudinal flux heating, the design of TFH devices is characterised by a large number of parameters, closely correlated each other. Besides, the distribution of heat sources and output temperature field in the workpiece is normally non-homogeneous. In turn, the non-homogeneity of temperature fields can provoke thermal deformations in the workpiece which have to be taken into consideration in the complete design of the device. Moreover, all of the problems typically should be solved for variable strip geometry and material properties [ccp3].
Different numerical packages are available for the solution of electromagnetic and thermal problems related to the analysis of TFH systems. These packages are able to solve both two and three dimensional problems. Their main drawbacks are the high runtime and the heavy procedure describing the geometry of the device. For this reason, an analytical-numerical tool has been developed by the Electrothermal heating Laboratory at University of Padova, Department of Electrical Engineering which is able to perform a parametrical analysis and to give very quickly a preliminary calculation of the main parameters of the device and the thermal transient behavior. The analysis tool has been linked to the developed multiobjective optimization procedures.

4.3.1 The model and Optimization Problem

A typical inductor for TFH (Transverse Flux induction Heating) system, is composed of two parts, each facing one side of the workpiece (metal strip), and is characterized by any number of poles, with different

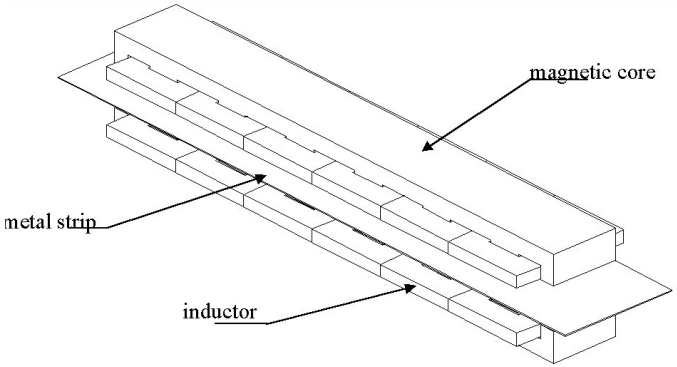

Figure 4.8: General view of a TFH device.

dimensions and supply [cjp8] (see an example in figure 4.8). The design variables (see cross section of coil in figure 4.9) are the half-internal width of the coil in the longitudinal direction **a**, the half-internal height in the transversal direction **b**, the width of the coil conductor **d**, and the working frequency **f** . The number of coils has been chosen equal to 4 i.e. two butterflies (a butterfly being a couple of inductor sections). The inductor is supplied by a current equal to 700 A, the velocity of the strip is v = 0.4 cm s-1. The material of the strip is silver; its width of the strip to be heated is fixed and equal to 100 mm.
The following two objective functions are defined:

- the **electrical efficiency** F_1 (to be maximised) of the inductor defined as the ratio between power transferred to the workpiece and power supplied to the inductor.
- the **maximum temperature gap** F_2 (to be minimised) in the y direction in the same instant. Congruency bounds have been imposed to design variables.

The analytical solution of the Helmholtz's equation in three dimensions gives the expressions of the electric field in the strip and in the air; the

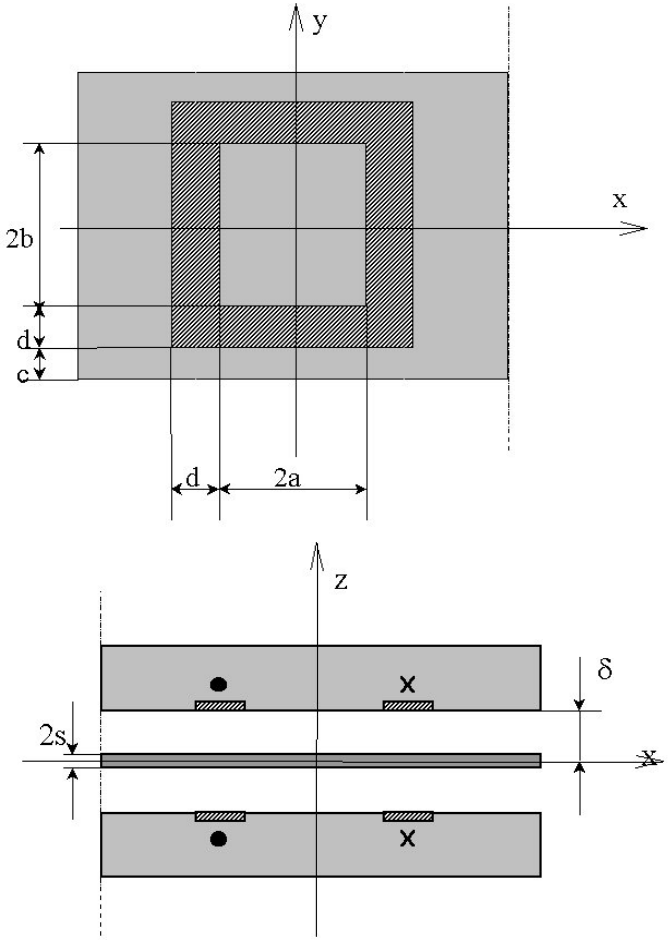

Figure 4.9: Top view and cross section of a TFH device.

power density distribution and all integral parameters of the system can be thus calculated. The analysis of the thermal transient is based on finite difference method starting from the solution of the electromagnetic problem described above.
The following constraint is imposed together with some box-constraints:

$$b + d < 50mm \tag{4.8}$$

Before tackling optimisation, several objective fiuction surfaces analyses have been performed, one for each pair of design variables. In figure 4.10 an example of conflict between the objective functions is reported; the values of a and b have been varied on a 100-point grid.

4.3.2 Discussion and results

Due to the high computational cost of each objective function evaluation (approximately 5 minutes on a PIV desktop) due to the precision required in approximating the POF, the optimization has been tackled via an hybrid stochastic-deterministic and local-global strategy. NSESA has been used as global search and PGBA as local search. The strategy is outlined in table 4.11 and compared with a full stochastic strategy.
Two are the key-points of such a strategy; the first one is the switching criterion to be used for stopping the evolutionary search and moving to local search, i.e. set up the value of K_2, ε_{STOP} being the maximum normalised distance between individuals for successive iterations. The second one is the metrics to be used in order to assign *npop* search directions to individuals when moving to local search. When convergence towards POF has to be represented, convergence indexes C_x and C_f can be profitably used. The two indexes monitor the convergence toward POS (in the design variable space) and toward POF (in the objective function space) respectively. More details on switching criteria can be found in [ccp3]. The global search is based on Pareto-ranking and thus does not require preference functions.
Three different solution are shown in figure 4.12 corresponding to columns in table 4.2. As can be seen when a fully stochastic strategy is run with

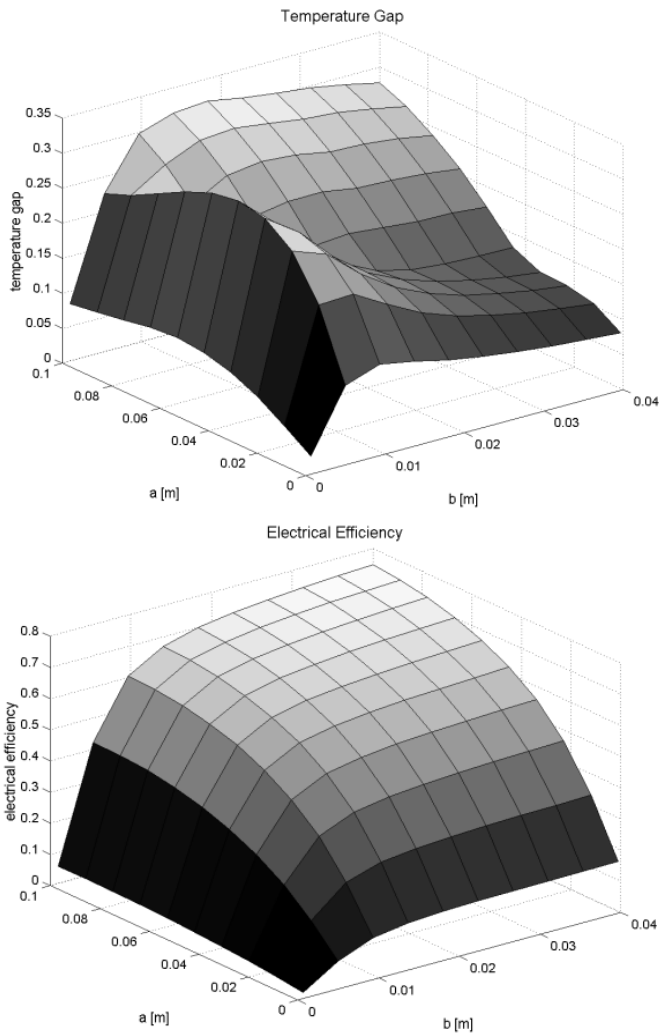

Figure 4.10: Objective function surfaces for the TFH problem versus two design variable.

```
BEGIN
◇ Build a random starting population (npop indiv.)
◇ Run NSESA up to partial conv.  (ε_STOP = K_2 ≪ K_1)
◇ Build npop scalar preference functions
◇ Run npop CGA or NMA up to full conv.(ε_STOP = K_1)
END
```

```
BEGIN
◇ Build a random starting population (npop indiv.)
◇ Run NSESA up to full conv.  (ε_STOP = K_1)
END
```

Figure 4.11: Combined global-local and conventional strategy (Fully global).

the same cost of the hybrid one, the solution is highly unsatisfactorily demonstrating the validity of the hybrid strategy. On the other hand the hybrid strategy with the simplex method as local search is able to give a bigger diversity in solution but, from an industrial point of view some solutions are to be discarded because of the too low efficiency value

figure	A	B	C
Strategy	NSESA+PSA	NSESA+PCGA	NSESA
global s.	128	150	206
local s.	422	56	-
Total cost	550	206	206
cpu-time [h]	17	7	7

Table 4.2: Number of objective function calls and cpu-time for TFH inductor optimization.

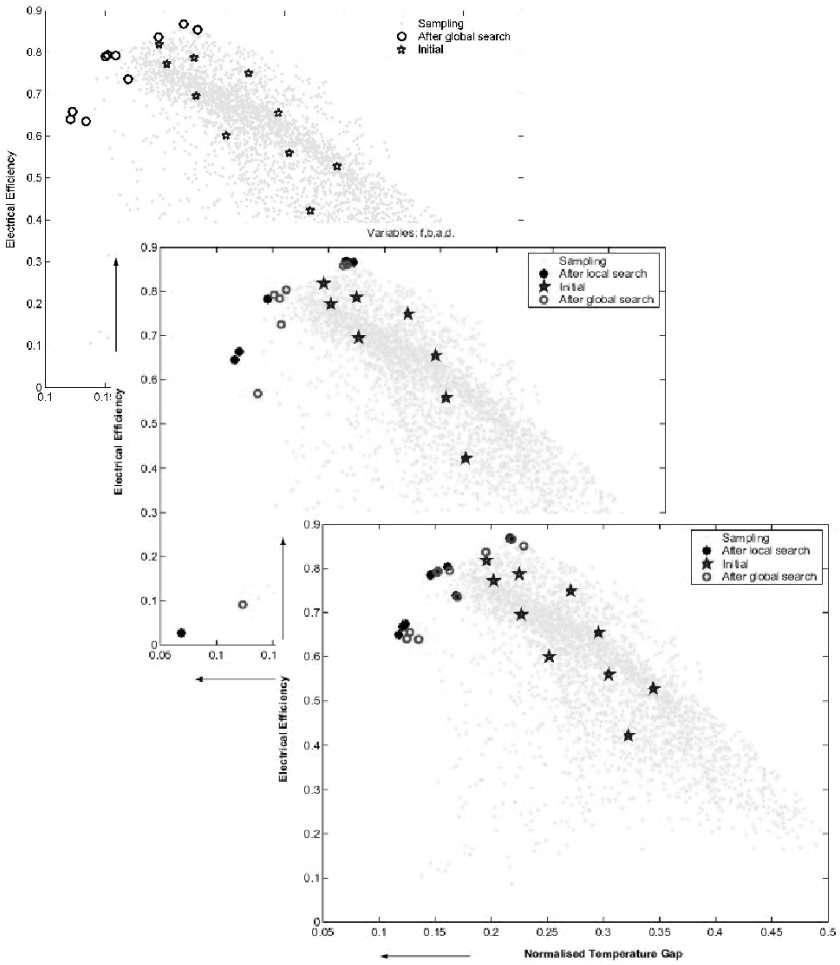

Figure 4.12: Optimization results for the TFH device (C,A,B cases described in table 4.2).

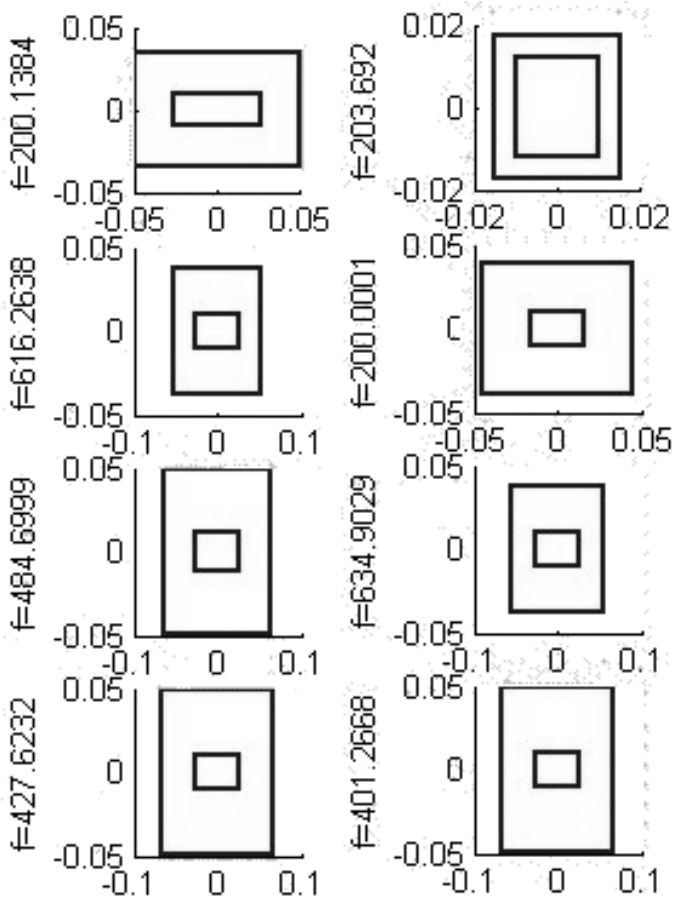

Figure 4.13: Cross section of Pareto optimal solutions ranked in F_1 increasing orded.

Chapter 5

Evolutionary Multiobjective Optimization and interpolation techniques: Towards GRS-MOEAs

5.1 Introduction: GRS Methods

The chapter is devoted to the effort, which is still in progress, in linking General Response Surface Methods (GRSM) and MultiObjective Evolutionary Algorithms (MOEAs).
On one hand we have GRS methods [cjp3,cjp4]that are a well established technique for single-objective optimization in case of time consuming objective function evaluation . The essential idea is to consider throughout the optimization two different objective functions; the first one is the true function which is to be evaluated in as few cases as possible due to its computational cost, the second one is the interpolation of the true objective function via some interpolation technique (polinomial, multiquadrics [24] or Neural Network [41])and it can be evaluated as many time as it is needed. A powerful stochastic global search algorithm (GA, ES, SA, DE) can be run on the interpolated function up to full convergence in order to be sure of escaping local minima, with no limits in objective function evaluation number. Moreover an iterative strategy alternating search of a new optimum and updating of the interpolation quality in the current optimum region is performed in order to increase convergence speed on one hand and to improve interpolation quality only in the area of current optimum with a dramatic reduction in the interpolation training set size. On the other hand we consider Evolutionary Multiobjective Optimization (EMO) as a well established computational research area [13] where several powerful methods are available for a fully convergent POF approximation (NSGAII [42], SPEA2 [46]).As already mentioned the computational cost of MOEAs is relevant and it may be unpractical when industrial design is concerned and the task of reducing objectives function calls is often mandatory. To this aim the link between GRSM and MOEAs seems to be an appealing alternative. Though very appealing such linking is not straightforward due to the fact that when dealing with MO problems the equivalent of the current optimum region of SO problems (an n-dimensional hypersphere centered on the current optimum) is a very complex and often non connected area of design domain search space; the iterative update-search strategy is thus non-trivial in this case.

5.1.1 Neural network for function approximation

A number of NN architectures are available for approximating functions by building response surfaces; amongst them, radial basis architectures

are extensively used for being particularly suitable to interpolation [41]. Such networks are two-layered. The first layer of neurons is characterized by radial basis transfer functions, often of the Gaussian type. The second layer is made of just one linear neuron, performing weighted sum of the first layer's output. Several methods are used for training such networks; in this work, they were chosen to be arranged as General Regression Neural Networks (GRNNs) [7]. This way, a smooth approximation of the surface is attainable, potentially better suited for an optimization procedure. Each objective function was approximated by means of a sequence of networks of increasing cost, where the cost of a network is meant as the number of elements in the training set (input/target couples) i.e. the number of true objective functions to be evaluated. Optimization was then performed, interfacing the NSESA to the NN-interpolated objective functions, so to extract the approximated POF. It is worth pointing out that, once a net is trained, it does not require any other function evaluation, unless an iterative strategy is built (see section 5.3); thus, the optimization can be considered to be inexpensive hereinafter, regardless of the number of individuals employed in the optimization run.

5.2 Non-iterative strategy

The first step of the strategy (see [cjp5]) consists of building NN response surfaces starting from a grid of values for each objective function. The accuracy in terms of both RMS and maximum errors is plotted in figure 5.1 A, for the first test problem; in figure 5.2 A the related results by NN approximation are shown in the objective space. The approximated POFs represented have been obtained from NN with different costs, whose approximation errors have been shown in 5.1 A; the exact front is also represented. The two lowest cost networks lead to degenerate fronts, each made up of just one point; the point corresponding to cost 25 is the farthest one from the utopia point. This means that for too poor interpolation of the objective functions, the character of the functions themselves is lost to such an extent that the problem is no longer multiobjective. For higher costs (from 225 on, in our simulation) the obtained fronts begin to resemble the exact one more closely.

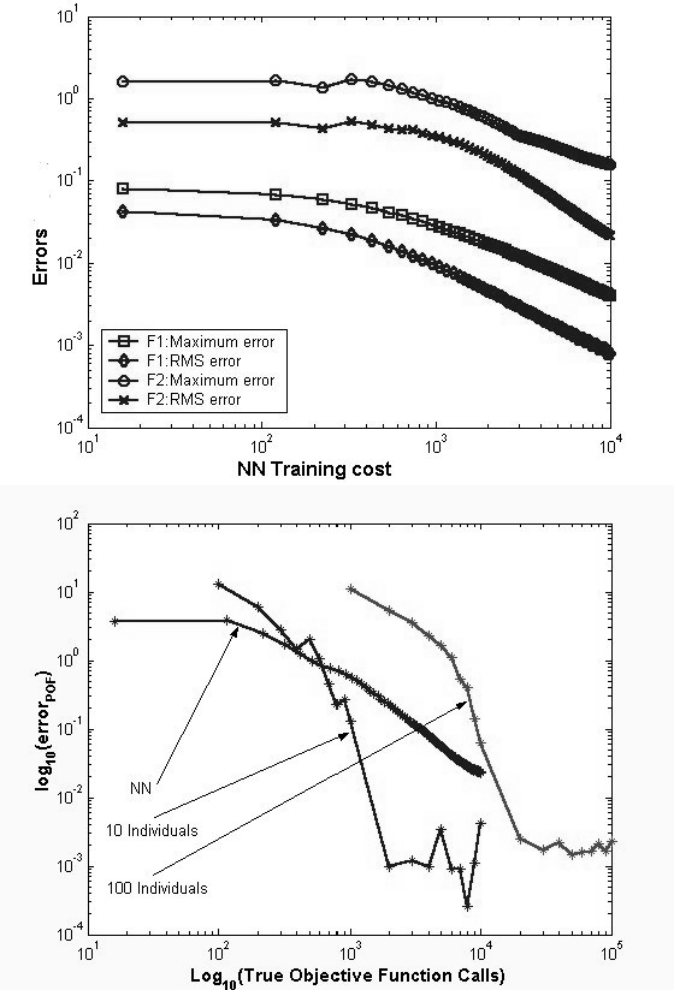

Figure 5.1: Shaffer's problem: objectives approximation errors for NN-interpolated function (top) and comparison on POF approximation error of the true objective function optimization with 10 or 100 individuals and the NN-interpolated objective function optimization (bottom).

As a further example we show in figure 5.3 several POFs for problem DTZ3 with two variables (see [10] for equations) corresponding to different NN training cost. The training set is always a 2D regular grid in the search space.

When the micromotor test problem is considered, an example of some approximated fronts obtained from NN-interpolated functions is shown in figure 5.4 A, where the POF resulting from a 105 point sampling of the design space is considered as the exact POF. The low cost NN gives an unacceptable POF and a cost of at least 1000 must be spent for an acceptable approximation.

In order to give some quantitative expression the approximation error of solutions obtained via NSGA (see [42]) on different NN interpolated functions can be computed in the following way:

$$e = \frac{1}{m}\sum_{j=1}^{m} \min_{i=1:n} \|\text{pof}_i - f_j^{NN}\|_2 \tag{5.1}$$

where **pof** is the true POF, $\mathbf{f}^{NN}$ is the NSGA m individuals solution on NN-interpolated functions. So doing, precision *versus* cost curve can be obtained and is shown in figure 5.3; Indeed, from this curve some a-priori information on the NN training cost for a satisfactory POF approximation may be derived.

As a final result on the micromotor, in figure 5.5 A and B we show a comparison between two different solutions, both obtained by means of NSESA: the first one is based on true objectives and involve ten individuals, the cost being equal to 5500; the second one is based of NN-interpolated objectives and involve 100 individuals, the training cost of the nets being equal to 5500. The 10-individual conventional simulation is definitely preferable with respect to accuracy (in 5.5 B squares dominate dots) but the sampling of both POF and POS is poor (only 10 solutions can be afforded at a cost of 5500). The 100-individual optimization based on NN-interpolated networks, on the contrary, is less accurate but gives a more uniform sampling of the front. The key point is that NN optimization cost is not dependent at all on the number of individuals, as the net is trained before the optimization starts, and no other true function

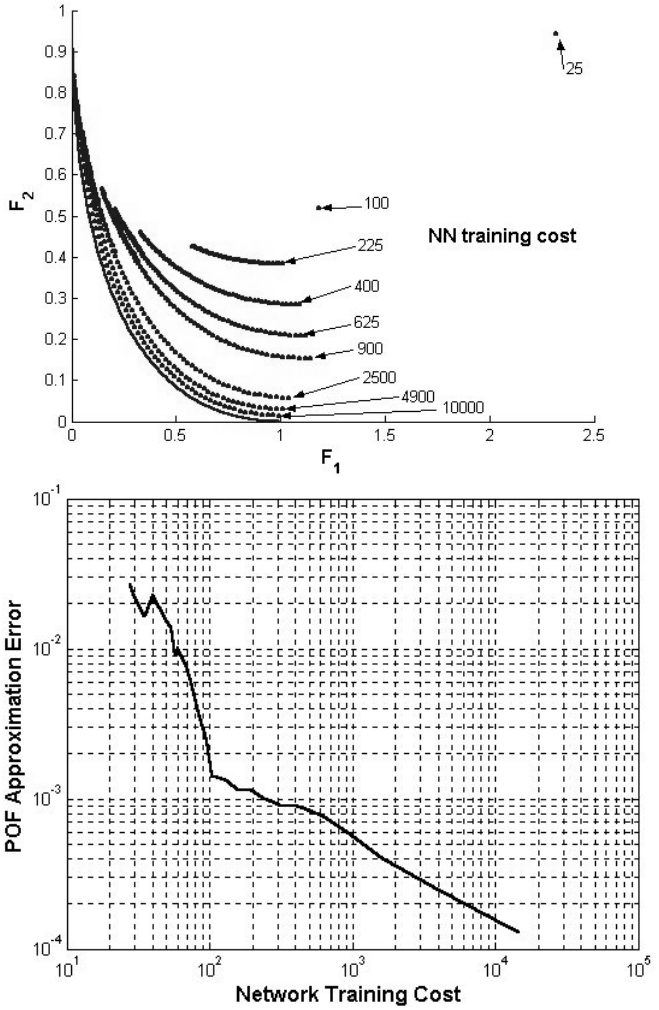

Figure 5.2: Micromotor optimization: approximated fronts for different NNs (A) and approximation error of the POF from NN-interpolated networks vs network training cost.

call is required during the evolutionary algorithm run. Consequently, the true function NSESA, run with few individuals, is preferable to neural networks when the main goal is accuracy, whilst, when a well-sampled front is sought, NN-NSESA proves to be more cost-effective, compared to the conventional NSESA with numerous individuals.
Although response-surface techniques with iterative improvement of approximation quality in the current optimum region are unpractical when considering approximation of POF, the use of interpolated function as objectives in a non-dominated sorting algorithm seems to be an efficient strategy when dealing with expensive evaluation of true objective evaluation. From a detailed study of POF approximation quality in terms of both approximation error and sampling frequency vs NN training cost the following remarks hold:

- if few yet very precise solutions are sought for, the true objectives non-dominated sorting algorithm is to be recommended,
- on the contrary, if many solutions with a satisfactory precision are expected, the NN-interpolated function can be used with a huge reduction of cost in terms of objective function evaluations,
- before building an iterative strategy the dependance of POF approximation error from NN interpolation accuracy is to be considered. This is an essential point that can give several guidelines for the iterative updating of NN training set in the full iterative strategy [cjp5]

5.3 Iterative strategy

The structure of a GRSM method for multiobjective optimization is essentially similar to the single-objective counterpart (see introductory part of the chapter) and is shown in figure 5.7. Three different objective function are considered: the true one, the interpolated one and an auxiliary one which is used for the addition of a point in the most unexplored area of the search space. More detail on this can be found in [cjp3] or [cjp4];

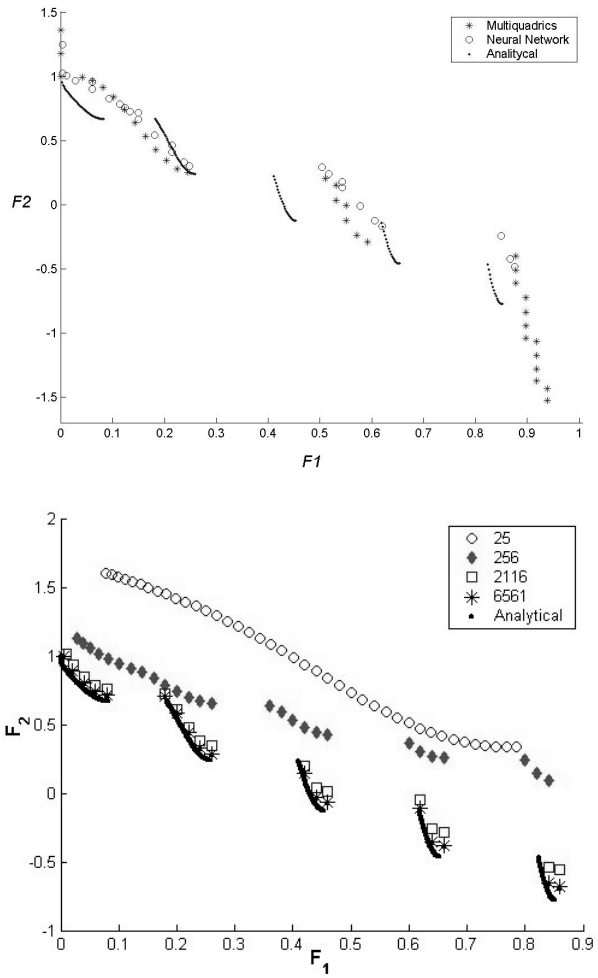

Figure 5.3: POF approximation error *versus* NN training cost (A) and fronts for DTZ3 problem with different NN training cost (B).

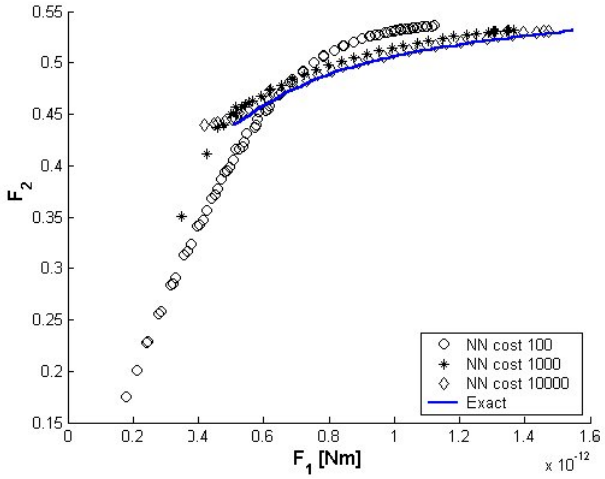

Figure 5.4: Micromotor test case: different POFs with different NN training cost.

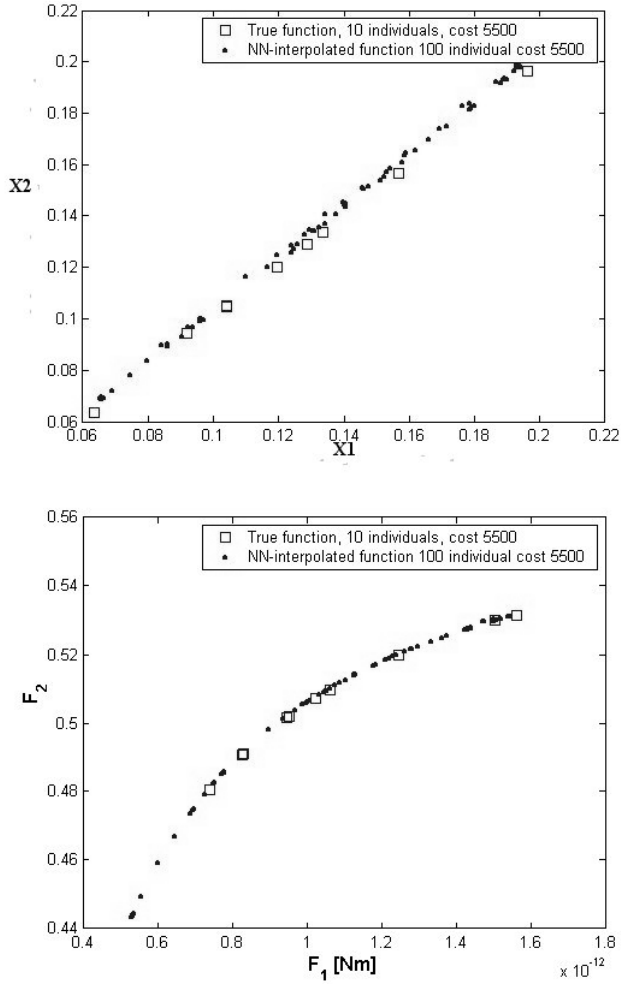

Figure 5.5: Micromotor optimization: comparison of true functions optimization (10 individuals) and NN-interpolated functions optimization (100 individuals) at the same cost (5500); design domain (B) and objective domain (A).

we outline here only those specificities that depends on tackling a multi-objective problem describing in detail the main steps of the algorithm. As will be shown, both problems - conflicting by their nature - of solution accuracy (in terms of both convergence and diversity) and of avoiding local fronts traps, are fully considered.

- **Step 1** Build an n-dimensional regular p^n points grid and evaluate the true objective functions for all points on the grid, where p is the number of points in each edge of the n-dimensional rectangular search space.

- **Step 2** Build the first NN interpolation using all points recorded in step 1 as training nodes and values.

- **Step 3** Start an iterative procedure, *iter* being the iteration counter. If $\langle iter, 2\rangle$=1 add a node in the interpolation nodes set in the most unexplored area of the whole search space, compute the true objectives values update NN-interpolation. The addition of information points increases the probability of jumping out of a local fronts. If $\langle iter, 2\rangle$=0 run a MOEA on current NN-interpolated functions and obtain a current POF; extract non-dominated solutions, compute true objective functions on this nodes and update training set and training nodes.

- **Step 4** If the termination criterion is satisfied stop the search, otherwise go to the next iteration.

The choice of a point in the most unexplored area of an n-dimensional rectangular search space to be added to interpolation set requires an optimisation procedure itself. Given a certain set of N_{NN} interpolation nodes the following objective function based on distances can be built:

$$F_{add}(X) = \frac{\sqrt{\sum_{i=1}^{N}(d_{av} - d_i)^2} - \min_{i=1:N} d_i}{d_{av}}; \tag{5.2}$$

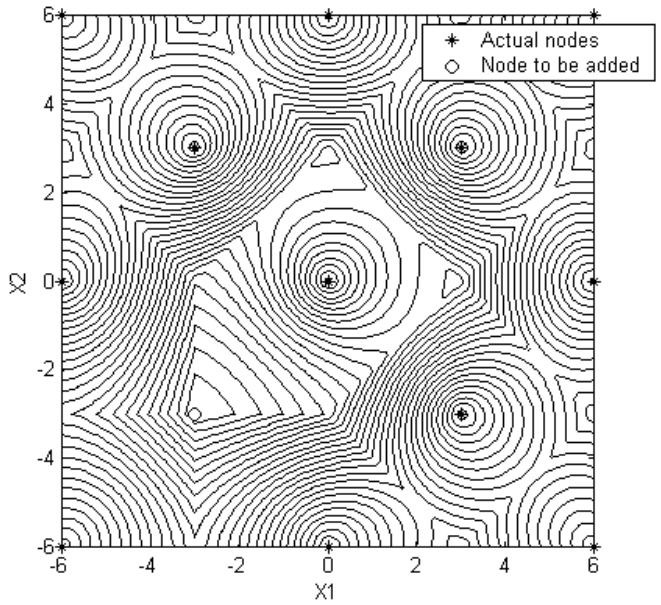

Figure 5.6: Example of addition of an information point throughout an auxiliary objective function minimization.

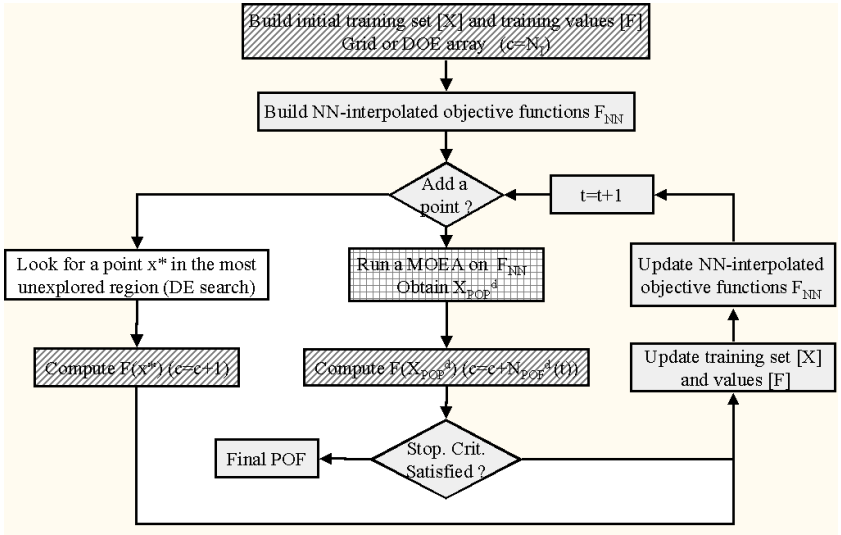

Figure 5.7: Principle flowchart of a GRS-MOEA.

where d_i is the Euclidean distance between X and the i-th interpolation node and d_{av} is the average distance. An example of a particularly symmetrical case is shown in figure 5.6 where the set of current actual nodes ($*$), the new node to be added ($\circ$) and the contour plot of F_{add} have been plotted. As can be seen the node is added where the F_{add} function has its minimum and the position indeed corresponds to the most unexplored area. Due to the possible presence of local minima for function F_{add} when the number of nodes increases this optimisation problem can be solved with a stochastic algorithm (DE). The flowchart of the described methodology is shown in figure 5.6.
Some preliminary results on function DTZ3 are shown in figure 5.8. A relevant reduction of true objective function evaluation is obtained (245 for test run in figure 5.8 versus approximately 2000 for an NSGA) at a given number of solutions on the POF (25). The application of such a strategy to industrial design problem is in progress.

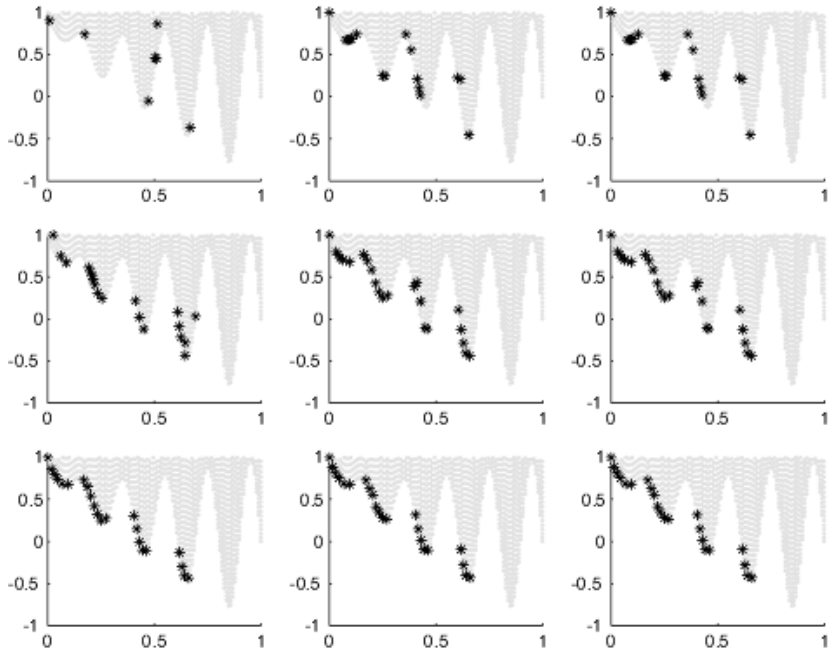

Figure 5.8: Test case for a GRSMOEA: story of current POF for problem dtz3

Conclusion

In the candidate's opinion, the following statement has been proven by the project:

- The analysis of Pareto Multiobjective Optimization theory shows that the use of scalar preference function is to be considered carefully and in a critical way.
- A posteriori choice of trade off among objectives from several available Pareto-optimal trade off solutions is to be preferable to a priori choice.
- Moreover the availability of several Pareto-optimal solutions is itself useful for the designer.
- Solving multiobjective industrial electromagnetic design problems with multiobjective Pareto optimization is practical if special methods are considered giving convergent and diverse solutions even when the number of affordable solutions is very small with respect to the typical number of individuals in an evolutionary strategy.

The most original contribution of the project seems to be the following:

- Application of Pareto MO optimization to electromagnetic shape design .
- Development of special computational strategies with good performances both on analytical test cases and practical industrial design.

Acknowledgments

The collaboration with the following persons is gratefully acknowledged :

- **Prof.P.Di Barba** and **Prof. A. Savini** for having encouraged me three years ago in taking MO Optimization of Electromagnetic devices as PhD subject, for continuous sharing of ideas and for the moving freedom they gave me.
- My PhD-colleague **Ing. A. Bramanti** and **Mr. R. Galdi** for sharing joy and sorrow of research with frequent serious discussion on various topics and brain relaxing chatting at CAD of Electromagnetic Devices Lab, Department of Elecrical Engineering, University of Pavia.
- **Professor J. Sykulski** and his staff, at the Department of Electronics and Computer Science, University of Southampton, UK, for joint research on GRSM methods and for my fruitful (not only for professional growing) 4 months stay in his lab.
- My colleague **Dr. P. Amato** at STMicroelectronics Soft Computing and Nano Organics Operation, for fostering me towards a clearer vision of MO optimization through pleasant discussion and for Latex editing help.
- **Dr. K. Rashid** for the pleasure of joint research on GRSM methods and for pleasant dinners in London and **Professor E. Freeman** for the hospitality in his lab during my stay in Southampton. Both of them are with the Department of Electrical Engineering at Imperial College, London, UK.
- **Prof. F. Dughiero** and the staff of the Electroheating Lab., Department of Electrical Engineering, University of Padova, IT, for deep discussion on the practical use on MO Optimization is real-life electromagnetic design, for kind hospitality in the lab., and for the permission to use their developed coupled electro-thermal analysis code, in the frame of a joint research project.
- **Ing. U. Piovan**, formerly with Tamini Trasformatori Srl, Melegnano, IT and presently with Weidmann Corp., CH for joint research work and stimulating discussion on the reactor test case.
- **Dr. R. Ashen**, with Infolytica Corp., UK for the assistance in linking MagNet FEM analysis code to developed MatLab optimization codes.

References

Papers authored or coauthored by the candidate

Journal Publications (cjp)

1. M. Farina *A Minimal Cost Hybrid Strategy for Pareto Optimal Front Approximation* In press on Evolutionary Optimization, special issue on Multiobjective Optimization, (2002).

2. P. Di Barba, M. Farina. *Multiobjective Shape Optimisation of Air Cored Solenoids* In press on COMPEL International Journal for computation and mathematics in Electrical and Electronic Engineering, (2002), Vol.21.

3. M. Farina, J. K. Sykulski. *Comparative Study of Evolution Strategies Combined with Approximation Techniques for Practical Electromagnetic Optimisation Problem* In press on IEEE Trans. Mag.,(2001).

4. K. Rashid, M. Farina J. A. Ramirez, J. K. Sykulski and E. M. Freeman , *A Comparison of Two Generalized Response Surface Methods for Optimisation in Electromagnetics* COMPEL International Journal for Computation and Mathematics in Electrical and Electronic Engineering, (2001), Vol.20, n.3, 740-753.

5. A. Bramanti, P. Di Barba, M. Farina, A. Savini. *Combining Response Surfaces and Evolutionary Strategies for Multiobjective Pareto Optimization in Electromagnetics.* in press on International Journal of Applied Electromagnetics and Mechanics, (2001).

6. P. Di Barba, M. Farina, A. Savini. *An improved technique for enhancing diversity in Pareto evolutionary optimization of electromagnetic devices.* COMPEL International. Journal for Computation and Mathematics in Electrical and Electronic Engineering, (2001), Vol.20, n.2, 482-496.

7. D .Boffi, M. Farina L. Gastaldi, *On the approximation of Maxwell's eigenproblem in general 2D domains* Computer and Structures, 79, (2001), 1089-1096

8. M. Battistetti, F. Colaone, P. Di Barba, F. Dughiero, M. Farina,S. Lupi, A. Savini, *Optimal design of an inductor for transverse flux heating using a combined evolutionary-simplex method.* COMPEL International Journal for computation and mathematics in Electrical and Electronic Engineering, 20, (2001), 2, 507-522.

9. P. Di Barba, M. Farina, U. Piovan, A. Savini. *Field simulation of forces on windings in a transformer for arc furnace.* COMPEL International Journal for computation and mathematics in Electrical and Electronic Engineering, (2000), Vol. 19 n.2, 381-387.

10. P. Di Barba, M. Farina, A. Savini. *Vector Shape Optimisation of an Electrostatic Micromotor using a Genetic Algorithm.* COMPEL International Journal for computation and mathematics in Electrical and Electronic Engineering, (2000), Vol. 19, n.2, 576-581.

11. P. Di Barba, M. Farina, A. Savini. *Multicriteria Strategy for the optimization of Air-cored solenoid Systems.* Studies in Applied Electromagnetics and Mechanics, IOS Press (1999), Vol. 18, 475-478.

12. P. Di Barba, M. Farina, A. Savini. *Progress in automated design of small and micro-electromechanical devices* Studies in Applied Electromagnetics and Mechanics, IOS Press (1999), Vol 18, 571-574.

Conference Proceedings (ccp)

1. M. Battistetti, P. Di Barba, F. Dughiero, M. Farina, S. Lupi, A. Savini, *Multiobjective Design Optimisation of an Inductor for Surface Heating:an Innovative Approach.* proceedings of IEEE CEFC 2000 Milwaukee US

2. P. Di Barba, M. Farina, A. Savini. *Multiobjective design optimization of real-life devices in electrical engineering: a cost-effective evolutionary approach* Proceedings of EMO01, Zurich, Lecture Notes in Computer Science, 2001, vol.1993, pag.560-573.

3. M.Farina A. Bramanti, P. Di Barba. *Combining Global and Local Search of Non-dominated Solutions in Inverse Electromagnetism* Proceedings of EUROGEN2001 Athens, Greece, September 2001.

4. P.Amato, M.Farina, G.Palma and D.Porto, *An ALife-Inspired Evolutionary Algorithm for Adaptive Control of Time-Varying Systems.* Proceedings of EUROGEN2001 Athens, Greece, September 2001.

Web Sites (ws)

1. `http://www.lania.mx/ ccoello/EMOO/EMOObib.html` a huge and continuously updated bibliography collection on EMO.
2. `http://www.mit.jyu.fi/ miettine` A web-site with important references and several downloadable software.
3. `http://www.iitk.ac.in/kangal/deb.htm` A web-site with important references and several downloadable software.
4. `http://www.tik.ee.ethz.ch/ zitzler/` A web-site with important references and several downloadable software.
5. `http://nimbus.mit.jyu.fi/` An interactive multiobjective optimization systemfor academc and research purposes.

Bibliography

[1] T. Back. *Evolutionary Algorithms in Theory and Practice*.

[2] Tapan P. Bagchi. *Multiobjective Scheduling by Genetic Algorithms*. Kluwer Academic Publishers, Boston, 1999.

[3] C. Carlsson and R. Fuller. Multiobjective optimization eith limguistic variables. *Proceedings of the Sixth European Congress on Intelligent Techniques and Soft Computing (EUFIT98, Aachen, 1998, Veralg Mainz, Aachen,*, 2:1038–1042, 1998.

[4] C.A. Coello Coello. A survey of constraint handling techniques used with evolutionary algorithms. *http://www.lania.mx/ ccoello/EMOO/EMOObib.html*.

[5] Carlos A. Coello Coello. An updated survey of evolutionary multiobjective optimization techniques: State of the art and future trends. In *1999 Congress on Evolutionary Computation*, pages 3–13, Piscataway, NJ, 1999. IEEE Service Center.

[6] C.M. Coello. A comprehensive survey of evolutionary-based multiobjective optimization techniques. *Knowledge and Information systems*, 3:269–308, 1999.

[7] Carlos Manuel Mira da Fonseca. *Multiobjective Genetic Algorithms with Application to Control Engineering Problems*. PhD thesis, Department of Automatic Control and Systems Engineering,University of Sheffield, September 1995.

[8] K. Deb. Multi-objective genetic algorithms: Problem difficulties and construction of test problems. *Tech. Rep. KX-23-45231 Comp. Science Dep., University of Dortmund, Germany*, 1999.

[9] K. Deb. Non-linear goal programming using multi-objective genetic algorithms. *Tech. Rep. KX-22-45201 Comp. Science Dep., University of Dortmund, Germany*, 1999.

[10] K. Deb. *Multi-objective Optimization Using Evolutionary Algorithms*. John Wiley and Sons, ISBN 0471 87339 X, Chichester, UK, 2001.

[11] K. Deb. Nonlinear goal programming using multi-objective genetic algorithms. *PJournal of the Operational Research Society*, 52(3):291–302, 2001.

[12] K. Deb E. Zitzler and L. Thiele. Comparison of multiobjective evolutionary algorithms on test functions of different difficulty. *Genetic and Evolutionary Computation Conference (GECCO-99) Bird-of-a-feather Workshop on Multi-criterion Optimization Using Evolutionary Methods*, pages 121–122, July 1999.

[13] K. Deb et al editors E. Zitzler. *Evolutionary Multi-Criterion Optimization, proceedings of EMO2001, Zurich*, volume 1993. 2001.

[14] C.M. Fonseca and P.J. Fleming. An overview of evolutionary algorithms in nultiobjective optimization. *Evolutionary Computation*, 3(1):1–16, 1995.

[15] C.M. Fonseca and P.J. Fleming. Multiobjective optimization and multiple constraints handling with evolutionary algotithms part i: unified formulation. *IEEE Trans. Sys. Man. and Cybern .A*, 28:26–37, 1998.

[16] C.M. Fonseca and P.J. Fleming. Multiobjective optimization and multiple constraints handling with evolutionary algotithms part ii: application examples. *IEEE Trans. Sys. Man. and Cybern .A*, 28:38–47, 1998.

[17] David E. Goldberg. *Genetic Algorithms in Search, Optimization and Machine Learning*. Addison-Wesley, New York,, 1989.

[18] R. S. H. A. Abbass and C. Newton. Pde: A pareto-frontier differential evolution approach for multi-objective optimization problems. *Proceedings of the Congress on Evolutionary Computation 2001 (CEC'2001),IEEE Service Center, Piscataway, New Jersey, pp. 971–978, May 2001*, 2.

[19] T. Hanne. *Intelligent strategie for meta multiple criteria decision making*. Kluwer Academic Publishers, Dordrecht, THE NEDERLANDS, 2001.

[20] M.P. Hansen and A. Jaszkiewicz. Evaluating the quality of approximations to the non-dominated set. *IMM Tach. Rep. IMM-REP-1998-7*, 1998.

[21] W. E. Hart. *Adaptive Global Optimization with local Search*. PhD thesis, University of California, San Diego, Department of Electrical Engineering, November 1994.

[22] J. Haslinger and P. Neittaanmaki. *Finite Element Approximation for Optimal Shape Design: Theory and Applications*. John Wiley & sons inc, Chichester, 1988.

[23] R.L Haupt and S.E Haupt. *Practical Genetic Algorithms*. John Wiley & sons inc, New York, 1998.

[24] K.F. Goddard J.K. Sykulski, A. H. Khoury. Minimal function calls approach with on-line learning and dynamic weighting for computationally intensive design optimization. *in press on IEEE Trans. Mag.*, 2001.

[25] P. Neittanmaki editors K. Miettinen. *Evolutionary Algorithms in Engineering and Computer Science, proceedings of EUROGEN99, Jyvaskyla,FI*. John Wiley & sons, ltd, New York, 1999.

[26] J. Knowles and D. Corne. Approximating the nondominated front using the pareto archived evolution strategy. *Evolutionary Computation*, 8(2), 2000.

[27] Joshua D. Knowles, Martin Oates, and David Corne. Advanced multi-objective evolutionary algorithms applied to two problems in telecommunications.

[28] F. Kursawe. Evolution strategies for vector optimization. *Proc 10th Int. Conf. MCDM, G.H. Tzeng and P. L. Yu, Eds, National Chiao Tung University, Hsinchu, Taiwan,*, pages 187–193, 1992.

[29] Y.W. Leung and Y. Wang. Multiobjective optimization by nessy algorithms. *Yech. Rep. Fraunhofer Institute for Production Systems and Design Technology, Berlin, Germay*, 1998.

[30] Y.W. Leung and Y. Wang. Multiobjective programming using uniform design and genetic algorithms. *IEEE Tansactions on System, Man and Cybernetics*, 30(3):293–304, 2000.

[31] L. Thiele M. Eisenring and E. Zitzler. Conflicting criteria in embedded system design. *IEEE Design & Test*, 17(2):51–59, April-June 2000.

[32] E. Zitzler M. Laumanns and L. Thiele. A unified model for multiobjective evolutionary algorithms with elitism. *Congress on Evolutionary Computation (CEC-2000)*, pages 46–53, July 2000.

[33] M.Gen and R. Cheng. *Genetic Algorithms and Engineering Design*. John Wiley & sons inc, New York, 1997.

[34] Kaisa Miettinen. *Nonlinear Multiobjective Optimization*. Kluwer Academic Publishers, Dordrecht, THE NEDERLANDS, 1999.

[35] Ch. Magele G. Molinari C. Paul K. Preis M. Repetto P. Alotto, A. V. Kuntsevitch and K. R. Richter. Multiobjective optimization in magnetostatics: A proposal for benchmark problems. *Technical report, Institut fr Grundlagen und Theorie Electrotechnik, Technische Universitt Graz, Graz, Austria,* `http://www-igte.tu-graz.ac.at/team/berl01.htm`, 1996.

[36] M. Rudnicki P. Neittaanmaki and A. Savini. *Inverse Problems and Optimal Design in Electricity and Magnetism*. Clarendon press, Oxford,, 1996.

[37] V. Pareto. *Course d'Economie Politique*. Libraire Drox, Geneve, 1964, first edition 1896.

[38] Yahya Rahmat-Samii and Eric Michielssen. *Electromagnetic Optimization by Genetic Algorithms*. John Wiley & sons,inc, New York,, 1999.

[39] J. Ringuest. *Multiobjective Optimization: Behavioral and Computational Considerations*. Kluwer Academic Publishers, Boston, 1992.

[40] J. D. Shaffer. *Multiple objective optimization with vector evaluated Genetic Algorithms*. PhD thesis, Vanderbily University, Nashville, TN, 1984.

[41] D.M. Skapura. *Buildin Neural Networks*. Addison-Wesley, New York,, 1997.

[42] N. Srinivans and K. Deb. Multiobjective optimization using nondominated sorting in genetic algorithm. *Evol. Comput.*, 2(3):221–248, 1994.

[43] A. M. Sultan and A.B. Templeman. Generation of pareto solutions by entropy-based methods. *in Multiobjective Programming and Goal Programming: Theories and application, M. Tamiz, ed., Berlin, Springher verlag*, pages 164–195, 1996.

[44] M. Zeleny. Multiple criteria decision making: Eight concepts of optimality. *Human System Management*, 17:97–107, 1998.

[45] E. Zitzler and L. Thiele. Multiobjective optimization using evolutionary algorithms - a comparative case study. *Parallel Problem Solving from Nature - PPSN-V*, pages 292–301, September 1998.

[46] Eckart Zitzler. *Evolutionary Algorithms for Multiobjective Optimization: Methods and Applications*. PhD thesis, Swiss Federal Institute of Technology, Computer Engineerin and Networks Laboratory, November 1999.

[47] Thiele L. Zitzler E. Multiobjective evolutionary algorithms: A comparative case study and the strength pareto approach. *IEEE Tansactions on Evolutionary Computation*, 3(4):257–271, 1999.